Aus der Klinik für Herz-, Thorax- und Gefäßchirurgie des Deutschen Herzzentrum Berlins, Stiftung des bürgerlichen Rechts

DISSERTATION

Physiologische Regelung für linksventrikuläre Herzunterstützungssysteme

zur Erlangung des akademischen Grades
Doctor medicinae (Dr. med.)

vorgelegt der Medizinischen Fakultät
Charité – Universitätsmedizin Berlin

von

Panagiotis Pergantis

aus Sparti, Griechenland

Datum der Promotion: 18.09.2020

Inhaltsverzeichnis

1. Zusammenfassung

1.1 Abstract

LVADs (left ventricular assist device) are part of the standard therapy of advanced heart failure. However, complications including right ventricular failure, pump thrombosis, arrhythmias, thromboembolic events, and aortic regurgitation still occur. The automatic adjustment of pump speed and pump flow to the ever-changing hemodynamic conditions and especially to the filling status of the left ventricle can imitate the Frank-Starling mechanism and may result in fewer suction events and more optimal unloading of the cardiovascular system. Various control strategies have been developed and evaluated in vitro. In the first simulation study we demonstrated the robust function of a physiological controller which uses the left ventricular volume as a control variable during acute pathophysiological events. In the second simulation study we developed a new controller which uses the systolic left ventricular pressure as a control parameter. This controller showed a reaction to hemodynamic changes which is similar to the physiological circulation and which led to fewer suction events in comparison to the standard controller with a fixed pump speed. The physiological control systems require sensors for continuous monitoring of variable hemodynamic parameters. As implantable pressure sensors are already being used in clinical practice, the use of pressure-based algorithms is preferred. In the clinical study we evaluated the utilization of the QRS amplitude in the electrocardiogram as a surrogate for cardiac preload in 19 patients with advanced heart failure. The change in acute preload was elicited by a 'passive leg raising' (PLR) maneuver. Transthoracic echocardiography and right heart catheterization were used to evaluate the preload. A relevant increase in mitral inflow and in all measured pressure parameters (pulmonary artery pressure, central venous pressure, pulmonary wedge pressure) was observed during the PLR. However, no increase was seen in the left ventricular volume. A weak yet statistically significant negative correlation between mean pulmonary artery pressure and QRS amplitude in leads V6 and II was observed with correlation coefficient (R) and 95% confidence intervals of R=−0.28 (−0.49, −0.04) and R=−0.29 (−0.50, −0.05), respectively. This study provided additional data regarding the correlation between cardiac preload and QRS amplitude in the electrocardiogram. The further development of physiological control strategies should involve chronic animal studies with heart failure and LVAD assisted cardiovascular systems.

1.2 Kurzfassung

LVADs (left ventricular assist device) gehören zum Standard in der Therapie der fortgeschrittenen Herzinsuffizienz. Komplikationen wie Rechtsherzinsuffizienz, Pumpenthrombose, Arrhythmien, thromboembolische Ereignisse und Aortenklappeninsuffizienz beeinträchtigen den Erfolg dieser Therapie. Die automatische Anpassung der Drehzahl und somit des Pumpenflusses an die immer wechselnden hämodynamischen Bedingungen und insbesondere an den Füllungsstatus des linken Ventrikels ähnelt dem Frank-Starling-Mechanismus und kann das Ansaugen und die inadäquate Entlastung des kardiovaskulären Systems vermeiden. Unterschiedliche Regelungsstrategien werden *in vitro* entwickelt und evaluiert. In der ersten Simulationsstudie zeigten wir die robuste Funktion eines auf dem linksventrikulären Volumen basierenden Kontrollers unter häufig auftretenden akuten pathophysiologischen Ereignissen. In der zweiten Simulationsstudie entwickelten wir einen Kontroller mit dem systolischen linksventrikulären Druck als Kontrollparameter. Wir untersuchten und demonstrierten, wie dieser Kontroller der Reaktion des physiologischen Kreislaufs unter verschiedenen hämodynamischen Veränderungen ähnelt. Im Vergleich zu dem Standardkontroller mit konstanter Drehzahl wurden mit dem entwickelten Kontroller Ansaugphänomene vermieden. Für die physiologische Regelung werden Sensoren zur kontinuierlichen Aufnahme von ausgewählten hämodynamischen Parametern benötigt. Da implantierbare Drucksensoren in der klinischen Praxis bereits verwendet werden, ist die Anwendung des druckbasierten Kontrollers leicht umsetzbar. In der klinischen Studie evaluierten wir die Anwendung der QRS-Amplitude des Elektrokardiograms als Surrogatparameter für die kardiale Vorlast bei 19 Patienten mit fortgeschrittener Herzinsuffizienz. Die akute Vorlastveränderung wurde durch ein *passive leg raising* (PLR) Manöver ausgelöst. Die Evaluation der Vorlast erfolgte mit transthorakaler Echokardiographie und Pulmonaliskatheter. Eine relevante Erhöhung des mitralen Einflusses und der gemessenen Druckwerte (Pulmonalisdruck, zentralvenöser Druck, pulmonaler kapillärer Verschlussdruck) während des PLR wurde erreicht. Echokardiographisch konnte keine relevante Volumenveränderung gezeigt werden. Eine schwache, aber statistisch signifikante negative Korrelation zwischen dem mittleren Pulmonalisdruck und der QRS-Amplitude in den Ableitungen V6 und II wurde mit respektiven Korrelationskoeffizienten und 95%- Konfidenzintervallen von $R=-0{,}28$ $(-0{,}49, -0{,}04)$ und $R=-0{,}29$ $(-0{,}50, -0{,}05)$ beobachtet. Eine Korrelation zwischen kardialer Vorlast und QRS-Amplitude wurde somit bei dieser Patientengruppe nachgewiesen. Für die weitere Evaluation der physiologischen Regelung sind chronische Tierversuche erforderlich.

2. Einleitung

2.1 LVAD (left ventricular assist device)

Die Herzinsuffizienz ist ein klinisches Syndrom mit unterschiedlichen Symptomen (zum Beispiel Belastungsdyspnoe), klinischen Zeichen (zum Beispiel periphere Ödeme) und Verläufen (akut oder chronisch). Die Folge aller pathophysiologischen Herzinsuffizienzmechanismen ist eine Kombination aus vermindertem Herzminutenvolumen (CO) und Erhöhung der intrakardialen Drücke[1]. Bei Patienten mit fortgeschrittener Herzinsuffizienz (unter anderem mit hochgradig eingeschränkter linksventrikulärer Pumpfunktion, wiederholten stationären Aufnahmen wegen kardialer Dekompensation und Abhängigkeit von Katecholaminen) gehört die Implantation von permanenten Kreislaufunterstützungssystemen, neben der Herztransplantation, zur Standardtherapie. In dieser Arbeit beschäftigten wir uns exklusiv mit linksventrikulären Herzunterstützungssystemen, im Folgenden LVAD (left ventricular assist device) genannt.

Die aktuell fast ausschließlich verwendeten LVADs (HeartMate 3, Abbott, Chicago, IL, USA und HeartWare HVAD, Medtronic, Minneapolis, MI, USA) sind Rotationspumpen, die einen kontinuierlichen Blutfluss erzeugen. In Deutschland werden jährlich mehr als 1000 solcher Systeme implantiert[2]. Der letzten Analyse des INTERMACS-Registers zufolge haben in den USA zwischen 2006 und 2017 über 18.000 Patienten einen LVAD eingesetzt bekommen, davon leben noch über 7.500 Patienten mit dem LVAD. Die durchschnittliche Therapiezeit liegt bei 20 Monaten; die Überlebensrate von einem Jahr bzw. fünf Jahren ist 83% bzw. 46%[3]. Trotz der sich immer verbessernden Überlebensrate, schränken Komplikationen den Erfolg der Therapie weiter ein. Rechtsherzinsuffizienz, Blutungskomplikationen, Pumpenthrombose, thromboembolische Ereignisse und Aortenklappeninsuffizienz sind wesentliche Komplikationen, die die Lebensqualität sowie das Überleben der Patienten beeinträchtigen.

LVADs zeigen eine erhöhte Nachlast- und verminderte Vorlastsensitivität[4] im Vergleich zum gesundem Herzen. Die Vorlast wird als die enddiastolische Dehnung der Kardiomyozyten und die Nachlast als der Widerstand stromaufwärts des LVADs bzw. des Herzens definiert[5]. Die physiologische Reaktion des Herzens auf eine Veränderung der Vorlast ist die Anpassung der Kontraktilität. Eine erhöhte Vorlast führt bei gesundem Myokard zu einer Erhöhung der Kontraktilität und somit des CO und umgekehrt, wie auch vom Frank-Starling-Mechanismus beschrieben[6]. Da die LVADs eine sehr geringe Vorlast- und gleichzeitig eine erhöhte Nachlastsensibilität haben, kann ihre Reaktion auf hämodynamische Veränderungen als unphysiologisch betrachtet werden.

Die in der klinischen Praxis verwendeten LVADs funktionieren mit einer konstanten Drehzahl. Die Drehzahl wird initial intra- und postoperativ sowie im Verlauf von den betreuenden Ärzten

anhand unterschiedlicher Kriterien festgelegt. Das Aufrechterhalten eines optimalen CO sowie die ausreichende Entlastung des linken Ventrikels, die anatomische Lage des intraventrikulären Septums, die Öffnung der Aortenklappe und die Rechtsherzfunktion sind dabei die wichtigsten Kriterien[7]. Die Bedürfnisse sowie die hämodynamischen Bedingungen der Patienten bleiben nach der LVAD-Implantation nicht stabil. Die zunehmende körperliche Aktivität erhöht den Bedarf an CO, um die Blutversorgung der Körpermuskulatur aufrechtzuerhalten. Der Abfall des intravasalen Blutvolumens durch die Aufhebung der Kompensationsmechanismen der Herzinsuffizienz, die diuretische Therapie oder Blutungskomplikationen führen zu einer Verminderung der kardialen Vorlast. Eine Verschlechterung der Rechtsherzfunktion kann durch die Rückwärtsstauung auch zu einer progredienten oder akuten Verminderung der Vorlast führen. Die konstant eingestellte Drehzahl erlaubt keine automatische Anpassung der LVAD-Funktion an die ständig wechselnden hämodynamischen Bedingungen.

Wenn die Drehzahl für das vorhandene linksventrikuläre Volumen (LVV) zu hoch eingestellt ist, kann es zu Ansaugen der kardialen Wand von der Einflusskanüle und somit zu einem Kollaps des linken Ventrikels (LV) und einem akuten Abfall des CO kommen (*overpumping*)[8]. Die Stagnierung des Blutes sowie die Wiederherstellung des Kreislaufs sind mit einem turbulenten Blutfluss und potentiell mit einer erhöhten Blutschädigung[9] verbunden. Ventrikuläre Tachykardien können von der Reizung des Myokards ausgelöst werden, und eine durch die anatomischen Veränderungen ausgelöste akute Verschlechterung der rechtsventrikulären Funktion kann auftreten. Dagegen führt eine relativ geringe Drehzahl zu nicht optimaler Entlastung des LV mit anschließender Stauung des Blutes im pulmonalen Kreislauf und zu Symptomen wie Luftnot oder auch zu akuten, lebensgefährlichen Komplikationen, wie Lungenödem, sowie zu einem inadäquaten CO (*underpumping*)[10]. Die nicht optimale Einstellung des LVADs und die daraus resultierende nicht adäquate Hämodynamik können auch zu Blutschädigung und Thrombose- oder Blutungskomplikationen führen[11]. Deswegen wird in der Praxis bei den regulären Verlaufskontrollen oder bei akuten Komplikationen die Drehzahl nach Sammlung von klinischen, echokardiographischen, hämodynamischen und laborchemischen Parametern sowie nach Abfrage der Pumpenparameter manuell angepasst[12]. Eine automatische, kontinuierliche, aktiv kontrollierte und physiologische Anpassung der Drehzahl an die ständig wechselnden hämodynamischen Bedingungen findet nicht statt.

2.2 Physiologische Regelung

Unterschiedlichen Forschungsgruppen haben intuitiv vorgeschlagen, dass die physiologische Regelung der LVADs die Funktion des gesunden Kreislaufs simulieren kann und somit zur

Vermeidung von Komplikationen und infolgedessen zur Verbesserung der Ergebnisse und der Lebensqualität der Patienten führen kann[10]. Trotz der konstanten Drehzahl findet eine passive Anpassung des Pumpenflusses zwar statt, da der Pumpenfluss stark von der Druckdifferenz zwischen dem LV und der Aorta abhängig ist. Diese passive Anpassung ist jedoch unphysiologisch und nicht ausreichend, da die durch die Herzinsuffizienz sehr eingeschränkte myokardiale Kontraktilität nur eine geringe Anpassungsmöglichkeit des CO durch die Ventrikelkontraktion zulässt. Die Erhöhung der Vorlastsensitivität des LVADs ermöglicht eine physiologische LVAD-Funktion. Diese auf dem Frank-Starling-Mechanismus basierende physiologische Regelung ermöglicht die Anpassung des CO an die wechselnden Bedürfnisse der Patienten und kann akute Komplikationen wie *under-* oder *overpumping* Ereignisse vermeiden, da die Drehzahl kontinuierlich und automatisch an den Füllungsstatus des LV angepasst wird.

Unsere Gruppe[13] entwickelte einen *preload responsive speed controller* (im Folgenden PRS-Kontroller), der als Inputparameter das enddiastolische Volumen des LV (LVEDV) verwendet. Der PRS-Kontroller erkennt Veränderungen des LVEDV und passt die Drehzahl und somit die Entlastung des LV und das CO automatisch an. Dieser Kontroller wurde mittels *in vitro* Methoden bzw. Simulationsstudien sowie *in vivo* Methoden, z.B. Tierversuche, evaluiert. *In vitro* konnte eine Überlegenheit des PRS-Kontrollers und anderen vorlastbasierten Algorithmen im Vergleich zu anderen Regelungsstrategien gezeigt werden[14]. In den akuten Tierversuchen[15] im Schweinemodell zeigte der PRS-Kontroller eine Superiorität in der Leistung und eine Reduktion der *overpumping* Ereignisse im Vergleich zu dem Standardkontroller mit konstanter Drehzahl (CS-Kontroller). In der ersten[16] Publikation dieser Arbeit erfolgte die erweiterte *in vitro* Evaluation dieses PRS-Kontrollers während der Simulation von akuten pathophysiologischen Ereignissen, wie die relevante Veränderung des intrathorakalen Druckes in Form eines Valsalva-Manövers und kardialer Extrasystolen.

In der Literatur werden viele physiologische Kontroller beschrieben. Der große Unterschied zwischen den unterschiedlichen Strategien ist die Kontrollvariable bzw. der Parameter, durch dessen kontinuierliche Messung der Feedbackmechanismus für die Regelung ermöglicht wird. Auf Nachlast basierende Regelungsstrategien verwenden Informationen über den aortalen Druck oder die Pulsatilität des Pumpenflusses sowie die Rotorenergie und passen danach die Drehzahl an. Diese Strategien basieren zwar nicht auf dem Frank-Starling-Mechanismus, können aber das Erreichen von Therapiezielen, wie die Erhaltung der Öffnung der Aortenklappe und der aortalen Pulsatilität, erleichtern. Eine direkte, kontinuierliche Messung von Vorlastparametern, wie der atriale und linksventrikuläre Druck (LVP) oder das LVV, ermöglicht die Erhöhung der Vorlastsensitivität, basierend auf dem realen Füllungsstatus des LV. Die vorlastbasierten

Strategien der physiologischen Regelung für die LVADs bieten eine aktive Anpassung der LVAD-Funktion, die sich dem physiologischen Kreislauf und dem Frank-Starling-Mechanismus am besten annähert[17].

In der zweiten[18] Publikation entwickelten wir einen Kontroller mit dem LVP als Kontrollparameter. In den oben genannten *in vitro* und *in vivo* Studien konnte eine gute Performance des PRS-Kontrollers im Vergleich zu dem CS-Kontroller gezeigt werden. Dieser Kontroller benutzt das LVEDV als Kontrollparameter. Normalerweise wird der linksventrikuläre enddiastolische Druck als Vorlastparameter betrachtet. In dieser Studie untersuchten wir die Anwendung des im Vergleich zu dem LVEDV und dem LVEDP einfacher automatisch erhobenen (siehe nächstes Kapitel), maximalen (systolischen) linksventrikulären Druckes (SP), gemessen am Eingang der Einflusskanüle als Kontrollparameter. Der neue Kontroller (SP-Kontroller) wurde dann *in vitro* unter akuten Vorlast-, Nachlast- und Kontraktilitätsveränderungen untersucht und mit dem PRS- und CS-Kontroller verglichen. Des Weiteren erfolgte die *in vitro* Untersuchung des Einflusses der unterschiedlichen Einstellungen des Algorithmus, des möglichen Sensordrifts und der myokardialen Kontraktilität auf die Funktion des SP-Kontrollers.

2.3 Sensoren

Ein essentieller Bestandteil der vorlastbasierten physiologischen Regelung ist die kontinuierliche, robuste und sichere Sammlung sowie Eingabe von Daten über einen ausgewählten Kontrollparameter. Hierbei werden kontinuierliche Informationen über den hämodynamischen Zustand der Patienten erfasst. Diese Informationen lösen durch unterschiedliche Algorithmen eine Reaktion vom Kontroller aus, die sich durch eine Anpassung der Drehzahl der Reaktion des gesunden kardiovaskulären Systems annähert. Je nach Art des Inputs werden diverse Regelungsstrategien in der Literatur vorgeschlagen[17]. Sowohl direkt gemessene als auch indirekt errechnete Werte über die Vorlast, die Nachlast und die Kontraktilität des linken Ventrikels werden als Kontrollparameter verwendet. Die Erhebung von Informationen durch die Bearbeitung von Pumpenparametern, wie dem Pumpenfluss und der Fluss-Pulsatilität, benötigen keine direkte Messung von hämodynamischen Parametern. Die direkte Messung der hämodynamischen Parameter bietet zwar eine kontinuierliche Überwachung des kardiovaskulären Systems, bedarf jedoch spezieller, implantierbarer Sensoren.

In der klinischen Praxis werden aktuell Drucksensoren für die Überwachung des Druckes im pulmonalen Kreislauf und somit der Vorlast des LV angewendet[19]. Durch die Messung der Bioimpedanz an der Körperoberfläche können Veränderungen im Volumenstatus der Patienten erkannt werden. Die Bestimmung der kardialen Impedanz durch die Schrittmacherelektroden wird

in der Praxis als Monitoringstrategie für den Verlauf der Herzinsuffizienz angewendet[20]. Diese Methoden benötigen allerdings spezielle Geräte und liefern indirekte Informationen über das LVV. Es gibt keine kommerziell verfügbaren, implantierbaren Volumensensoren.

Die Amplitude des QRS-Komplexes vom Elektrokardiogram (EKG) wurde schon im Jahr 1956 von A. Brody als Indikator für das LVV vorgeschlagen[21]. Diverse Studien haben seitdem diese Korrelation mit sowohl positiven[22–26] als auch negativen Ergebnissen[27] evaluiert. Madias[28] et al. schlagen die Anwendung der QRS-Amplitude als Überwachungsparameter für den chronischen Verlauf der Herzinsuffizienz vor. Der Nachweis dieser Verbindung bei Herzinsuffizienzpatienten könnte die Anwendung eines einfach gemessenen Parameters als Kontrollvariable für die vorlastbasierte physiologische Regelung der LVADs ermöglichen.

In der dritten[29] Publikation evaluierten wir die Korrelation zwischen der Amplitude des QRS-Komplexes in den Ableitungen II, III und V6 des Oberflächen-EKGs und der linksventrikulären Vorlast bei Patienten mit fortgeschrittener Herzinsuffizienz. Die Erhöhung der Vorlast wurde mit einem *passive leg raising (PLR)* Manöver ausgelöst. Die Vorlast wurde anhand echokardiographischer Bestimmung des LVV und invasiver hämodynamischer Druckmessung evaluiert.

3. Methodik

3.1 Simulationsstudien

3.1.1 Hybrid- Mock- Circulation

Zur Entwicklung und Evaluation von LVADs werden unterschiedliche präklinische Methoden benutzt. Hierzu zählen numerische Modelle, die eine virtuelle Simulation des kardiovaskulären Systems ermöglichen, technische Simulationsmodelle mit echtem Anschluss von LVADs, die den physikalischen Einfluss auf die hämodynamischen Bedingungen sowie die Messung von Flüssen, Volumen und Drücken ermöglichen, und Tiermodelle für die *in vivo* Evaluation. Für die Simulationsstudien in diesem Projekt wurde ein *hybrid mock circulation* (HMC) Modell benutzt, das aus der Kombination eines validierten numerischen Modells des kardiovaskulären Systems[30] mit Anpassung zur Simulation von Ansaugen[31], eines LVADs und einer Schnittstelle zwischen mechanischen und hydraulischen Anteilen entstanden ist. Dieses Modell ermöglicht die Untersuchung von Prototypen und Software-Alternativen bzw. Regelungsmethoden für die LVADs[32] sowie die Simulation von Komplikationen, zum Beispiel Ansaugphänomenen. Das HMC Modell ermöglicht die genaue Untersuchung der Auswirkung bestimmter Veränderungen an multiplen hämodynamischen Parametern, wie die myokardiale

Kontraktilität, der systemische und pulmonale Gefäßwiderstand, das zirkulierende Volumen, aber auch die Drehzahl des LVADs auf das kardiovaskuläre System und die LVAD-Funktion. Das numerische Modell wurde mit Matlab/Simulink auf Real-Time Windows Target (The Mathworks Inc., Natick, MA, USA) bearbeitet. Für diese Studien wurde eine *mixed-flow turbodynamic* Blutpumpe (Deltastream DP2, Medos Medizintechnik AG, Stolberg, Germany) als LVAD benutzt. Die zwei ersten Publikationen sind Simulationsstudien, durchgeführt am HMC Modell.

3.1.2 Auswirkung von akuten pathophysiologischen Ereignissen auf die LVAD-Funktion

Das numerische Modell wurde so erweitert, dass die Auswirkung der Veränderungen des intrathorakalen Druckes (ITP) gezeigt werden konnte. Im Einzelnen wurde das venöse und arterielle Kreislaufsystem in intra- und extrathorakale Komponenten aufgeteilt. Zusätzlich wurde eine venöse Klappe zur Vermeidung von Regurgitationen im venösen System hinzugefügt. Die Simulation des ITP erfolgte durch das Addieren dieses numerischen Druckes und der vorhandenen Druckwerte der intrathorakalen Komponenten des HMC. Es wurden zwei pathophysiologische Ereignisse untersucht: Der akute Anstieg des intrathorakalen Druckes im Valsalva-Manöver (VM) und die ventrikulären Extrasystolen (PVC). Die Simulation des VM erfolgte durch Anwendung eines ITP von 30 mmHg für 10 Sekunden und Anpassung der Herzfrequenz laut klinischen Daten. Die Veränderung der Regularität des Herzrhythmus mit entsprechender Anpassung der diastolischen Phase der simulierten Herzkammern ermöglichte die Simulation von PVC. 4 aufeinanderfolgende PVC wurden implementiert.

Initial wurden beide Ereignisse unter einem physiologischen Kreislauf mit Daten aus klinischen Studien verglichen. Für den gesunden Kreislauf wurde eine normale myokardiale Kontraktilität und eine Herzfrequenz von 70/min in Ruhe mit einem Anstieg auf 90/min unter VM angewendet. Der pathologische Kreislauf wurde mit einer reduzierten myokardialen Kontraktilität von 34% der normalen und einer erhöhten Herzfrequenz von 90/min simuliert. Im pathologischen Kreislauf war ein LVAD angeschlossen. Drei unterschiedlichen Kontroller wurden untersucht. Der erste war der CS-Kontroller. Der zweite war der bis dato von unserer Gruppe angewendete PRS-Kontroller, der den aus einem fortlaufenden Zeitfenster von 3 Sekunden erhobenen LVEDV (maximaler numerischer Wert des LVV) als Kontrollvariable[13] benutzte. Der dritte war eine für diese Studie angepasste Version des PRS-Kontrollers mit *beat-to-beat* LVEDV-Erkennung. Folgende Parameter wurden aufgenommen, um die Auswirkung dieser Kombinationen auf das kardiovaskuläre System und den LVAD zu evaluieren: Drehzahl (PS), Pumpenfluss (PF), Herzminutenvolumen (CO), Druck in der Einflusskanüle (PIP) und mittlerer arterieller Druck (AoP). Ein negativer PIP weist auf Ansaugphänomene hin.

3.1.3 Linksventrikulärer systolischer Druck als Input- Variable für physiologische Regelung

Zur Entwicklung eines druckbasierten physiologischen Kontrollers erfolgte initial die *in vitro* Evaluation der Korrelation zwischen dem systolischen Druck (SP) und der Vorlast, der Nachlast und der myokardialen Kontraktilität. Die Vorlastveränderungen wurden durch Anpassung des zirkulierenden Volumens und die Nachlastveränderungen durch Anpassung des systemischen Gefäßwiderstandes für diese Simulationsstudie ausgelöst. Die Kontraktilität sowie die Herzfrequenz konnten direkt am numerischen Modell eingestellt werden. Durch Evaluierung dieser Veränderungen im physiologischen, pathologischen und mit LVAD mit konstanter Drehzahl (CS LVAD) assistiertem Kreislauf konnte eine direkte Abhängigkeit des gemessenen SP mit Vorlastveränderungen im assistierten Kreislauf gezeigt werden. Im pathologischen Kreislauf führen Veränderungen im LVV zu geringen Veränderungen im LVP, da das System sich im Plateau-Teil der Frank-Starling-Kurve befindet. Im mit LVAD assistierten Kreislauf ermöglicht die reduzierte Kontraktilität und das durch die kontinuierliche Entlastung kleine, fast konstante SV den direkten Einfluss des LVV auf den SP. Das System befindet sich vor dem Plateau-Teil, dementsprechend können Veränderungen am Volumen relevante Veränderungen im SP auslösen. Die Daten dieser Simulationen wurden für die Entwicklung und Kalibrierung des SP-Kontrollers benutzt. Der verwendete Algorithmus war folgender: Ndes= ksp(SP – SPref) + Nref, wobei Ndes die vom SP-Kontroller produzierte Drehzahl, ksp die Proportionalverstärkung, und SPref und Nref der respektive SP und die Drehzahl, definiert für erwünschte CO-Werte mit einem CS LVAD, sind. Laut dieser Formel erhöht der SP-Kontroller die Drehzahl, wenn der SP steigt, und umgekehrt. Ziel ist die Aufrechterhaltung des CO und die Vermeidung von Ansaugen. Die ksp-Werte bzw. die Sensitivität des Kontrollers wurden durch eine *in vitro* Sensitivitätsanalyse bestimmt. Dieser direkte Zusammenhang zwischen SP und Vorlast im pathologischen Kreislauf mit LVAD diente als die Basis für die Entwicklung des SP- Kontrollers.

Unterschiedliche Konfigurationen von physiologischem Kreislauf, pathologischem Kreislauf, pathologischem Kreislauf mit LVAD mit CS-Kontroller und pathologischem Kreislauf mit LVAD mit SP-Kontroller wurden unter den oben beschriebenen Veränderungen der Vorlast, Nachlast und Kontraktilität untersucht. Der Einfluss der unterschiedlichen ksp-Werte sowie des Sensordrifts auf die Performance des SP-Kontrollers wurden evaluiert. Die Annäherung des physiologischen Kreislaufs sowie die Vermeidung von *over-* und *underpumping* wurden als Kriterien für die Evaluation des SP-Kontrollers benutzt.

3.2 Prospektive klinische Studie

3.2.1 Studiendesign

Zur Evaluation der Korrelation zwischen QRS-Amplitude und linksventrikulärer Vorlast bei Herzinsuffizienzpatienten wurde eine prospektive Studie im Deutschen Herzzentrum Berlin durchgeführt. Eingeschlossen wurden 19 Patienten mit fortgeschrittener Herzinsuffizienz (LVEF<25%) aus der Evaluierungsliste für LVAD-Implantation oder Herztransplantation der Herzinsuffizienz-Ambulanz. Die akuten Veränderungen der linksventrikulären Vorlast wurden mit einem *passive leg raising (PLR)* Manöver ausgelöst. Die Studie verlief in drei Phasen für jeden Patienten. In der ersten Phase (Phase 0) lagen die Patienten auf dem Untersuchungstisch in leichter Linksseitenlage zur Erleichterung der echokardiographischen Untersuchung. Nach Erhebung aller Daten in dieser Position erfolgte die Erhöhung der unteren Extremitäten um 45 Grad, wobei die Position des Oberkörpers unverändert blieb (Phase 1). Nach Erhebung der Daten erfolgte der Rückkehr in die Ausgangsposition und die letzte Datenerhebung (Phase 2).

Es wurden kontinuierliche elektrokardiographische und hämodynamische Daten sowie Daten über die thorakale Impedanz, gemessen in der Ableitung II des Monitor-EKGs, und die respiratorischen Bewegungen durch die Aufnahme der CO_2-Kurve gesammelt. Bei Patienten mit liegendem Pulmonaliskatheter im Rahmen der klinischen Evaluierung und unabhängig von der Studie, wurden zusätzlich erweiterte hämodynamische Daten aufgenommen. Es wurden drei echokardiographische Datensätze pro Phase erhoben. Bei Patienten mit Schrittmacheraggregaten erfolgte zusätzlich die Messung der intrakardialen QRS-Amplitude. Alle aufgenommen Daten waren synchronisiert. Die Aufnahme und Verwaltung der Studiendaten erfolgte in einer REDCap[33] Datenbank im DHZB.

Die Bearbeitung der aufgenommenen Daten erfolgte semiautomatisch mit MATLAB (R2018a, The Mathworks Inc., Natick, MA, USA). Die QRS-Amplitude wurde vom maximalen und minimalen Punkt der QRS-Komplexe errechnet. Alle kontinuierlichen Parameter wurden über 10 Sekunden gemittelt, um den Einfluss der respiratorischen Bewegungen auszublenden. Die echokardiographisch aufgenommen Daten wurden von einem zweiten Untersucher mit IntelliSpace Cardiovascular 2.2 (Philips Medical Systems, Best, The Netherlands) ausgewertet.

3.2.2 Statistische Analyse

Die R Version 3.3.1 (R Core Team 2016. R: A language and environment for statistical computing. R Foundation for Statistical Computing, Vienna, Austria) wurde für alle statistischen Analysen bei einem Signifikanzniveau von 0,05 benutzt. Der Fischer's Exact Test und der $\chi 2$-Test wurden für

den Vergleich von kategorischen Variablen zwischen zwei unabhängigen Gruppen und Mann-Whitney-U-Test für kontinuierliche Variablen benutzt. Der Friedmann Test wurde für die Evaluation der Unterschiede zwischen den drei Phasen angewendet. Die Korrelation zwischen mPAP und QRS-Amplitude wurde mit der r *repeated measures correlation* Methode [34] für jeden Patienten in jeder Phase analysiert und gegen die Hypothese untersucht, dass der Slope 0 war. Alle Tests waren zweiseitig und explorativ.

4. Ergebnisse

4.1 Simulationsstudien

4.1.1 Auswirkung von akuten pathophysiologischen Ereignissen auf die LVAD-Funktion

Die Implementation von VM und PVC im simulierten physiologischen Kreislauf ergab realistische CO- und aortale Druckwerte (AoP). Im Fall des VM konnten während der Phase des erhöhten ITP ein Abfall des CO von 5 L/min auf 2,5 L/min und ein AoP-Abfall beobachtet werden. Oszillationen im CO während der PVC wurden erwartungsgemäß beobachtet. Im pathologischen Kreislauf mit LVAD mit CS-Kontroller kam es während des VM zu negativen Druckwerten an der Einflusskanüle bzw. zu Ansaugphänomenen mit Abfall des CO und der aortalen Pulsatilität. Die beobachteten CO-Oszillationen während der PVC waren denen des physiologischen Kreislaufs ähnlich. Im Gegensatz kam es im pathologischen Kreislauf mit LVAD mit PRS-Kontroller zu keinen Ansaugphänomenen. Der Abfall des LVEDV während des erhöhten ITP führte zu einer Verminderung der Drehzahl bis auf 1800 rpm (Ausgangswert 4100 rpm) vom PRS-Kontroller. Dadurch wurde die weitere Entlastung des schon unterfüllten Ventrikels vermieden. Allerdings wurden ein CO-Abfall bis auf 1,5 l/min, ein mittlerer AoP-Abfall bis auf 60 mmHg und ein geringer umgekehrter PF beobachtet. Der PRS-Kontroller mit *beat-to-beat* LVEDV-Erkennung lieferte eine zeitigere Erkennung der Veränderung des EDV und somit eine prompte Reaktion. Im Gegensatz zu dem Standard-PRS-Kontroller wurde eine geringere Drehzahlreduktion (bis auf 2500 rpm) mit entsprechend geringerem CO-Abfall bis auf 2,5 L/min sowie kein umgekehrter PF beobachtet. Während der PVC wurde mit beiden Kontrollern eine ähnliche Reaktion beobachtet. Initial kam es zu einer Drehzahlreduktion während der PVC und anschließend zu einer Drehzahlerhöhung während der normalen Kontraktion, als Folge des aufgrund der PVC erhöhten LVEDV. Nach Abschluss des VM und der PVC waren alle Veränderungen reversibel und das System kehrte in die Ausgangsposition zurück.

4.1.2 Linksventrikulärer systolischer Druck als Input-Variable für physiologische Regelung

Während der Vorlast- und Nachlastveränderungen war die Reaktion des physiologischen Kreislaufs und des SP-Kontrollers ähnlich. Die resultierenden LVP-Werte waren stets vom Niveau des Ansaugens entfernt, im Gegensatz zu dem CS-Kontroller, bei dem beide Vorlast- und Nachlastveränderungen zu Ansaugen führten. Während der akuten Kontraktilitätsveränderungen wurde allerdings eine unphysiologische Reaktion des SP-Kontrollers beobachtet. Obwohl im CS-Kontroller ein akuter Abfall der Kontraktilität keinen signifikanten Einfluss auf das CO hatte, führte dies im Fall des SP-Kontrollers zu einem relevanten Abfall des CO, einem niedrigeren SP und einem höheren EDP, was in der Praxis ein *underpumping*-Ereignis auslösen kann. Die unterschiedlichen Nref- und SPref-Werte hatten einen geringen Einfluss auf die Performance des SP-Kontrollers und für die breit ausgewählten und getesteten Werte wurde kein Ansaugen beobachtet. Unterschiedliche ksp-Werte wurden unter den oben genannten Veränderungen getestet, wobei nur unter sehr kleinen Werten Ansaugphänomene mit dem SP-Kontroller beobachtet werden konnten. Der SP-Kontroller zeigte eine optimale Performance auch unter höheren Sensordrift-Werten bis 25%. Der SP-Kontroller zeigte eine stärkere Abhängigkeit von der Kontraktilität. Die ausgewählte Standardkontraktilität für den pathologischen Kreislauf für die Simulationen war 34%. Eine erhöhte Kontraktilität von 50% (wie zum Beispiel bei myokardialer Erholung) führte im Vergleich zum physiologischen Kreislauf zu überproportionaler Erhöhung des CO. Dagegen führte eine reduzierte Kontraktilität von 10% zu unterproportionaler Erhöhung des CO während der Vorlasterhöhung.

4.2 Prospektive klinische Studie

Es erfolgte der Einschluss von 19 Herzinsuffizienzpatienten. Bei einem Patienten gab es während der Studie eine akute Veränderung im Herzrhythmus, so dass diese elektrokardiographischen Daten nicht miteingeschlossen wurden. 15 Patienten waren männlich, 4 weiblich. Alle Patienten litten unter einer dilatativen Kardiomyopathie, 26% von ihnen hatten eine ischämische Ätiologie. Erweiterte hämodynamische Daten vom Pulmonaliskatheter konnten bei 9 Patienten erhoben werden. Adäquate Daten für die echokardiographische LV-Volumetrie konnten bei 7 Patienten erhoben werden. Zum Ausblenden des möglichen Effektes der Veränderung der Position und Form des Herzens während der drei Phasen blieb der Oberkörper stets stabil. Dies erschwerte die Aufnahme von aussagekräftigen echokardiographischen Loops bei den übrigen Patienten. Die meisten Patienten hatten eine leicht bis mittelgradig eingeschränkte rechtsventrikuläre Pumpfunktion (53%), der Rest (47%) eine normale. Bei 68% der Patienten war der Herzrhythmus

kontinuierlich vom Schrittmacher getriggert oder unterstützt im Rahmen der kardialen Resynchronisationstherapie.

Während des PRL wurde eine signifikante Veränderung in folgenden Vorlastparametern beobachtet: mittlerer Pulmonalisdruck (mPAP) (p=0,014), zentralvenöser Druck (CVP) (p=0,009), pulmonaler kapillärer Verschlussdruck (PCW) (p=0,001), mitraler Einfluss (E-Welle) (p=0,015). Darüber hinaus konnte eine relevante Veränderung in indirekten echokardiographischen Parameter für die linksventrikuläre Druckbelastung E/A (p=0,002) und E/E′ (p=0,047) (Tabelle 1) gezeigt werden. Die Auswertung der volumetrischen Daten ergab keine statistische Signifikanz, allerdings ist die transthorakale Volumetrie wahrscheinlich nicht genau genug, um solche Veränderungen zu erfassen, insbesondere bei nicht optimaler Schallbarkeit. Es wurden keine Veränderungen in den rechtsventrikulären Dimensionen sowie im Diameter der *Vena cava inferior* beobachtet. Der Grund dafür ist wahrscheinlich die Weiterleitung des zusätzlichen Volumens in den pulmonalen Kreislauf durch die erhaltene Rechtsherzfunktion. Es wurde keine signifikante Veränderung der aufgenommenen möglichen Störfaktoren beobachtet. Die thorakale Impedanz, die Herzfrequenz, das inspiratorische Tidalvolumen, der Blutdruck und der echokardiographisch gemessene Abstand zwischen Thoraxwand und linksventrikulärer Spitze blieben während der drei Phasen unverändert.

	N	Phase 0	Phase 1	Phase 2	p_{all}	p_{01}	p_{12}	p_{02}
Pulmonaliskatheter								
mPAP (mmHg)	10	30.3 [16.4, 35.8]	32.8 [20.9, 38.6]	31.7 [19.2, 40]	0.014	0.011	Ns	ns
CVP (mmHg)	11	6 [0, 10]	9 [2, 12]	5 [1, 8]	0.009	ns	0.011	ns
PCWP (mmHg)	9	11 [8, 21]	17 [12, 28.5]	11 [9.5, 22]	0.001	0.003	0.003	ns
Transthorakale Echokardiographie								
LVV (mL)	8	251 [216, 283]	233 [213, 262]	247 [227, 283]	ns	ns	Ns	ns
E Welle(m/s)	17	0.72 [0.61, 0.94]	0.81 [0.66, 1.13]	0.75 [0.54, 1.02]	0.015	0.029	0.012	ns
E/A (~)	16	1.55 [0.75, 2.02]	1.71 [0.8, 2.4]	1.36 [0.74, 2]	0.002	ns	0.003	0.020
E/E′ (~)	17	12.9 [8.4, 16.8]	11.8 [9.3, 18]	13.5 [9.3, 19.3]	0.047	ns	Ns	0.029
VCI (mm)	13	13 [10.5, 17]	14 [10.5, 16]	14 [11.5, 16.5]	ns	ns	Ns	ns

RVEDD1 (mm)	12	38.5 [33, 48.8]	40 [35.8, 53.3]	36 [30, 46.5]	ns	ns	Ns	ns
RVEDD2 (mm)	10	28 [22.8, 32.5]	27 [23.8, 33]	25.5 [18.8, 27.3]	ns	ns	Ns	ns

Tabelle 1: p_{all}: p-Wert über alle Phasen, p_{01}: p-Wert zwischen Phase 0 und Phase 1, p_{12}: p-Wert zwischen Phase 1 und Phase 2, p_{02}: p-Wert zwischen Phase 0 und Phase 2. mPAP: mittlerer Pulmonalisdruck, CVP: zentralvenöser Druck, PCWP: pulmonaler kapillärer Verschlussdruck, VCI: Vena cava inferior, RVEDD1 und RVEDD2: rechtventrikulärer enddiastolischer Diameter 1 und 2, N: Patientenzahl, ns: nicht signifikant Adaptiert von Dual, Pergantis et al[29].

Die QRS-Amplitude über alle Patienten, gemessen anhand der Ableitungen I, II und V6, zeigte keine signifikante Veränderung über die drei Phasen der Studie. Eine tendenzielle reversible Veränderung konnte in der Ableitung V6 und in der Summe der QRS-Amplituden von den Ableitungen I und II beobachtet werden; eine statistische Signifikanz wurde allerdings nicht erreicht. Ein Abfall in der intrakardialen QRS-Amplitude wurde während des PLR beobachtet, allerdings auch ohne statistische Signifikanz. Die *repeated measures correlation* lieferte eine statistisch signifikante negative Korrelation zwischen QRS-Amplitude und mPAP in den Ableitungen V6 mit R= -0,28 (-0,49, -0,04) (p=0,024) und II mit R= -0,29 (-0,50, -0,05) (p=0,016) (Abbildung 1).
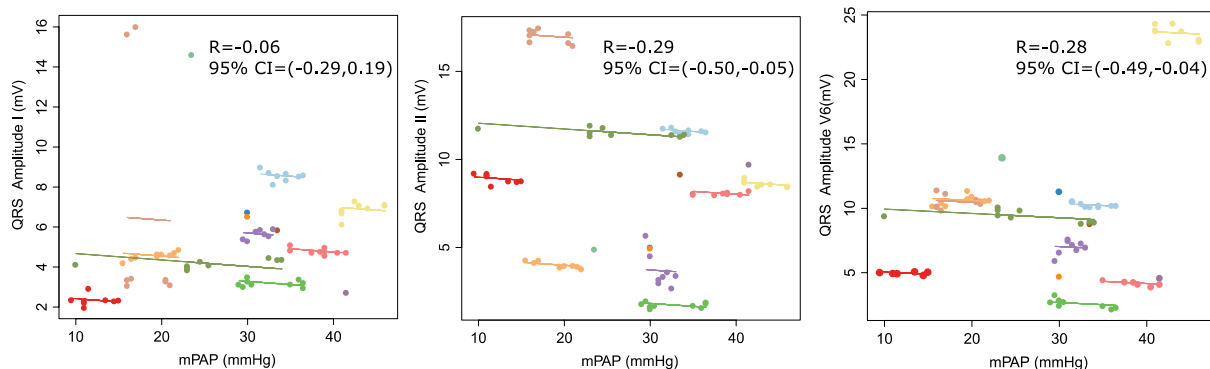

Abbildung 1: *Darstellung der Korrelation zwischen mPAP und QRS-Amplitude in den Patienten mit Pulmonaliskatheter für die drei EKG-Ableitungen I, II, V6. Statistisch signifikante Korrelation wurde in den Ableitungen II und V6 beobachtet. Jede Linie repräsentiert einen Patienten. R ist der Korrelationskoeffizient, 95% CI sind die 95%igen Konfidenzintervalle[29].*

5. Diskussion

Wir untersuchten die Funktion des PRS-Kontrollers mit zwei unterschiedlichen Erkennungsstrategien während der Simulation von zwei akuten pathophysiologischen Ereignissen und verglichen diese mit der Performance des CS-Kontrollers. Durch die Anwendung der physiologischen Regelung konnten Ansaugphänomene vermieden werden. Die Erkennungsstrategie mit dem "fortlaufendem Zeitfenster" ergab eine stärkere Anpassung bzw. Reduktion der Drehzahl und infolgedessen des Pumpenflusses und des aortalen Druckes. Parallel wurde ein umgekehrter Fluss beobachtet, was zu Strömungsunregelmäßigkeiten und gegebenenfalls Blutschädigung führen kann. Dies wurde mit dem *beat-to-beat-*

Erkennungsalgorithmus nicht beobachtet. Aufgrund der erhöhten Sensitivität dieses Algorithmus konnten allerdings während der PVCs unerwünschte Oszillationen in der Drehzahl und dem Pumpenfluss beobachtet werden. Der Kontroller mit dem fortlaufendem Zeitfenster erkannte diese akuten Veränderungen des LVV nicht und löste keine Veränderungen an der Drehzahl aus, weshalb die Variation des CO geringer war.

Im Alltag dieser Patienten kommen solche Ereignisse häufig vor. Der intrathorakale Druck ändert sich mit jedem Atemzug. Übliche Aktivitäten wie das Heben von Lasten oder Stuhlgang führen zu einer intensiven Erhöhung des ITP. Oft lösen solche Ereignisse bei den LVADs einen Alarm über niedrigen Pumpenfluss aus. Abgesehen von den möglichen Komplikationen, die mit *under-* oder *overpumping* verbunden sind, verängstigen diese Alarme die Patienten und erhöhen die Arbeitslast für das behandelnde Team. Die physiologische Regelung bietet die Möglichkeit, diese Ereignisse zu vermeiden und somit die Komplikationsrate möglicherweise zu reduzieren sowie die Lebensqualität der Patienten zu verbessern. Die genaue Art des Inputs als auch das Ausmaß der Reaktion des physiologischen Kontrollers können potentiell zu anderen Komplikationen führen, die mit intensivierten Oszillationen des Pumpenflusses und Strömungsunregelmäßigkeiten verbunden sind. Da es sich um eine Simulationsstudie handelt, können solche Ergebnisse wegweisend für die weitere Entwicklung von Regelungsstrategien sein. Notwendig für die physiologische und biologische Evaluation ist die weitere Untersuchung in Tierversuchen und eventuell am Menschen.

In der zweiten Studie entwickelten und untersuchten wir einen physiologischen Kontroller, der den SP als Input verwendet. Während akuter Veränderungen in der Vor- und Nachlast kam es zu keinen Ansaugphänomenen und die CO-Variationen ähnelten dem physiologischen Kreislauf. Eine weitere Sensitivitätstestung ergab einen Verstärkungswert von 40 rpm/mmHg. Eine Veränderung des SP um 1 mmHg löst somit eine Veränderung der Drehzahl um 40 rpm bei einem Ausgangswert von 4180 rpm aus. Darunter waren die Unterschiede in den CO-Werten zwischen dem SP-Kontroller und dem physiologischen Kreislauf kleiner als 0,55 l/min (quadratisches Mittel) während der Vorlast- und Nachlastveränderungen. Ansaugphänomene wurden nicht beobachtet. Die Simulation von sehr ausgeprägten akuten Veränderungen in der Kontraktilität ergab eine unerwünschte Reaktion des SP-Kontrollers. Unter dem oben genannten Verstärkungswert kam es bei einem akuten Abfall der myokardialen Kontraktilität auf 10% (LVEF<10%) zu Ansaugen. Solche akuten und relevanten Veränderungen der Kontraktilität werden allerdings überwiegend während akuten, schwerwiegenden Komplikationen, wie zum Beispiel Myokardinfarkt, septischem Schock oder Tachykardie, beobachtet. Während solchen

Zuständen wird nicht erwartet, dass die physiologische Regelung eine Lösung anbietet, da die medizinische Notfallversorgung der Patienten notwendig ist.

Der SP-Kontroller braucht für die Erhebung der Druckwerte einen Drucksensor, der möglicherweise in oder auf der Einlasskanüle positioniert werden kann. Die Entwicklung und Integrierung eines solchen Sensors ist einfacher als die eines Volumensensors, da es schon ähnliche biokompatible Sensoren auf dem Markt gibt. Die höheren numerischen Werte des SP im Vergleich zu dem diastolischen Druck erlauben eine genauere und robustere automatische Erkennung der Veränderung dieses Parameters, da diese Werte sich weiter weg vom Bereich des Sensordrifts befinden. Unsere Gruppe evaluierte die Performance[15] des SP-Kontrollers und des volumenbasierten PRS-Kontrollers in einem akuten Tierversuch im Schweinemodell. Unter Veränderungen der Vor- und Nachlast konnten im Gegensatz zu dem CS-Kontroller weniger (PRS-Kontroller) oder keine (SP-Kontroller) Ansaugphänomene beobachtet werden. Der SP-Kontroller stellt eine einfachere und leichter umsetzbare Alternative zum volumenbasierten PRS-Kontroller für die physiologische Regelung dar.

In der klinischen Studie wurde die Korrelation zwischen Vorlast und Amplitude des QRS-Komplexes, gemessen durch ein konventionelles EKG, in Patienten mit fortgeschrittener Herzinsuffizienz untersucht. Die ausgewählte, nicht invasive Methode für die Vorlasterhöhung war das PLR-Manöver. Eine signifikante und meistens reversible Erhöhung der durch den Pulmonaliskatheter gemessenen Druckwerte zeigte eine relevante Veränderung in der kardialen Vorlast. Außerdem wurde eine signifikante Erhöhung im mitralen Einfluss bei allen Patienten beobachtet. Eine Veränderung im LVV konnte allerdings nicht beobachtet werden, wobei hier vermutlich die relativ niedrige Sensitivität der transthorakalen Echokardiographie eine Rolle spielte. Es ist aber zu erwarten, dass nur kleine Veränderungen im LVV bei diesen Patientengruppen erreicht werden können, da das Herz aufgrund der verminderten Kontraktilität und des erhöhten LVEDV im steilen Bereich der Frank-Starling-Kurve funktioniert. In diesem Bereich führen relativ kleine Veränderungen des Volumens zu größeren Veränderungen im Druck. Eine Veränderung in der QRS-Amplitude über alle Patienten wurde nicht beobachtet. Laut dem Brody-Effekt korreliert physikalisch das LVV mit der QRS-Amplitude. Aufgrund der relativ geringen Volumenveränderung bei diesen Patienten war wahrscheinlich in diesem Studiendesign die Veränderung in der QRS-Amplitude zu gering, um eine statistische Signifikanz zu erreichen.

In der Subgruppe der Patienten mit einem Pulmonaliskatheter konnte allerdings eine statistische Signifikanz zwischen den Veränderungen in der QRS-Amplitude und dem mPAP beobachtet werden, was sich mit anderen Quellen in der Literatur deckt. Es wurden keine bedeutenden

Unterschiede zwischen den Subgruppen beobachtet. Diese Korrelation wurde in den Ableitungen V6 und II beobachtet bzw. sowohl in einer prekordialen als auch in einer Extremitätenableitung.

In der Literatur werden unterschiedliche Bias beschrieben, die die Korrelation zwischen der Vorlast und der QRS-Amplitude des oberflächigen EKGs beeinflussen können. Durch dieses Studiendesign wurde versucht, die mögliche Auswirkung dieser Faktoren zu untersuchen oder auszublenden. Die durch die externen Elektroden gemessene thorakale Impedanz blieb während des PLR unverändert. Veränderungen in Hämatokrit oder Kalium waren nicht erwartet, da die Vorlasterhöhung mit einer Autotransfusion bzw. Verschiebung des eigenen Blutes im Körper ausgelöst wurde und somit die Konsistenz des Blutes unverändert blieb. Madias[28] et al. schlagen vor, dass die Veränderungen im EKG eine Folge des mit dem Verlauf der chronischen Insuffizienz veränderten Blutvolumens des Körpers und eines möglichen myokardialen Ödems sein kann. Durch das akute Design unserer Studie kamen diese Faktoren nicht in Frage. Eine Veränderung der Position des Herzens im Thorax kann die QRS-Amplitude im auf der Körperoberfläche gemessenen EKG beeinflussen. Obwohl das PLR so angepasst wurde, dass der Oberkörper der Patienten stabil blieb, könnte eine zu der Thoraxwand relative Bewegung der Herzwand Einfluss auf die QRS-Amplitude gehabt haben. Zusammenfassend könnte die untersuchte Korrelation entweder eine Folge des Brody-Effektes oder der Wandbewegung des Herzens sein.

Das nicht invasive Design der Studie erlaubte keine großen Vorlastveränderungen, genauso wenig wie eine genauere, aber für die Patienten belastende und potentiell gefährliche, Volumetrie, wie zum Beispiel mit einem Druck-Volumen Induktionskatheter oder einer transösophagealen Echokardiographie. Durch Veränderung der Drehzahl des LVADs können akute und reversible Veränderungen des LVV kontrolliert ausgelöst werden. Solche Protokolle gehören zu dem klinischen Alltag der Behandlung dieser Patienten und sind komplikationsarm. Die Untersuchung der Veränderung der QRS-Amplitude während solcher relevanten, nachvollziehbaren und für die Patienten sicheren LVV-Veränderungen würde die genauere Evaluation dieser Korrelation erlauben, wie in der vor kurzem publizierten Studie von Imamura et al[35], in der eine Korrelation zwischen dem CVP und der Impedanz der Schrittmacherelektroden in LVAD-Patienten gezeigt werden konnte.

Für diese Patienten ist die Druckmessung wahrscheinlich eine genauere Methode zur Beurteilung der kardialen Vorlast. Die relativ größeren Veränderungen in den Druckwerten als in den Volumenwerten erlauben eine einfachere automatische Erkennungsstrategie für die Algorithmen der physiologischen Regelung. Außerdem gibt es Drucksensoren, die bereits im klinischen Alltag verwendet werden. Diese Studie liefert neue, klinische Daten von Herzinsuffizienzpatienten in der

seit Jahrzehnten mehrfach evaluierten möglichen Anwendung der einfach aufgenommenen QRS-Amplitude als Überwachungsparameter für die kardiale Vorlast.

5.1 Schlussfolgerungen

- Der volumenbasierte physiologische Kontroller zeigte *in vitro* eine robuste Funktion während der Simulation von VM und PVC.
- Der druckbasierte physiologische Kontroller zeigte *in vitro* eine dem physiologischen Kreislauf ähnliche Funktion und konnte im Vergleich zu dem Standardkontroller mit konstanter Drehzahl Ansaugphänomene während akuter hämodynamischer Veränderungen vermeiden.
- Eine Korrelation zwischen mPAP und QRS-Amplitude bei Patienten mit fortgeschrittener Herzinsuffizienz wurde in der klinischen Studie beobachtet. Allerdings konnten durch das zur Sicherheit der Patienten minimalinvasive Studiendesign keine relevanten Veränderungen des LVV beobachtet werden.

5.2 Ausblick

Die vorlastbasierte physiologische Regelung kann zur Verbesserung der Ergebnisse der LVAD-Therapie beitragen. Der in diesem Projekt entwickelte druckbasierte physiologische Kontroller kann aufgrund des Vorhandenseins von Drucksensoren leichter in der Praxis angewendet werden. Die weitere Evaluation der Funktion des SP-Kontrollers sowie die klinische Relevanz dieser Art von physiologischer Regelung sollte in chronischen Tierversuchen evaluiert werden. Im Rahmen der Entwicklung eines Volumensensors mit Anwendung der Korrelation zwischen LVV und QRS-Amplitude sollte diese Korrelation in einem Studiendesign getestet werden, das relevante, kontrollierte Volumenveränderungen erlaubt, wie im Fall der kontrollierten Drehzahlveränderung in LVAD-Patienten.

6. Literaturverzeichnis

1.   (Poland) PP (Chairperson), Adriaan A. Voors* (Co-Chairperson) (The Netherlands), Stefan D. Anker (Germany) Héctor Bueno (Spain), John G. F. Cleland (UK), Andrew J. S. Coats (UK) Volkmar Falk (Germany), Jose Ramon Gonzalez-Juanatey (Spain), Veli-Pekka Harjola (Finland), Ewa A. Janko BP (Germany), Jillian P. Riley (UK), Giuseppe M. C. Rosano (UK/Italy) LMR (Spain), Frank Ruschitzka (Switzerland) FHR (The N, Netherlands) P van der M (The. 2016 ESC Guidelines for the diagnosis and treatment of acute and chronic heart failure The Task Force for the diagnosis and treatment of acute and chronic heart failure of the European Society of Cardiology (ESC) Developed with the special contribution of. Eur Heart J. 2016;891–975.

2.   Meinertz T. Deutscher Herzbericht 2018 - Sektorenübergreifende Versorgungsanalyse zur Kardiologie, Herzchirurgie und Kinderherzmedizin in Deutschland. Dtsch Herzstiftung. 2018;

3.   Kormos RL, Cowger J, Pagani FD, Teuteberg JJ, Goldstein DJ, Jacobs JP, Higgins RS, Stevenson LW, Stehlik J, Atluri P, Grady KL, Kirklin JK. The Society of Thoracic Surgeons Intermacs Database Annual Report: Evolving Indications, Outcomes, and Scientific Partnerships. Ann Thorac Surg. 2019;107(2):341–53.

4.   Salamonsen RF, Mason DG, Ayre PJ. Response of Rotary Blood Pumps to Changes in Preload and Afterload at a Fixed Speed Setting Are Unphysiological When Compared With the Natural Heart. Artif Organs. 2011;

5.   Klabunde RE. Cardiovascular Physiology Concepts Second Edition. Lippincott Williams & Wilkins. 2012.

6.   Sequeira V, van der Velden J. Historical perspective on heart function: the Frank–Starling Law. Biophys Rev. 2015;7(4):421–47.

7.   Potapov E V, Antonides C, Crespo-Leiro MG, Combes A, Färber G, Hannan MM, Kukucka M, de Jonge N, Loforte A, Lund LH, Mohacsi P, Morshuis M, Netuka I, Özbaran M, Pappalardo F, Scandroglio AM, Schweiger M, Tsui S, Zimpfer D, Gustafsson F. 2019 EACTS Expert Consensus on long-term mechanical circulatory support. Eur J Cardio-Thoracic Surg. 2019;56(2):230–70.

8.   Reesink K, Dekker A, Nagel T Van Der, Beghi C, Leonardi F, Botti P, Cicco G De, Lorusso R, Veen F Van Der, Maessen J. Suction Due to Left Ventricular Assist : Implications for Device Control and Management. 2007;31(7):542–9.

9.   Cowger JA, Romano MA, Shah P, Shah N, Mehta V, Haft JW, Aaronson KD, Pagani FD. Hemolysis: A harbinger of adverse outcome after left ventricular assist device implant. J Hear Lung Transplant [Internet]. 2014 Jan 1;33(1):35–43. Available from: http://linkinghub.elsevier.com/retrieve/pii/S1053249813015283

10.   Alomari AHH, Savkin A V, Stevens M, Mason DG, Timms DL, Salamonsen RF, Lovell NH. Developments in control systems for rotary left ventricular assist devices for heart failure patients: A review. Vol. 34, Physiological Measurement. 2013.

11.   Imamura T, Nguyen A, Kim G, Raikhelkar J, Sarswat N, Kalantari S, Smith B, Juricek C, Rodgers D, Ota T, Song T, Jeevanandam V, Sayer G, Uriel N. Optimal haemodynamics during left ventricular assist device support are associated with reduced haemocompatibility-related adverse events. Eur J Heart Fail. 2019;21(5):655–62.

12.   Imamura T, Chung B, Nguyen A, Sayer G, Uriel N. Clinical implications of hemodynamic assessment during left ventricular assist device therapy. Vol. 71, Journal of Cardiology. 2018. p. 352–8.

13.   Ochsner G, Amacher R, Wilhelm MJ, Vandenberghe S, Tevaearai H, Plass A, Amstutz A, Falk V, Schmid Daners M. A Physiological Controller for Turbodynamic Ventricular Assist Devices Based on a Measurement of the Left Ventricular Volume. Artif Organs [Internet]. 2014;38(7):527–38. Available from: http://www.ncbi.nlm.nih.gov/pubmed/24256168

14.   Petrou A, Lee J, Dual S, Ochsner G, Meboldt M, Schmid Daners M. Standardized Comparison of Selected Physiological Controllers for Rotary Blood Pumps: In Vitro Study. Artif Organs. 2018;42(3):E29–42.

15.   Ochsner G, Wilhelm MJ, Amacher R, Petrou A, Cesarovic N, Staufert S, Röhrnbauer B, Maisano F, Hierold C, Meboldt M, Daners MS. In Vivo Evaluation of Physiologic Control Algorithms for Left Ventricular Assist Devices Based on Left Ventricular Volume or Pressure. ASAIO J. 2017;63(5):568–77.

16.   Petrou A, Pergantis P, Ochsner G, Amacher R, Krabatsch T, Falk V, Meboldt M, Daners MS. Response of a physiological controller for ventricular assist devices during acute patho-physiological events: An in vitro study. Biomed Tech [Internet]. 2017 Feb 9;62(6):623–33. Available from: http://www.degruyter.com/view/j/bmte.ahead-of-print/bmt-2016-0155/bmt-2016-0155.xml

17.   Tchantchaleishvili V, Luc JGY, Cohan CM, Phan K, Hübbert L, Day SW, Massey HT. Clinical implications of physiologic flow adjustment in continuous-flow left ventricular assist devices. ASAIO J. 2017;63(3):241–50.

18.   Petrou A, Ochsner G, Amacher R, Pergantis P, Rebholz M, Meboldt M, Schmid Daners M. A Physiological Controller for Turbodynamic Ventricular Assist Devices Based on Left Ventricular Systolic Pressure. Artif Organs. 2016;40(9).

19.   Abraham WT, Adamson PB, Bourge RC, Aaron MF, Costanzo MR, Stevenson LW, Strickland W, Neelagaru S, Raval N, Krueger S, Weiner S, Shavelle D, Jeffries B, Yadav JS. Wireless pulmonary artery haemodynamic monitoring in chronic heart failure: A randomised controlled trial. Lancet. 2011;377(9766):658–66.

20.   Porterfield JE, Larson ER, Jenkins JT, Escobedo D, Valvano JW, Pearce JA, Feldman MD. Left ventricular epicardial admittance measurement for detection of acute LV dilation. J Appl Physiol. 2011;110(3):799–806.

21.   BRODY DA. A theoretical analysis of intracavitary blood mass influence on the heart-lead relationship. Circ Res. 1956;4(6):731–8.

22.   Ishikawa K, Nagasawa T, Shimada H. Influence of hemodialysis on electrocardiographic wave forms. Am Heart J. 1979 Jan;97(1):5–11.

23.   Ishikawa K, Shirato C, Yanagisawa A. Electrocardiographic changes due to sauna bathing. Influence of acute reduction in circulating blood volume on body surface potentials with special reference to the Brody effect. Br Heart J. 1983;50(5):469–75.

24.   Feldman T, Borow KM, Neumann A, Lang RM, Childers RW. Relation of electrocardiographic R-wave amplitude to changes in left ventricular chamber size and position in normal subjects. Am J Cardiol. 1985;55(9):1168–74.

25.   Vitolo BYE, Ph MDD, Madoi S, Palvarini M, Sponzilli C, Maria RDE, Cir E, Colombo AE, Vallino F, D M, Sarugoia M, D M. Relationship Between Changes in R Wave Voltage and Cardiac Volumes . A Vectorcardiographic Study During Hemodialysis. J Electrocardiol. 1987;20(2):138–46.

26.   Vancheri F, Barberi O. Relationship of qrs amplitude to left ventricular dimensions after acute blood volume reduction in normal subjects. Eur Heart J. 1989;10(4):341–5.

27.   Caiani EG, Auricchio A, Potse M, Krause R, Pellegrini A, Lang RM, Vaïda P, Elettronica D, Bioingegneria I, Milano P, Ticino FC, Italiana S, Segalen UB. Evaluation of the Relation between Changes in R-wave Amplitude and LV Mass and Dimensions in a Model of " Reversed Hypertrophy ." Comput Cardiol (2010). 2013;40:867–70.

28.   Madias JE. The resting electrocardiogram in the management of patients with congestive heart failure: Established applications and new insights. Vol. 30, PACE - Pacing and Clinical Electrophysiology. 2007. p. 123–8.

29.   Dual SA, Pergantis P, Schoenrath F, Keznickl-pulst J, Falk V, Meboldt M, Daners MS. Acute changes in preload and the QRS amplitude in advanced heart failure patients. Biomed Phys Eng Express [Internet]. 2019;5(4):45015. Available from: http://dx.doi.org/10.1088/2057-1976/ab23e8

30.   Colacino FM, Moscato F, Piedimonte F, Arabia M, Danieli GA. Left ventricle load impedance control by apical VAD can help heart recovery and patient perfusion: A numerical study. ASAIO J. 2007;53(3):263–77.

31.   Ochsner G, Amacher R, Daners MS. Emulation of ventricular suction in a hybrid mock circulation. In: 2013 European Control Conference, ECC 2013. 2013. p. 3108–12.

32.   Ochsner G, Amacher R, Amstutz A, Plass A, Schmid Daners M, Tevaearai H, Vandenberghe S, Wilhelm MJ, Guzzella L. A Novel Interface for Hybrid Mock Circulations to Evaluate Ventricular Assist Devices. IEEE Trans Biomed Eng [Internet]. 2013;60(2):507–16. Available from: http://ieeexplore.ieee.org/lpdocs/epic03/wrapper.htm?arnumber=6362188

33.   Harris PA, Taylor R, Minor BL, Elliott V, Fernandez M, O'Neal L, McLeod L, Delacqua G, Delacqua F, Kirby J, Duda SN. The REDCap consortium: Building an international community of software platform partners. Vol. 95, Journal of Biomedical Informatics. 2019.

34.   Bakdash JZ, Marusich LR. Repeated Measures Correlation. Front Psychol [Internet]. 2017 Apr 7 [cited 2018 Oct 9];8:456. Available from: http://journal.frontiersin.org/article/10.3389/fpsyg.2017.00456/full

35.   Imamura T, Moss JD, Flatley E, Rodgers D, Kim G, Raikhelkar J, Sarswat N, Kalantari S, Nguyen A, Juricek C, Burkhoff D, Song T, Ota T, Jeevanandam V, Sayer G, Uriel N. Estimation of Central Venous Pressure by Pacemaker Lead Impedances in Left Ventricular Assist Device Patients. ASAIO J. 2019;

Anteilserklärung

Panagiotis Pergantis hatte folgenden Anteil an den folgenden Publikationen:

Publikation 1: Petrou A*, **Pergantis P***, Ochsner G, Amacher R, Krabatsch T, Falk V, Meboldt M, Schmid Daners M. Response of a physiological controller for ventricular assist devices during acute pathophysiological events: An in vitro study. Biomed Tech. 2017. ***Geteilte Erstautorenschaft,** Impact Factor 2017: 1,096

Beitrag im Einzelnen: Konzeption der Studie, Literaturrecherche (insbesondere Recherche nach Daten von klinischen Studien mit Valsalva-Manöver zur „Kalibrierung" des Simulationsmodells), Datenauswertung, Schreiben von Anteilen des ersten Publikationsentwurfs (klinische Relevanz, Pathophysiologie der akuten Ereignisse), Überarbeitung von Textpassagen, anteilige Bearbeitung der Reviews.

Publikation 2: Petrou A, Ochsner G, Amacher R, **Pergantis P**, Rebholz M, Meboldt P, Schmid Daners M. A Physiological Controller for Turbodynamic Ventricular Assist Devices Based on Left Ventricular Systolic Pressure. Artif Organs. 2016, Impact Factor 2016: 2,403

Beitrag im Einzelnen: Datenanalyse und Datenauswertung, Überarbeitung von Textpassagen, anteilige Bearbeitung der Reviews.

Publikation 3: Dual SA*, **Pergantis P***, Schoenrath F, Keznickl-Pulst J, Falk V, Mebold M, Schmid Daners M. Acute changes in preload and the QRS amplitude in advanced heart failure patients. Biomed Phys Eng Express 2019. ***Geteilte Erstautorenschaft,** noch kein Impact Factor zugeteilt, da seit 2015 aktiv. Verlag: IoP Publishing

Beitrag im Einzelnen: Konzeption der Studie, Schreiben des Ethikantrages und Verteidigung vor der Ethikkommission, Literaturrecherche, Rekrutierung der Patienten und Datenerhebung (Studienarzt), Datenauswertung (klinisch erhobene Daten wie echokardiographische Daten, Daten vom Pulmonaliskatheter), Datenanalyse, anteilige statistische Analyse (deskriptive Statistik), Mitschreiben des ersten Publikationsentwurfs mit der ersten Koautorin, Überarbeitung der Textpassagen, Bearbeitung der Reviews.

_____

Unterschrift des Doktoranden

Anastasios Petrou[a], Panagiotis Pergantis[a], Gregor Ochsner, Raffael Amacher,
Thomas Krabatsch, Volkmar Falk, Mirko Meboldt and Marianne Schmid Daners*

Response of a physiological controller for ventricular assist devices during acute patho-physiological events: an *in vitro* study

Abstract: The current paper analyzes the performance of a physiological controller for turbodynamic ventricular assist devices (tVADs) during acute patho-physiological events. The numerical model of the human blood circulation implemented on our hybrid mock circulation was extended in order to simulate the Valsalva maneuver (VM) and premature ventricular contractions (PVCs). The performance of an end-diastolic volume (EDV)-based physiological controller for VADs, named preload responsive speed (PRS) controller was evaluated under VM and PVCs. A slow and a fast response of the PRS controller were implemented by using a 3 s moving window, and a beat-to-beat method, respectively, to extract the EDV index. The hemodynamics of a pathological circulation, assisted by a tVAD controlled by the PRS controller were analyzed and compared with a constant speed support case. The results show that the PRS controller prevented suction during the VM with both methods, while with constant speed, this was not the case. On the other hand, the pump flow reduction with the PRS controller led to low aortic pressure, while it remained physiological with the constant speed control. Pump backflow was increased when the moving window was used but it avoided sudden undesirable speed changes, which occurred during PVCs with the beat-to-beat method. In a possible clinical implementation of any physiological controller, the desired performance during frequent clinical acute scenarios should be considered.

Keywords: physiological control; premature ventricular contraction (PVC); suction; Valsalva maneuver (VM); ventricular assist device (VAD); volume measurement.

Introduction

Implantable ventricular assist devices (VADs) have become a viable solution for the ever growing population of heart failure patients. The continually improving clinical outcome of the VAD-therapy [28] play an important role on this result. According to data presented in [12], which was derived from more than 15,000 patients, the 1 year and 2 year survival rates with turbodynamic VADs (tVADs) currently reach 80% and 70%, respectively, while the quality of life remains improved after 2 years compared to pre-implantation. More than 90% of the VAD patients receive a tVAD. Although a reduction of adverse events has been reported during the last few years, complications of this therapy such as hemolysis, cardiac arrhythmias, pump thrombosis, gastrointestinal bleeding, right ventricular (RV) failure and left ventricular (LV) overloading, still pose a problem. Despite the increased durability of newer generation of pumps, a stable incidence of device malfunction and exchange due to all causes is evident [12, 34].

Several research groups [1, 3, 6, 15, 21, 22, 26, 33] have proposed physiological control as a solution to reduce or even eliminate overpumping and underpumping events, which are presumably related to adverse events, such as hemolysis, pump thrombosis and RV failure. These control strategies are based on various signals, such as the LV pressure (LVP), the LV volume (LVV), the aortic pressure

[a]These authors contributed equally to the study.

*Corresponding author: Marianne Schmid Daners, pd|z Product Development Group Zurich, Department of Mechanical and Process Engineering, ETH Zurich, CLA G21.1 Tannenstr. 3, 8092 Zurich, Switzerland, Phone: + 41 44 632 2447, E-mail: marischm@ethz.ch
Anastasios Petrou and Mirko Meboldt: pd|z Product Development Group Zurich, Department of Mechanical and Process Engineering, ETH Zurich, 8092 Zurich, Switzerland
Panagiotis Pergantis, Thomas Krabatsch and Volkmar Falk: German Heart Institute Berlin, Department of Cardiothoracic and Vascular Surgery, Augustenburger Platz 1, 13353 Berlin, Germany
Gregor Ochsner: pd|z Product Development Group Zurich, Department of Mechanical and Process Engineering, ETH Zurich, 8092 Zurich, Switzerland; and Institute for Dynamic Systems and Control, Department of Mechanical and Process Engineering, ETH Zurich, 8092 Zurich, Switzerland
Raffael Amacher: Wyss Translational Center Zurich, ETH Zurich, 8092 Zurich, Switzerland

(AoP), or the pump flow. Their goal is to adjust the speed and ultimately the blood flow of a tVAD such that the resulting cardiac output (CO) meets the perfusion requirements of the circulation. By matching the pump flow to the hemodynamic status of the patient, adverse events related to overpumping and underpumping can be prevented and the physiological adaptation of the CO is restored.

All physiological controllers extract one or more indices from either a measured or an estimated signal of the heart-tVAD system. These indices are fed into a control system which adjusts the desired speed of the tVAD. In [21, 22] the authors implemented a beat-to-beat extraction algorithm for their control indices, namely the end-diastolic pressure (EDP) and mean pump flow, respectively. In [3, 6, 26, 33] the authors proposed signal processing algorithms, which extract the indices of the end-diastolic volume (EDV), the pump pressure difference, the pump speed pulse, or the EDP over a time window with a pre-defined fixed length. Particularly, in [26] and [6] a moving window with a length of 3 s of the measured signals was implemented in order to extract their respective control inputs, whereas Wang et al. [33] proposed a moving 1 s time window. The suction detection algorithm developed in [3] uses a moving maximum search algorithm for the identification of the diastolic level of the pulsation of the pump differential pressure. Additionally, authors in [9] used low-pass filtering methods, such as the non-linear morphological filter, in order to feed their controller with the required mean pump flow.

The controller presented in [26] was evaluated by *in vitro* experiments, which represent wide-range variations of cardiovascular parameters and simulate resting or exercising conditions. Similar experiments for testing physiological controllers either *in silico* or *in vitro* are presented in [3, 15, 21, 23]. In contrast, authors in [18] investigated the response of several physiological controllers during more sudden changes in hemodynamic parameters. These changes were related to exercise (CO increase) and head-up tilt (CO decrease), simulated through a detailed numerical model [16]. Additional cases that lead to such sudden changes are related to patho-physiological events such as respiration (deep expiration or inspiration), strain (Valsalva or Mueller maneuver, coughing or heavy lifting) or arrhythmia.

Approaches to simulate such patho-physiological events either numerically or by manipulating mechanical components have been proposed. In [17], the authors presented a numerical model of a human circulation that incorporates the influence of the intra-thoracic pressure (ITP) and can therefore potentially simulate respiration and the Valsalva maneuver (VM). However, the simulation of these events and their use for evaluating physiological

controllers was not in the scope of their study. A study focused on VM simulation has been presented in [14], however without investigating a VAD-assisted circulation. In [32], the authors simulated VM in their mock circulation loop (MCL), which is built for evaluating bi-ventricular assist devices (BiVADs). They were able to reproduce VM by manipulating the mechanical valves of their MCL, which represented the systemic and pulmonary vascular resistances, in order to apply a resistance increase, thereby emulating the influence of an increase of the ITP. These simulations were later used to evaluate physiological controllers for BiVAD support cases [30]. Amacher et al. [2] simulated premature ventricular contractions (PVCs) in order to evaluate arrhythmia detection algorithms, when a pulsatile speed mode of a tVAD, synchronized to the heart cycle, was implemented.

The current paper describes how our numerical model of the human blood circulation [24] was extended to simulate specific patho-physiological events, namely PVCs and VM, by manipulating the heart rate (HR) and the ITP. For both extensions, we focused on the hemodynamics in the LV of a pathological circulation assisted by a tVAD, which was either controlled by one of several configurations of the preload responsive speed (PRS) controller [26] or set at a constant speed. The core algorithm of the PRS controller remained unchanged, but the EDV extraction algorithm was modified to influence the aggressiveness of the controller. The pros and cons of fast and slow response during PVCs and VM were analyzed and compared to the clinical case of the constant speed control. The potential of the proposed extended human blood circulation model for testing new control algorithms is indicated and possible complications of standalone physiological controllers discussed. The need for additional algorithmic features that will support the core of the physiological controller is highlighted to guarantee preventing undesired overpumping and underpumping events.

Materials and methods

Hybrid mock circulation

We conducted experiments on a hybrid mock circulation (HMC) based on the hardware-in-the-loop concept, which has been developed in our group [24]. Figure 1 shows a picture of the hardware part of the HMC, while its caption defines the parts and their manufacturer. In our experiments, a non-implantable mixed-flow turbodynamic blood pump that allows implementing various control approaches substituted the tVAD (c). The pump is connected to two pressure-controlled reservoirs (a), (b) and a back flow pump (d) ensures that the fluid level in the two reservoirs remains constant during the experiments.
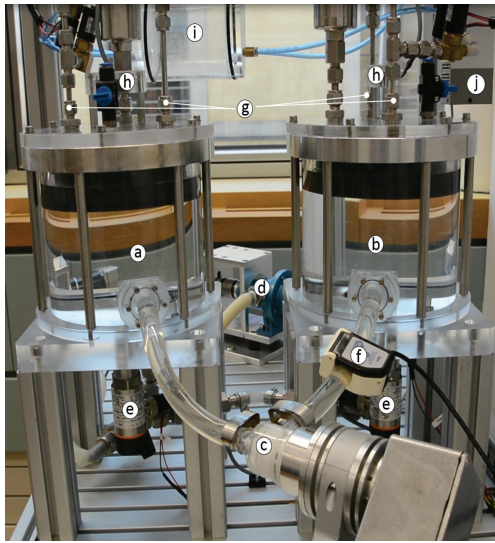
Figure 1: Picture of the hardware part of our hybrid mock circulation consisting of two pressure-controlled reservoirs (a) and (b), a blood pump head (Deltastream DP2, Xenios AG, Heilbronn, Germany) (c) equipped with an encoder (ME22, PWB Encoders GmbH, Eisenach, Germany) and an industrial motor controller (Accelus, ASP-090-09, Copley Controls Corp., Canton, MA, USA), a backflow pump (Moyno 500 Pumps-200 Series, Moyno, Inc., Springfield, OH, USA) (d), two fluid-pressure sensors (PN2009, IFM Electronic GmbH, Essen, Germany) (e), one ultrasonic flow probe (TS410/ME-11PXL, Transonic Systems, Inc., Ithaca, NY, USA) (f), one proportional solenoid inlet valve (PVQ33-5G-23-01F, SMC Pneumatics, Tokyo, Japan) and two proportional solenoid outlet valves (PVQ33-5G-40-01F, SMC Pneumatics, Tokyo, Japan) per reservoir (g), two fluid-level sensors (GP 2Y0D810Z0F, Sharp, Osaka, Japan) (h), a vacuum receiver (i) and a vacuum pump (ZL112-K15LOUT-E26L-Q, SMC Pneumatics, Tokyo, Japan) (j).

The fluid level is measured by infrared range finders (h) and fed to the back flow pump-controller. The pressure in each reservoir is controlled using one proportional solenoid inlet valve and two proportional solenoid outlet valves (g) per reservoir, a vacuum receiver (i) and a vacuum pump (j), and one fluid-pressure (e) sensor per reservoir.

The reference signals for the pressure controllers of the two reservoirs are computed in real-time by a validated numerical model of the human blood circulation [7], based on the measured pump flow (f). This numerical model consists of lumped-parameter elements. Thus, the veins of the upper and lower limb circulation, the inferior vena cava, etc. are implemented with one classic Windkessel model, which does not allow an implementation of the ITP on the vessels and organs of the thorax separately. Therefore, the numerical model was extended for the current investigation as described below.

Hemodynamic influence of intrathoracic pressure variations and arrhythmia

In order to define the required modifications of the existing numerical model, the hemodynamic influence of ITP variations and PVCs

had to be identified. For this purpose, the response of both a physiological and a pathological circulation during these events was analyzed based on clinical studies and is presented below.

The VM causes an increase in the ITP without hyperinflation of the lungs. In the physiological circulation, increased ITP causes a decrease in the RV preload and RV filling, leading to a decrease in LV preload and CO. In the pathological circulation, the decrease of CO is significantly smaller or even inverted compared to the healthy heart. That happens due to the blood pooling in the pulmonary vascular system which can compensate the decrease in the LV preload, thus preserving the LV EDV. The preserved LV EDV, in combination with the decrease in the LV afterload in the failing heart, is responsible for the altered influence of VM on CO and AoP in heart failure [20, 27, 29]. Similar ITP changes are observed during coughing, strain, bowel movement, heavy lifting etc. [20].

Arrhythmias cause abrupt changes in the CO. Bradycardia causes a decrease in the CO and an overload of the cardiopulmonary system. Tachycardia, both ventricular and supraventricular, impairs the diastolic filling of the ventricles, leading to a decrease of the CO. Extrasystoles cause a decrease in both LV and RV EDV by generating PVCs and disrupting the diastolic phase. Arrhythmias in the setting of left VAD therapy can lead to suction events because of a decrease in LV preload, for instance during bradycardia or tachycardia, leading to a reduction of the RV SV or directly in LV EDV during extrasystoles [27].

Extension of the numerical model

The numerical model has already been extended in order to emulate suction [25]. For the current study, we further extended it in order to account for the influences of ITP variations, based on the analysis presented above. Figure 2 shows the structure of the extended model. The systemic venous and arterial systems are now divided into an intrathoracic and an extrathoracic part. The resistance of the intrathoracic and extrathoracic veins, namely $R_{sv,it}$ and $R_{sv,et}$, respectively, are used to simulate the collapse of the large vessels when the transmural pressure is negative. Furthermore, we added a venous valve in order to prevent regurgitation of the venous return [11]. The ITP is implemented by adding its value to all pressure values inside the thoracic cavity. Table 1 lists the values of all new parameters introduced into the extended model as well as their source. The remaining parameters used in the model were the same as presented in [7].

Simulation of the Valsalva maneuver

Figure 3A and C show the input signals to simulate the VM. The ITP was increased manually by 30 mm Hg at t ∈ (5, 15) s, and the HR varied according to clinical data presented in [14]. The amplitude of the ITP for the VM was defined such that the resulting AoP waveform matched those presented in clinical studies [11, 14, 29, 31].

Simulation of arrhythmia

Figure 3B and D show the input signals to simulate arrhythmia. We introduced several PVCs, as they were defined in [2]. For that, we altered the cardiac cycle of the time-varying elastance model of the simulated ventricles and atria. Soon after the end of the systole,
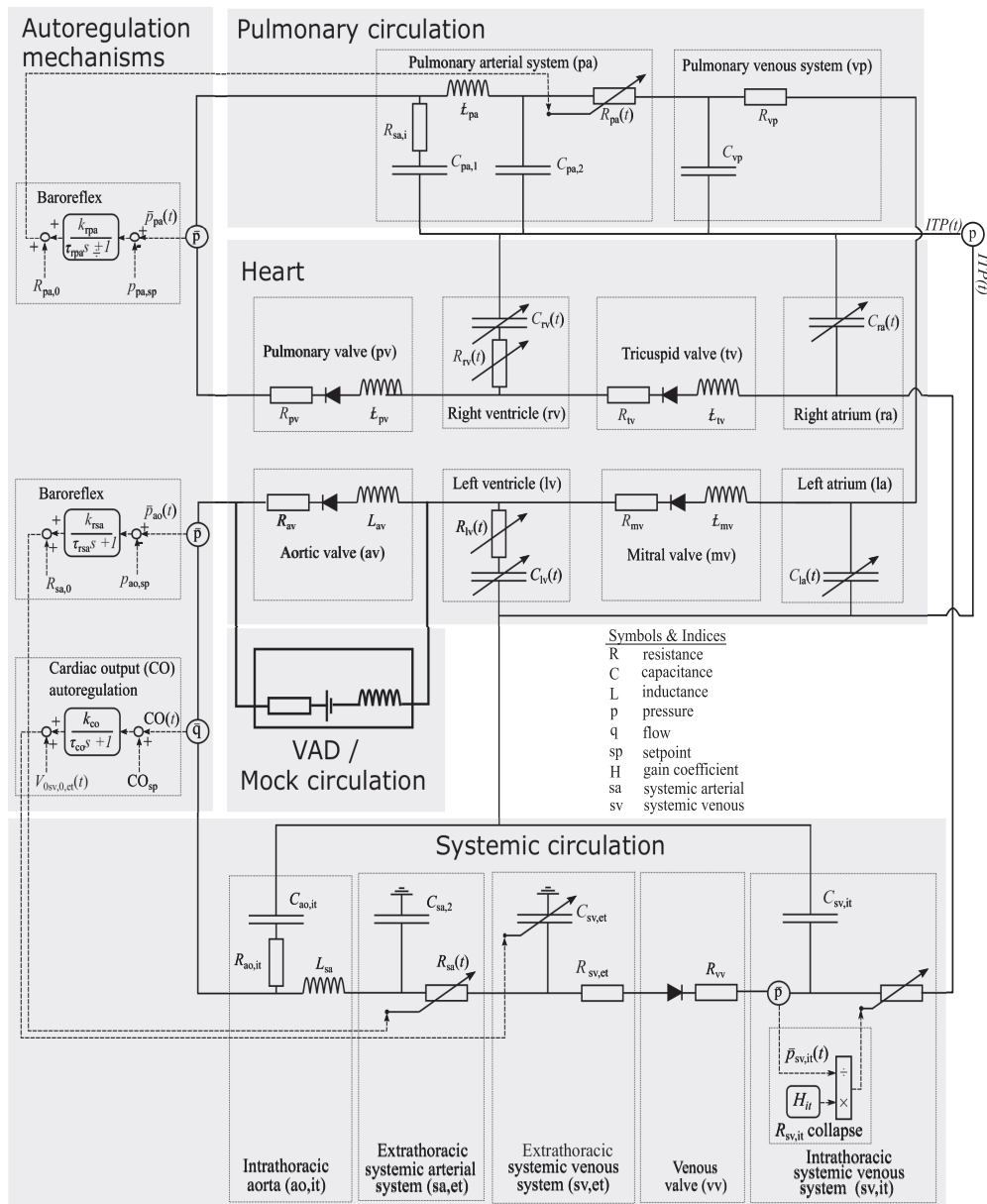
Figure 2: Electrical analog of the extended numerical model of the human blood circulation to include the influence of the intrathoracic pressure (ITP) on the organs of the thoracic cavity.
The systemic arterial and venous systems each consist of an intrathoracic and an extrathoracic part.

another ventricular contraction is triggered, while the subsequent diastolic phase is prolonged.
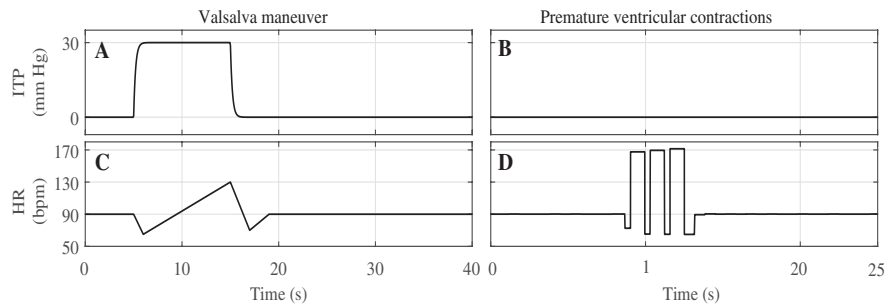
Experiments

For the physiological circulation, the HR was fixed at 70 bpm and increased up to 90 bpm during the VM event. The pathological circulation was simulated by decreasing the contractility of the LV to 34% of physiological contractility and increasing the HR to 90 bpm. For each experiment we ran the HMC until steady state was reached and then started either the VM or the PVCs experiment as depicted in Figure 3. The numerical model was executed with Matlab/Simulink running Real-Time Windows Target (The Mathworks Inc., Natick, MA, USA) and all signals were recorded at 1 kHz. A glycerol water mixture with viscosity of 2.8 mPa·s was used for all the experiments.

Table 1: Numbers and references used for the extended numerical model of the human blood circulation.

Parameter	Description	Value	Units	References
$V_{0sv,0,et}(t)$	Extrathoracic unstressed venous volume	3088	ml	[5, 24]
$V_{0sv,0,it}$	Intrathoracic unstressed venous volume	162	ml	[5, 24]
$C_{sv,et}$	Extrathoracic venous system compliance	55	ml/mm Hg	[14]
$C_{sv,it}$	Intrathoracic venous system compliance	10	ml/mm Hg	[14]
H_{it}	Intrathoracic vena cava collapse gain coefficient	0.547	mm Hg^2·s/ml	[7]

The extrathoracic unstressed venous volume is a variable input, all other parameters are constant.

Figure 3: Defined values for the parameters that were varied during the experiments.
Panels (A) and (C) show the variation of the intrathoracic pressure (ITP) and the heart rate (HR) during the Valsalva maneuver (VM). Panels (B) and (D) show the ITP and the HR during the implementation of premature ventricular contractions.
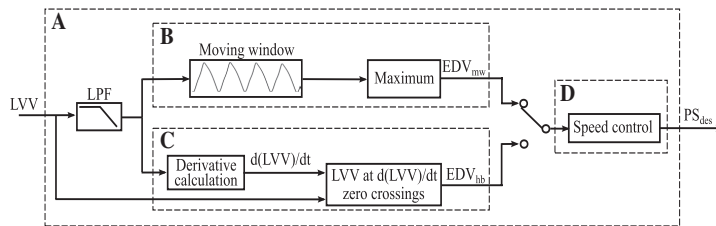
Figure 4: Structure of the PRS controller configurations of the tVAD (A).
The left ventricular volume (LVV) is processed and the end-diastolic volume is extracted either from the maximum of a moving window (EDVmw) (B) or at every heartbeat (EDVhb) (C). The extracted EDV is fed to the preload responsive speed (PRS) controller algorithm, which computes the desired pump speed (PSdes). The detailed structure of (D) is presented in [26].

Pump control configurations

Three different control configurations (C1–C3) of a tVAD were tested, as described below. The input to the PRS controller was the simulated LVV signal; the output was the desired pump speed (Figure 4A).

1) Constant speed (C1)

   For the C1 configuration, the PRS controller was disabled and the tVAD was operated at a constant speed. The speed was set to 4100 rpm, which yielded a CO of 5 l/min at rest.

2) Nominal PRS controller (C2)

   For the C2 configuration, we used the PRS controller as presented in [26], i.e. with a sliding window (Figure 4B) of 3 s to extract the EDV value. The lower limit for the pump speed was set to 1800 rpm.

3) Modified PRS controller with beat-to-beat EDV detection algorithm (C3)

   For the C3 configuration, we modified the signal-processing algorithm of the nominal PRS controller in order to extract the EDV value at every heartbeat. Figure 4C depicts the structure of the beat-to-beat EDV extraction algorithm. First, the simulated LVV signal is low-pass filtered with a second-order IIR filter with a cut-off frequency of 2.5 Hz. Second, the derivative of the signal is computed. When the derivative of the LVV signal changes sign the LVV signal is at a maximum, which corresponds to the EDV. Due to the continuous flow of a tVAD, no isovolumetric contraction occurs and the LVV signal has one distinct maximum. Therefore, the zero detection of the LVV derivative works reliably *in vitro*. The PRS controller structure (Figure 4D) remained unchanged, as presented in [26].

Results

Figure 5 shows the CO and the AoP of a physiological circulation during the VM [panels (A) and (C)] and four PVCs [panels (B) and (D)]. The four phases of VM and the four PVCs are separated by dashed lines. After the onset of VM (phase 1) and a sudden AoP increase due to the increase of the ITP, the AoP decreased and made a trough during phase 2, while the CO decreased from 5 l/min to 2.5 l/min. In phase 3, at the end of VM, the AoP dropped suddenly together with the ITP. AoP recovered and increased up to 160 mm Hg. After a final oscillation, the AoP returned to its initial value. Accordingly, the CO increased up to approx. 7 l/min in phase 4 and then returned to 5 l/min.

During the PVCs, sudden CO drops can be observed, while the mean AoP decreased from 105 mm Hg to 90 mm Hg. After the last PVC both the CO and the AoP increased slightly above their initial values (end of phase 4) before they returned to their initial values (t > 20 s).

Figure 6 shows the effect of VM (left-hand side) and PVCs (right-hand side) on a pathological circulation assisted with a tVAD operated at a constant speed (C1). The figure shows the pump speed (PS) and flow (PF), the CO, the transmural pump inlet pressure (PIP) and the AoP. The PIP signal shows that suction (negative pressure) occurred during the VM. At the same time, the CO decreased and the AoP pulsatility was diminished. All signals recovered to the steady-state value after the end of the VM. During PVCs, all signals except the pump speed showed strong oscillations, but quickly returned to their steady-state values after the last PVC.

Figure 7 shows the effect of the VM and PVCs on a pathological circulation assisted with a tVAD controlled by the nominal PRS controller (C2). During the VM, due to the reduced LVV, the controller reduced the pump speed down

to its minimum value of 1800 rpm at t = 12 s. The pump flow decreased as well as back flow occurred, while the CO decreased down to 1.5 l/min. The PIP signal shows that no suction occurred, while the mean AoP dropped down to approx. 60 mm Hg. During PVCs, the PS slowly adapted to the decreased LVV resulting from the arrhythmic beats. After the end of PVCs, the increased LV feeling led to a PS increase until it returned to a steady state. The mean PF, CO and AoP fluctuated according to the PS variations.

Figure 8 shows the effect of the VM and PVCs on a pathological circulation assisted with a tVAD controlled by the modified PRS controller (C3). In this case, the PS adaptation during the VM led to a minimum value of approx. 2500 rpm at t = 12 s. The PF decreased as well, but now back flow occurred. The minimum CO observed is 2.5 l/min. The maximum PIP dropped down to approx. 60 mm Hg and the mean AoP down to 80 mm Hg. A further AoP drop down to 60 mm Hg occurred after the end of VM. The PS adapted to the PVCs by decreasing the speed, whereas it increased during the normal contractions (8 s < t < 12.5 s). Pump flow, CO and AoP varied similarly to PS.

Figure 9 shows the performance of the EDV detection methods for the configurations C2 and C3 during the experiments. An LVV decrease occurred during the VM [Figure 9 – panels (A) and (C)]. Clearly, the EDV detection algorithm of C2 shows a delayed detection during the LVV decrease compared to C3, which detected the EDV accurately at every beat. Panels (B) and (D) in Figure 9 show the irregular LVV waveform during the PVCs. The C3 configuration detected not only the EDV of the normal contraction but also the maximum volume during the premature ventricular contraction. Due to the 3 s moving window, the C2 configuration did not capture the sudden EDV drops during PVCs.
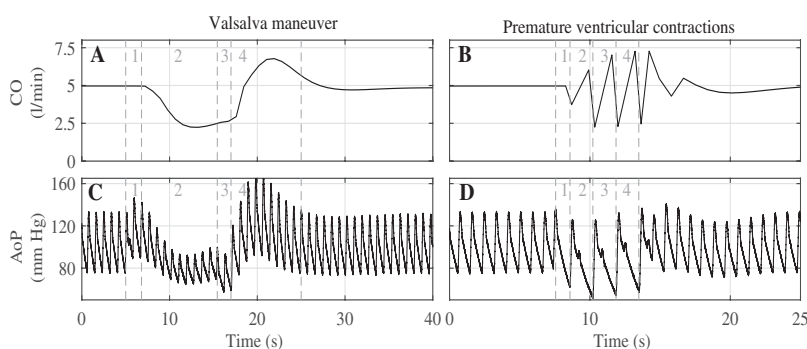

Figure 5: Cardiac output (CO) and aortic pressure (AoP) signals of a physiological circulation during the simulated Valsalva maneuver (VM) and premature ventricular contractions (PVCs). VM (A) and (C) and four PVCs (B) and (D).
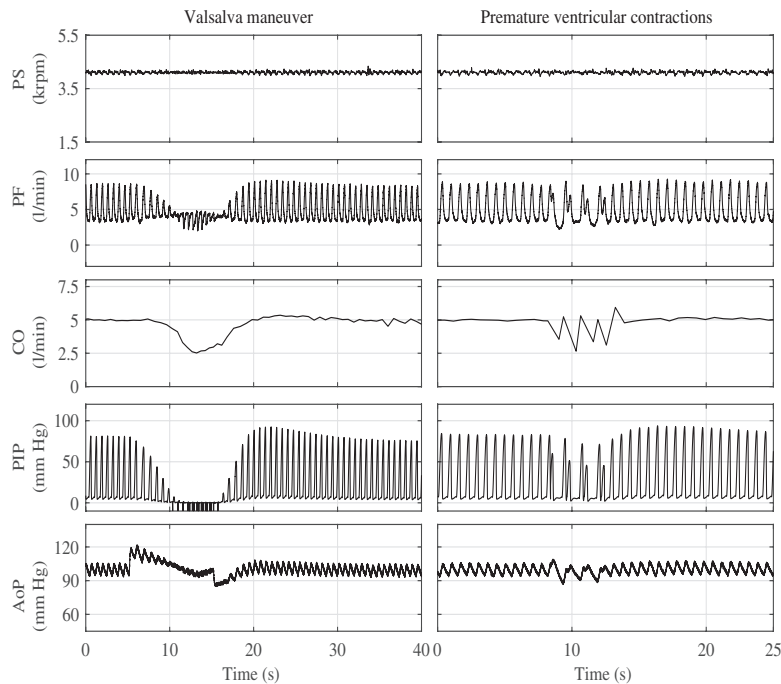Dashed lines indicate the four phases of the VM and the four PVCs.

Figure 6: Performance of a pathological circulation assisted by a tVAD operated at a constant speed (C1) during the Valsalva maneuver (VM) (left-hand side panels) and premature ventricular contractions (PVCs) (right-hand side panels).
PS, Pump speed; PF, pump flow; CO, cardiac output; PIP, pump inlet pressure; AoP, aortic pressure.
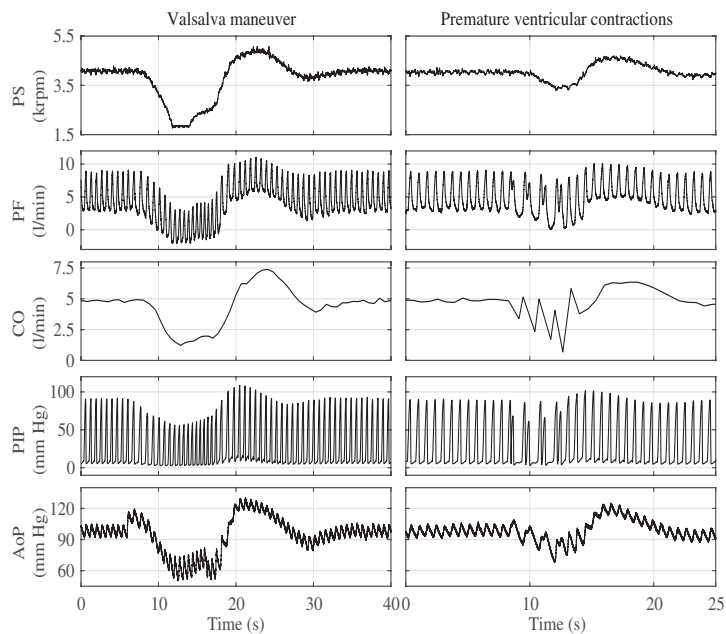

Figure 7: Performance of a pathological circulation assisted by a tVAD controlled by the nominal PRS controller (C2) during the Valsalva maneuver (left-hand side panels) and premature ventricular contractions (right-hand side panels).
PS, Pump speed; PF, pump flow; CO, cardiac output; PIP, pump inlet pressure; AoP, aortic pressure.

Figure 8: Performance of a pathological circulation assisted by a tVAD controlled by the modified PRS controller (C3) during the Valsalva maneuver (left-hand side panels) and premature ventricular contractions (right-hand side panels).

PS, Pump speed; PF, pump flow; CO, cardiac output; PIP, pump inlet pressure; AoP, aortic pressure.
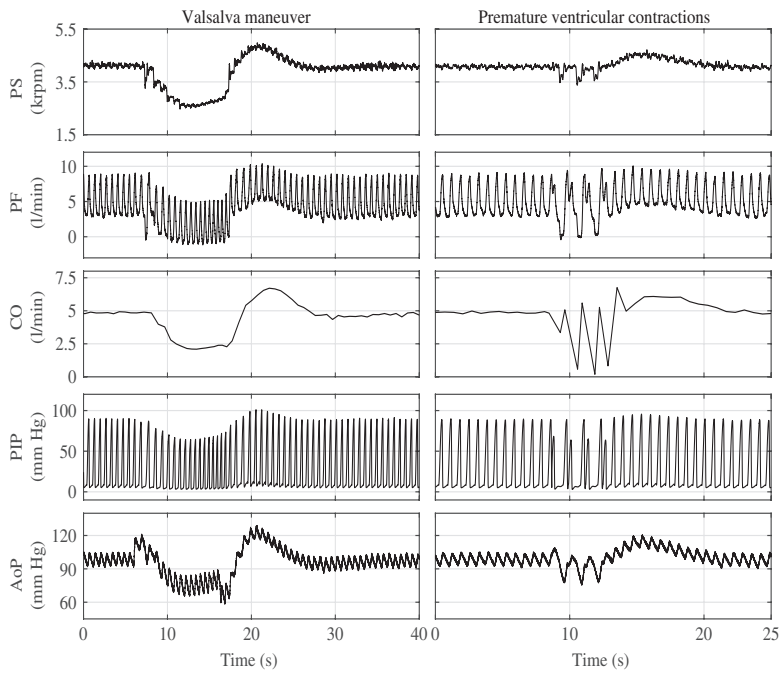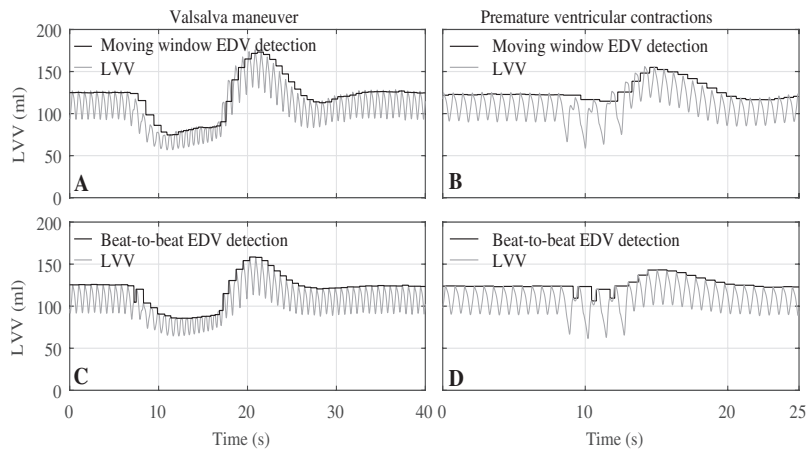

Figure 9: Comparison of two algorithms to extract the end-diastolic volume (EDV) from the left ventricular volume (LVV) signal during Valsalva maneuver [panels (A) and C)] and premature ventricular contractions [panels (B) and (D)].

Panels (A) and (B) show the performance of the 3-s moving window extraction algorithm used in C2. Panels (B) and (D) show the performance of the beat-to-beat EDV extraction algorithm used in C3.

Discussion

In this study, we investigated special patho-physiological situations that can lead to sudden changes of the venous return and therefore, suction or LV overloading. We simulated the VM on our HMC by introducing a change in the ITP. We increased the ITP to 30 mm Hg over 10 s, as it is reported from clinical experiments [8, 19, 29]. Such an

ITP increase can also occur during daily strain conditions of the patients, such as bowel movement, heavy lifting, coughing and posture changes [13]. The observed AoP signals of the physiological heart matched well with those reported in studies about clinical experiments [13, 29]. The four phases of VM seen in clinical recordings of arterial blood pressure were identified (Figure 5).

In the failing circulation without tVAD, a square-wave AoP response would be expected during the VM due to the blood pooling in the congested pulmonary vascular system, i.e. due to sustained LV preload [19, 29]. This was not observed in our experiments with the controlled tVAD support, where the AoP waveform during the VM was similar to that observed in the physiological circulation. This was to be expected, because the pulmonary vascular system was not congested in this case.

PVCs were simulated as described in [2], where the simulated results were validated based on the MIT-BIH arrhythmia database [10]. The moving window method detected the gradual LVV decrease resulting from the consecutive PVCs (Figure 7), while the beat-to-beat method was able to capture the sudden LVV changes between the irregular beats (Figure 8). No suction occurred during PVCs with neither of the configurations C1, C2, or C3. The case of sustained tachycardia was not included in our experiments, because we focused on the detection of abrupt and temporary hemodynamic changes.

The goal of this study was to investigate whether a beat-to-beat extraction of the EDV is required for a clinical physiological controller, or if a simpler method with a moving window is sufficient. We used the PRS controller [26] as a test controller. As it was developed in our group, we could faithfully configure and implement it. However, the results allow drawing conclusions for other physiological controllers, which rely on a certain feature that is extracted from the signal. The controllers presented in [1, 3, 6, 15, 21, 22, 26, 33] all use one of the two approaches investigated in the current study. Additionally, the presented numerical model can be a useful tool while tuning physiological controllers or defining their sampling rate, as such factors influence the aggressiveness of its response.

For our study, the lack of an implantable, long-term LV volume sensor is not addressed. We acknowledge the use of admittance catheters or sonomicrometry as a short-term, real time volume measurement for *in vivo* research studies, but these technologies are not suitable to be used in patients for long term. In the clinic, echocardiography or magnetic resonance imaging systems are normally used for the measurement of EDV, but they require computationally expensive post processing. In our group, we focus on the development of an implantable LV volume sensor that will be suitable for clinical applications.

The constant speed operation (C1) and the nominal PRS physiological controller (C2) were compared during the VM and the PVCs (Figures 6 and 7). The C2 configuration led to a pump speed and flow decrease during PVCs, which in turn decreased CO and AoP. After the end of the PVCs, a slight overshoot of all signals occurred due to the abrupt venous return recovery. This overshoot was absent in the case of C1 and the CO and AoP changes resembled better the physiological ones (Figure 5). During the VM, the physiological controller (C2) was able to prevent suction, whereas suction was observed with the constant speed (C1). The pump speed and flow adaptation of C2 led to stronger reduction of the CO during the VM, which is more physiological, but leads to a critically low AoP. The AoP waveform during constant speed operation resembled more that of a pathological circulation as presented in [19, 29], where the overshoot is attenuated.

Two different methods for extracting the index of the PRS controller were evaluated (C2 and C3). Both configurations performed better than the constant speed operation (C1) with respect to suction prevention. C3 outperformed C2 due to its faster response resulting from the beat-to-beat detection. The moving window of C2 introduced a delay (Figure 9). Comparing signals during VM between Figures 7 and 8, it is well visible that with C2, there was a greater drop in pump speed (lower speed limit was reached) than with C3. This lower speed resulted in turn in lower pump flow and CO. Backflow through the pump was higher with C2, thereby presumably increasing the probability for blood damage and thrombus formation due to blood recirculation and stagnation zones [4]. Furthermore, the lower pump flow with C2 led to lower AoP. Such low AoP may cause organ dysfunction and affect the quality of life of the patient. Thus, C2 led to less physiological hemodynamics compared to C3. With C1, the AoP sustained in physiological limits, but suction occurred. These outcomes show that the aggressiveness of a physiological controller may be hard to be identified when aiming to design an optimal controller. Additional algorithms to monitor parallel cases of suction, backflow, low AoP and adaptation of the response of the core physiological controller seems to be required for a better performance of a physiological controller.

During the PVCs with C3, the LVV dropped due to the additional contraction of the heart and the shortened diastolic phase. Thus, sudden speed changes occurred (Figure 8). Disturbances of the measured signal can lead to misdetection of the EDV with a beat-to-beat algorithm and therefore, undesirable speed changes. Furthermore,

such an extraction algorithm is considered to be more complex thus increasing the sensitivity to measurement noise, the probability for wrong feature extraction and ultimately reducing the stability margins of the controller in a clinical implementation. On the other hand, a moving window algorithm is considered quite simple, robust and independent of the HR of the native heart. However, the lack of fast adaptation to short-time acute events can lead to momentarily high flows during premature contractions and intermittent suction events or strong maneuvers. Considering all these results, a trade-off is observed between a fast response, which can more likely prevent overpumping and underpumping and a slower response, which is more robust. For a clinical implementation, robustness should be the major goal.

One direct impact of physiological control could be the avoidance of low-flow alarms, which occur frequently in clinical practice. They directly affect the workload of the clinical staff and thus increase treatment costs. Typical everyday activities like coughing, bowel movement, heavy lifting, sleep apnea or even deep breathing can affect ITP and lead to abrupt blood flow changes. With physiological control, the pump flow will be adapted to such activities and the risks of overpumping and underpumping events can be reduced drastically. The clinical routines for monitoring VAD-patients would need to be revised, as low-flows will, hopefully, not constitute such a critical condition for the patients any more. This can also contribute to reduce the psychological stress of the patients and thus improve their quality of life as well as the workload of the health care professionals. However, the development of physiological controller that can achieve all this positive impact constitutes a multi-objective task. It seems that a very fast suction prevention may result to non-physiological hemodynamics, thus reducing the positive effect of a controller. Therefore, the statement that a physiological controller is superior to constant speed should be carefully stated and the comparison between them should be based on realistic, clinically frequent scenarios.

The development of a tVAD and its regulatory approval require extensive *in vivo* testing. Because these tests are expensive and ethically problematic, it is very important to gain as much knowledge as possible from *in vitro* tests. Therefore, it is important to test physiological controllers against all possible patho-physiological events that may occur and thereby influence the performance of the controller. With our extended numerical model of the human blood circulation, we propose an additional tool for testing physiological controllers that can contribute to boost the trust in *in vitro* testing and thus reduce the amount required in *in vivo* trials.

References

[1] AlOmari AHH, Savkin AV, Stevens M, et al. Developments in control systems for rotary left ventricular assist devices for heart failure patients: a review. Physiol Meas 2013; 34: R1–R27.

[2] Amacher R, Ochsner G, Ferreira A, Vandenberghe S, Schmid Daners M. A robust reference signal generator for synchronized ventricular assist devices. IEEE Trans Biomed Eng 2013; 60: 2174–2183. ISSN 1558-2531.

[3] Arndt A, Nüsser P, Lampe B, Müller J. Physiological control of a rotary left ventricular assist device: robust control of pressure pulsatility with suction prevention and suppression. In: World Congress on Medical Physics and Biomedical Engineering, Munich, Germany, Volume 25/7. IFMBE Proceedings, September 7–12. Berlin Heidelberg: Springer, 2009. pp. 775–778.

[4] Behbahani M, Behr M, Hormes M, et al. A review of computational fluid dynamics analysis of blood pumps. Eur J Appl Math 2009; 20: 363.

[5] Bergan JJ, Bunke-Paquette N. The vein book. Oxford: Oxford University Press 2014.

[6] Bullister E, Reich S, Sluetz J. Physiologic control algorithms for rotary blood pumps using pressure sensor input. Artif Organs 2002; 26: 931–938.

[7] Colacino FM, Moscato F, Piedimonte F, Arabia M, Danieli GA. Left ventricle load impedance control by apical vad can help heart recovery and patient perfusion: a numerical study. ASAIO J 2007; 53: 263–277.

[8] Felker GM, Cuculich PS, Gheorghiade M. The valsalva maneuver: a bedside "biomarker" for heart failure. Am J Med 2006; 119: 117–122.

[9] Gaddum NR, Stevens M, Lim E, et al. Starling-like flow control of a left ventricular assist device: *in vitro* validation. Artif Organs 2014; 38: E46–E56.

[10] Goldberger AL, Amaral LA, Glass L, et al. Physiobank, physiotoolkit, and physionet components of a new research resource for complex physiologic signals. Circulation 2000; 101: e215–e220.

[11] Hall JE, Guyton AC. Textbook of medical physiology. London: Saunders 2011.

[12] Kirklin JK, Naftel DC, Pagani FD, et al. Seventh intermacs annual report: 15,000 patients and counting. J Heart Lung Transplant 2015; 34 :1495–1504.

[13] Klabunde R. Cardiovascular physiology concepts. Baltimore, MD, USA: Lippincott Williams & Wilkins 2011.

[14] Liang F, Liu H. Simulation of hemodynamic responses to the valsalva maneuver: an integrative computational model of the cardiovascular system and the autonomic nervous system. J Physiol Sci 2006; 56: 45–65.

[15] Lim ET, Alomari AH, Savkin AV, et al. A method for control of an implantable rotary blood pump for heart failure patients using noninvasive measurements. Artif Organs 2011; 35: E174–E180.

[16] Lim E, Chan GS, Dokos S, et al. A cardiovascular mathematical model of graded head-up tilt. PLoS One 2013; 8: e77357.

[17] Lim E, Dokos S, Cloherty SL, et al. Parameter-optimized model of cardiovascular-rotary blood pump interactions. IEEE Trans Biomed Eng 2010; 57: 254–266.

[18] Lim E, Salamonsen RF, Mansouri M, et al. Hemodynamic response to exercise and head-up tilt of patients implanted with a rotary blood pump: a computational modeling study. Artif Organs 2015; 39: E24–E35.

[19] Little WC, Barr WK, Crawford MH. Altered effect of the valsalva maneuver on left ventricular volume in patients with cardio-myopathy. Circulation 1985; 71: 227–233.

[20] MacDougall J, McKelvie R, Moroz D, Sale D, McCartney N, Buick F. Factors affecting blood pressure during heavy weight lifting and static contractions. J Appl Physiol 1992; 73: 1590–1597.

[21] Mansouri M, Salamonsen RF, Lim E, Akmeliawati R, Lovell NH. Preload-based starling-like control for rotary blood pumps: numerical comparison with pulsatility control and constant speed operation. PLoS One 2015; 10: e0121413. ISSN 1932-6203.

[22] Moscato F, Arabia M, Colacino FM, Naiyanetr P, Danieli GA, Schima H. Left ventricle after load impedance control by an axial flow ventricular assist device: a potential tool for ventricular recovery. Artif Organs 2010; 34: 736–744.

[23] Moscato F, Arabia M, Naiyanetr P, Danieli G, Schima H. Control of a rotary blood pump for defined ventricular unloading: a potential tool for ventricular recovery. In: World Congress on Medical Physics and Biomedical Engineering. Munich, Germany, Volume 25/7. IFMBE Proceedings, September 7–12, 2009. Berlin Heidelberg: Springer, pp. 502–505.

[24] Ochsner G, Amacher R, Amstutz A, et al. A novel interface for hybrid mock circulations to evaluate ventricular assist

devices. IEEE Trans Biomed Eng 2013; 60: 507–516. ISSN 1558-2531.

[25] Ochsner G, Amacher R, Schmid Daners M. Emulation of ventricular suction in a hybrid mock circulation. In: Proceedings of the 12th European Control Conference, New York City, NY, USA 2013. pp. 3108–3112.

[26] Ochsner G, Amacher R, Wilhelm MJ, et al. A physiological controller for turbodynamic ventricular assist devices based on a measurement of the left ventricular volume. Artif Organs 2013; 38: 527–538. ISSN 0160-564X.

[27] Samet P. Hemodynamic sequelae of cardiac arrhythmias. Circulation 1973; 47: 399–407.

[28] Schumer EM, Ising MS, Slaughter MS. The current state of left ventricular assist devices: challenges facing further development. Expert Rev Cardiovasc Ther 2015; 13: 1–9.

[29] Sharpey-Schafer E. Effects of valsalva's manoeuvre on the normal and failing circulation. Br Med J 1955; 1: 693.

[30] Stevens MC, Wilson S, Bradley A, Fraser J, Timms D. Physiological control of dual rotary pumps as a biventricular assist device using a master/slave approach. Artif Organs 2014; 38: 766–774.

[31] Ten Harkel A, Van Lieshout J, Van Lieshout E, Wieling W. Assessment of cardiovascular reflexes: influence of posture and period of preceding rest. J Appl Physiol 1990; 68: 147–153.

[32] Timms DL, Gregory SD, Stevens MC, Fraser JF. Haemodynamic modeling of the cardiovascular system using mock circulation loops to test cardiovascular devices. In: Engineering in Medicine and Biology Society, EMBC, 2011 Annual International Conference of the IEEE. New York City, NY, USA: IEEE, 2011. pp. 4301–4304.

[33] Wang Y, Koenig SC, Slaughter MS, Giridharan GA. Rotary blood pump control strategy for preventing left ventricular suction. ASAIO J 2015; 61: 21–30.

[34] Xie A, Phan K, Yan TD. Durability of continuous-flow left ventricular assist devices: a systematic review. Ann Thorac Surg 2014; 3: 547.

A Physiological Controller for Turbodynamic Ventricular Assist Devices Based on Left Ventricular Systolic Pressure

*Anastasios Petrou, *†Gregor Ochsner, ‡Raffael Amacher, §Panagiotis Pergantis,
*Mathias Rebholz, *Mirko Meboldt, and *Marianne Schmid Daners

*Product Development Group Zurich; †Institute for Dynamic Systems and Control, Department of Mechanical and
Process Engineering, ETH Zurich; ‡Wyss Translation Center Zurich, ETH Zurich, Zurich, Switzerland; and
§Department of Cardiothoracic and Vascular Surgery, German Heart Institute Berlin, Berlin, Germany

Abstract: The current article presents a novel physiological feedback controller for turbodynamic ventricular assist devices (tVADs). This controller is based on the recording of the left ventricular (LV) pressure measured at the inlet cannula of a tVAD thus requiring only one pressure sensor. The LV systolic pressure (SP) is proposed as an indicator to determine the varying perfusion requirements. The algorithm to extract the SP from the pump inlet pressure signal used for the controller to adjust the speed of the tVAD shows robust behavior. Its performance was evaluated on a hybrid mock circulation. The experiments with changing perfusion requirements were compared with a physiological circulation and a pathological one assisted with a tVAD operated at constant speed. A sensitivity analysis of the controller parameters was conducted to identify their limits and their influence on a circulation. The performance of the proposed SP controller was evaluated for various values of LV contractility, as well as for a simulated pressure sensor drift. The response of a pathological circulation assisted by a tVAD controlled by the introduced SP controller matched the physiological circulation well, while over- and underpumping events were eliminated. The controller presented a robust performance during experiments with simulated pressure sensor drift. **Key Words:** Ventricular assist device—Physiological control—Left ventricular systolic pressure—Pressure measurement.

The blood propulsion by the healthy heart provides all tissue of the human body with oxygen and nutrients and removes waste products. The heart's hydraulic output is regulated by various interacting mechanisms, which ensure that the perfusion meets the continuously varying requirements (1). In case of heart failure, the severe left ventricular (LV) dysfunction impairs the cardiac contraction and consequently reduces the cardiac output (CO). Heart failure constitutes a common, costly, and even fatal condition, mainly in developed countries (2). The treatment of heart failure depends on the severity of the disease (3). For severe heart failure, heart transplantation remains the gold standard

treatment. However, this treatment is limited by a donor heart shortage and, therefore, the long-term application of mechanical circulatory support systems has been increasing (4,5).

Ventricular assist devices (VADs) constitute such a mechanical circulatory support system. VADs are mechanical blood pumps, which support the pumping function of the failing heart. Most VADs are implanted in the LV and pump blood into the aorta, in parallel to the remaining heart (6). VAD technology has improved over the last decades and nowadays, their performance in terms of survival is comparable to that of heart transplantations (7). However, adverse events still occur at a high rate (5) and require further technological improvements in future systems. One limitation of today's VADs is their constant speed operation, which may lead to over- and underpumping situations as the perfusion requirements change. Adverse events that are presumably promoted by over- and underpumping

are hemolysis and thromboembolic events due to suction, as well as right heart failure or lung edema caused by volume or pressure overloading (8–10). Consequently, the physiological adaptation of VADs is a promising technological enhancement to improve the outcome of the VAD therapy.

A variety of control strategies for VADs has been developed to achieve physiological adaptation (11). The two major challenges in the development of a physiological controller are the selection of the sensory feedback signal and the design of an algorithm, which adjusts the pump speed based on this measurement. Many controllers are based on pump intrinsic signals, like the motor current, the pump speed, or the heart rate (HR), which can be calculated from the motor current waveform (12–15). Other physiological controllers based on either measured or estimated flow (16–18), atrial pressure (19), pump pressure head (20–22), end-diastolic volume (EDV) (23), or end-diastolic pressure (EDP) (24,25) have been developed, evaluated, and published.

Most of them try to imitate the Frank–Starling mechanism (1), which describes how the CO of a healthy heart depends on after- and preload. In case of a pathological heart, this mechanism is unable to meet the perfusion requirements due to the impaired functioning of the LV. Even though the flow of a VAD also depends on the after- and preload, its sensitivity differs greatly from the Frank–Starling mechanism. The current paper presents a novel physiological controller for turbodynamic VADs (tVADs), which imitates the Frank–Starling mechanism based on the measured pump inlet pressure (PIP) using the systolic pressure (SP) of the PIP signal as input to the controller. From here on, we refer to it as SP controller.

The SP controller proved a physiological adaptation of the tVAD's speed during after- and preload variations and followed the perfusion requirements of a simulated patient well. The algorithmic steps to extract the SP from the PIP and the adjustment of the tVAD speed are presented. The relationship between the LV SP and the LV filling as well as the sensitivity of the SP controller's parameters and the influence of the LV contractility and the pressure sensor drift were analyzed.

MATERIALS AND METHODS

Hybrid mock circulation

All experiments were conducted on the hybrid mock circulation (HMC) presented in (26). The HMC mimics the cardiovascular system by a numerical model (27) that is connected to the tVAD by a numerical-hydraulic interface. A nonimplantable mixed-flow turbodynamic blood pump (Deltastream DP2, Medos Medizintechnik AG, Stolberg, Germany) that allows implementing various control approaches substitutes the tVAD in order to conduct all the experiments. Various pathophysiological scenarios have been simulated to test physiological control algorithms (23). Unstressed venous volume, arterial resistance, LV contractility, and HR can be varied independently. In order to imitate a pathological circulation with the HMC, the contractility of the LV was reduced and the HR was increased. The specific settings for each experiment are described in the Experiments section.

Systolic pressure as physiological index

In the following paragraphs, we analyze the possibility to use the SP as a measure for preload. For this purpose, pressure–volume (PV) loops of a physiological circulation, a pathological circulation without tVAD support, and a pathological circulation assisted by a tVAD operated at constant speed were generated using the HMC. For each case, we investigated the dependence of SP on the after-, preload, and contractility. Figure 1 depicts all these PV loops, which are qualitatively validated by (28,29).

In a physiological circulation, the SP is mainly determined by the afterload and by the contractility of the LV (1). Afterload refers to the pressure or the resistance against which the heart must work to eject blood during systole. During isovolumetric contractions, the intraventricular pressure increases until the aortic valve opens and the ejection phase starts. Additionally, the arterial compliance and resistance as well as the resistance of the aortic valve influence the SP. Figure 1A shows the dependence of the SP on the afterload, whereby the SP increases as afterload increases and decreases as afterload decreases, respectively. Figure 1B shows that preload changes affect the SP similarly to afterload changes. A preload increase (EDV increase) results in an increase of stroke volume (SV) and correspondingly CO, resulting in an aortic pressure (AoP) increase and consequently in an SP increase (28). A preload reduction will have the opposite effects, that is, decreased SV, CO, AoP, and SP. Figure 1C shows the dependence of the SP on the contractility. A contractility increase results in a small increase in SP, while the EDV decreases, and vice versa.

Figure 1D–1F shows the PV loops of a pathological circulation where the contractility of the simulated heart was reduced, during after-, preload, and
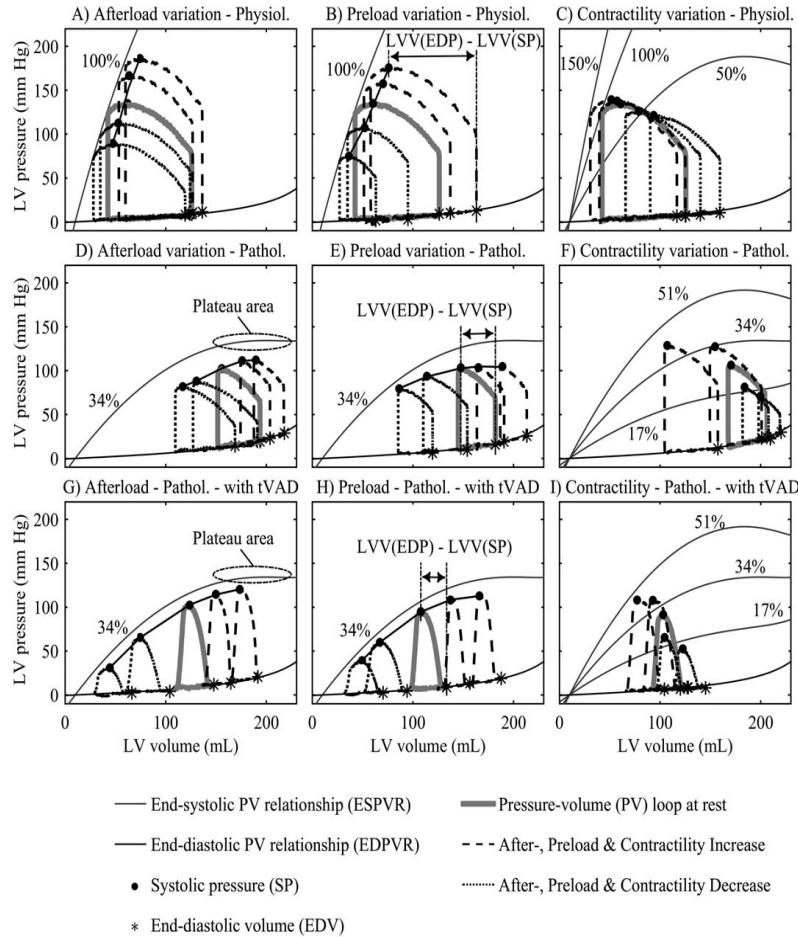
FIG. 1. (A, D, G) show pressure–volume (PV) loops for five different afterload values. (B, E, H) show PV loops for five different preload values. (C, F, I) show PV loops for five different contractility values. (A, B, C) depict the PV loops of a physiological (Physiol.) circulation; (D, E, F) depict the PV loops of a pathological (Pathol.) circulation; (G, H, I) depict the PV loops of a pathological circulation assisted with a constant speed tVAD. The systolic pressure (SP) and end-diastolic volume (EDV) values are measured and marked for all PV loops. In the pathological circulation the left ventricular (LV) contractility is reduced and therefore, small changes of SP values are detected during increased after- and preload. The end-systolic and end-diastolic PV relationship curves are illustrated, as well as their plateau area. The contractility values expressed in percentage of the normal physiological contractility (100%) are indicated alongside the ESPVR curves. The difference between the LV volume at end-diastolic pressure (EDP) and the LV volume at SP (LVV(EDP) – LVV(SP)) is indicated by two dash-dotted vertical lines.

contractility variations. Due to the decreased contractility, the slope of the end-systolic–pressure–volume relationship (ESPVR) curve decreased as well (28). Thus, smaller intraventricular pressures for the same after- and preload conditions are generated (Fig. 1D,1E) compared to the physiological circulation (Fig. 1A,1B). Additionally, during both after- and preload increase, the heart is unable to further increase its intraventricular pressure and the influence on the SP is limited (Fig. 1D,1E). Figure 1D depicts this limitation through the plateau area of the ESPVR curve (28).

During contractility variations the pathological heart responds similarly to the physiological, that is, the SP decreases during a contractility decrease and vice versa. Figure 1G–1I shows the same after-, preload, and contractility variation experiments conducted with a pathological circulation assisted with a tVAD set at a constant speed, which yields to 5 L/min at rest. In that case, the influence of all variations on the shape of the PV loops is different, because the continuous unloading of the LV with the tVAD reduces the SV (28,29).
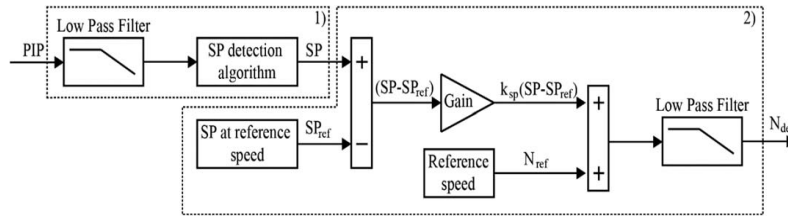
FIG. 2. Structure of the SP controller. First, the systolic pressure (SP) is extracted and its difference from the reference systolic pressure SP_{ref} is calculated. Second, the resulting SP difference is multiplied by the proportional gain k_{sp} of the controller and the product is added to the reference speed of the controller in order to define the desired pump speed N_{des}. The reference speed N_{ref} and the corresponding systolic pressure SP_{ref} are obtained during the patient specific calibration process.

The influence of afterload on the SP is still large; however, the shape of the PV loops in Fig. 1G shows that this is not a direct influence. Unlike the PV loops in Fig. 1A, those in Fig. 1G show a great variation of the EDV, that is, the LV filling. This means that the afterload has a direct effect on the filling of the LV, which in turn dictates the SP. This effect can be explained by the reduced and almost constant SV. Vertical lines in the panels B, E, and H in Fig. 1 indicate the difference between the EDV and the LV at maximum pressure. Clearly, with a small SV this difference is also small under tVAD support. In this case, as long as the filling is below the indicated plateau area, the SP directly depends on the LV filling and can therefore be seen as a measure of preload. Figure 1I shows that the contractility of the LV also influences the SP, which can therefore not be viewed as contractility independent.

We developed our controller according to the behavior of SP during after- and preload variations. The limitation of such a controller during contractility variations is addressed and discussed in the Results and Discussion sections. The use of the SP value as physiological index for a tVAD controller requires that the PV loops of the LV remain below the plateau area and above the suction area (as depicted in Fig. 1G,1H). This requirement can be fulfilled by using a physiological controller to regulate the pump speed. The following section presents the algorithmic steps of such a controller.

Systolic pressure controller

We developed a controller for tVADs based on SP to restore the physiological hemodynamics by increasing the tVAD assistance to the LV when SP increases and vice versa. The SP controller is a proportional controller which adapts the pump speed proportionally to the SP. The measured PIP is the input to the controller and the desired pump speed (N_{des}) is the output. Figure 2 shows the structure of the SP controller. It consists of two parts: First, the PIP is low-pass filtered with a first-order infinite impulse response (IIR) filter. The maximum pressure, that is, the SP, is detected within a fixed time interval of 2 s to ensure that an SP value is detected even for low heart rates. Second, the SP control algorithm is executed according to

$$N_{des} = k_{sp}(SP - SP_{ref}) + N_{ref},$$

where k_{sp} is the proportional gain (rpm/mm Hg), SP_{ref} is the SP obtained during calibration (mm Hg), and N_{ref} is the pump speed during calibration (rpm). The controller linearly relates a signal that varies with after- and preload variations (the SP) to the pumping work by controlling the N_{des}, and thus imitates the Frank–Starling mechanism.

For this study, the parameters N_{ref} and SP_{ref} of the SP controller were identified with the following calibration process. First, we manually identified the constant pump speed that yielded a desired CO at rest. The chosen speed was saved as N_{ref} and the corresponding SP was saved as SP_{ref}. The gain k_{sp} was not identified during the calibration process, but defined by conducting an in vitro sensitivity analysis, which is presented in the Experiments and Results sections.

Experiments

Figure 3 depicts the prescribed variations of cardiovascular parameters for our experiments. The parameters for after- and preload variations correspond to the variations presented in (23), with a wider range of parameters. We additionally conducted experiments with a varying contractility. Specifically, we varied the HR, the unstressed venous volume, the systemic vascular resistance, and the contractility in order to represent the after-, preload, and contractility variations. The experiments were designed not to mimic a specific daily situation, but to allow for an independent investigation of the effects of the
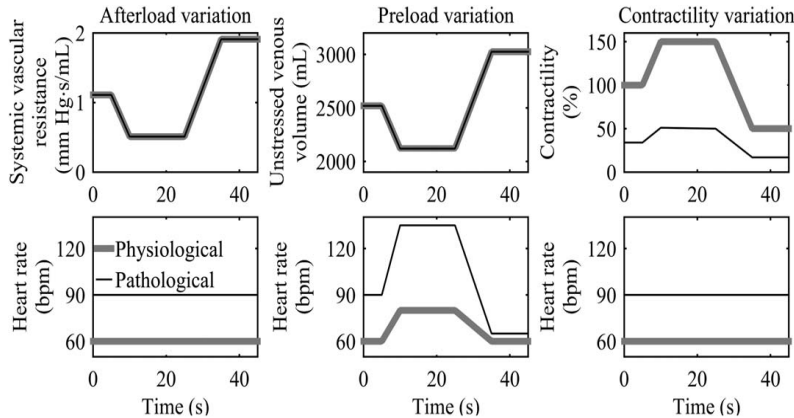
FIG. 3. Defined cardiovascular parameters for the after-, preload, and contractility variation experiments. During the preload variation experiment, the systemic vascular resistance was controlled by the baroreflex; during the afterload variation experiment, the unstressed venous volume was controlled by the CO autoregulation. The contractility was maintained at 34 or 100% for both variations. For the contractility variations experiments, both, systemic vascular resistance and unstressed venous volume were fixed at the values attained in the resting condition (corresponding to 0 s $< t <$ 5 s of after- and preload variation).

after-, preload, and contractility variations on the performance of the SP controller. In addition, the focus of the experiments was on fast and wide-ranging variations of cardiovascular parameters, which are challenging for a desired physiological VAD controller.

For each experiment, the HMC ran for 20 s with a constant pump speed and fixed physiological parameters to allow the system to reach steady state at the resting condition. Then, one of the experiments was started. The duration of after- and preload variations was 45 s. For the contractility variation experiment, the duration was increased to 100 s to reach steady state after each variation. During the experiments, the LV pressure was continuously measured (PN2009, IFM Electronic GmbH, Essen, Germany). This measurement was given as an input to the SP controller.

Table 1 lists the specific configurations used for the experiments. We conducted four different studies to evaluate these configurations. Each study included the comparison of different configurations of Table 1 and experiments of Fig. 3. Table 2 lists the studies conducted, as well as the corresponding configurations tested, and the variations applied. Configurations C1-C7 and C10-C11 were evaluated under after-, preload, and contractility variations whereas C8 and C9 were only evaluated under after- and preload variations and the contractility was held constant. Further investigations of the performance of the SP controller included various configurations, which are listed in

Table 2. All four studies, listed in Table 2, are described below:

1. Baselines and nominal SP controller: Comparison of the performance of a pathological circulation assisted with the nominal SP controller (C3) with the performances of a physiological circulation (C1) and with a pathological circulation assisted with a tVAD running at constant speed (C2). The gain k_{sp} was set to 40 rpm/mm Hg, and the desired CO was chosen to be 5 L/min, which yielded a reference speed N_{ref} of 4180 rpm during calibration.

2. Sensitivity of the SP controller on the controller parameters: The second study analyzes the performance of the SP controller for different values for the controller parameters. Particularly, the influence of the SP controller's gain k_{sp} and reference speed N_{ref} on the CO and the SP was investigated. The high and low values for the N_{ref} were chosen such that a CO of 5.5 and 4.5 L/min, respectively, resulted at rest. The high and low values for k_{sp} were identified based on different limits. The high gain was identified by gradually increasing it, until strong CO oscillations were observed during the experiments, which occurred at k_{sp} = 220 rpm/mm Hg. The low gain was identified by gradually decreasing it, until the pump operates close to suction (SP close to 0 mm Hg), which occurred at k_{sp} = 10 rpm/mm Hg. Both configurations C6 and C7 were compared to the nominal SP controller C3.

TABLE 1. *Settings of the different experiment configurations*

Configuration (#)	Predefined parameters			Variables obtained during calibration process		Contractility during after- and preload variations (%)	Sensor drift (mm Hg)
	tVAD support	CO at rest (L/min)	Controller gain k_{sp} (rpm/mm Hg)	Reference speed N_{ref} (rpm)	Reference SP SP_{ref} (mm Hg)		
C1	—	5	—	—	—	100	—
C2	Constant speed	5	—	4180	—	34	—
C3	SP controller	5	40	4180	91	34	0
C4	SP controller	4.5	40	3750	102	34	0
C5	SP controller	5.5	40	4500	73	34	0
C6	SP controller	5	10	4180	91	34	0
C7	SP controller	5	220	4180	91	34	0
C8	SP controller	5.85	40	4180	118	60	0
C9	SP controller	4.7	40	4180	32	10	0
C10	SP controller	5.28	40	4180	91	34	+15
C11	SP controller	4.87	40	4180	91	34	−15

CO, cardiac output; SP, systolic pressure; tVAD, turbodynamic ventricular assist device.

3. Sensitivity of the SP controller on the contractility: The third study investigated the influence of various contractility conditions on the circulation assisted with a tVAD controlled with the SP controller, during after- and preload variations. Both experiments were conducted for different constant contractility values from 10 to 60%. The RMS values with respect to the nominal SP controller at a 34% contractility (C3) were calculated.

4. Sensitivity of the SP controller on sensor drift: The performance of the nominal SP controller during all three variations was evaluated when the pressure sensor is affected from drift. The drift was simulated by adding or subtracting a constant offset to the actual LV pressure measurement. The maximum offset was ±25 mm Hg.

RESULTS

Baselines and nominal SP controller

Figure 4 shows the result of the baselines and SP controller performance. Three configurations are compared: the physiological circulation (C1), the pathological circulation assisted with a constant speed tVAD (C2), and the pathological circulation assisted with a tVAD controlled by the SP controller (C3). The CO response of the circulation supported by the SP-controlled tVAD is similar to that of the physiological circulation. In contrast, when the tVAD is operated at constant speed, the CO response is attenuated and suction events occur (at $t > 38$ s during preload variation and at 20 s $< t <$ 28 s during afterload variation). When the contractility increases, the CO of C1 and C2 remains almost constant, while it slightly increases when the SP controller is applied. During the contractility decrease, the CO of C1 decreases while the EDP increases up to 12 mm Hg. With C3, the CO decreases even more than with C1, while the EDP increases up to 25 mm Hg. Study 1 in Tables 2 and 3 shows the CO RMS values of C2 and C3 configurations with respect to C1. The CO RMS values of C3 for after- and preload variation experiments are closer to zero compared to C2, proving the more physiological response of the pump when the SP

TABLE 2. *List of conducted studies, tested configurations, and applied variations*

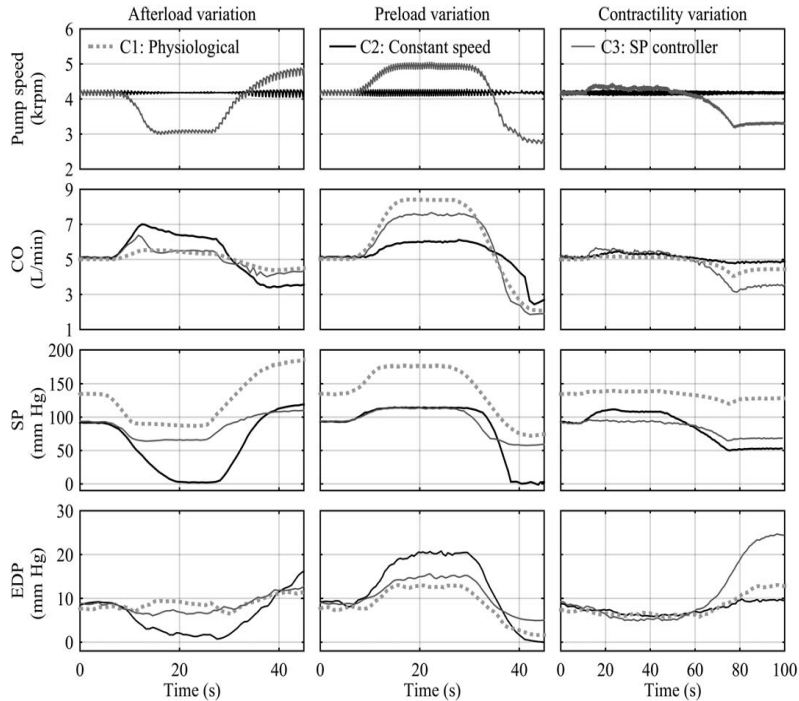| Study	Description	Configurations tested	Preload variation	Afterload variation	Contractility variation
1	Baselines and nominal SP controller	C1-C3	✓	✓	✓
2A	Sensitivity of the SP controller on the controller parameters	C3-C5	✓	✓	✓
2B		C3, C6, C7	✓	✓	✓
3	Sensitivity of the SP controller on the contractility	C8, C9	✓	✓	×
4	Sensitivity of the SP controller on sensor drift	C10-C11	✓	✓	✓

FIG. 4. Experimental results of study 1. After-, preload, and contractility variation experiments for the physiological circulation (C1), the pathological circulation assisted with a constant speed tVAD (C2), and the pathological circulation assisted with a tVAD controlled by the SP controller (C3). The resulting signals for pump speed, cardiac output (CO), systolic pressure (SP), and end-diastolic pressure (EDP) are depicted.

controller is applied. However, the C2 configuration presents better CO results (based on RMS values) than the C3 during the contractility variations.

Figure 5 shows the PV loops of C3 during all three experiments. The LV volume remains within a physiological range and the SP varies according to the LV filling in both after- and preload variation experiments. During the strong contractility variations, this is not the case. Figure 6 depicts the detection of the SP from the PIP signal during the preload variation according to the detection algorithm presented in the Materials and Methods section. The SP value is reliably detected every 2 s. A delay is introduced due to the filtering and the fixed time interval used.

Sensitivity of the SP controller on the controller parameters

Figure 7 shows a comparison of two configurations with a different value for the reference speed (C4 and C5) in comparison with the nominal SP controller (C3) during the preload experiment. SP signals show that no overpumping events (suction) occurred in both cases despite the maladjustment

of the reference speed. Figure 8 shows a comparison of two configurations with a different value for the controller gain (C6 and C7) in comparison with the nominal SP controller (C3) during the preload experiment. With $k_{sp} = 220$ rpm/mm Hg (C7), CO and pump speed oscillations occurred during the preload increase, which indicates small stability margins. In contrast, with $k_{sp} = 10$ rpm/mm Hg (C6), the controller dictates small speed changes only, which resulted in very low SP values during the preload decrease at $t > 40$ s, similar to the constant speed operation of the tVAD (C2). The calculated RMS values for various reference speeds and gain parameters with respect to the nominal SP controller are listed in Tables 2 and 3. The CO RMS values for the two reference speeds tested in C6 and C7 do not differ much. However, we observed more aortic valve flow when the reference speed was low (C4). The speed, and in turn CO, oscillations shown in Fig. 8 during the preload variation, were also observed during the afterload and the contractility variation. However, they already occurred at lower controller gains, namely at $k_{sp} = 140$ rpm/mm Hg during the afterload variation

42

TABLE 3. *Calculated root mean square values for cardiac output in Liters/minute for all studies conducted, all after-, preload, and contractility variations implemented and configurations evaluated. For study 1 the configurations are compared with the physiological circulation (C1), whereas for studies 2A, 2B, 3, and 4 the configurations are compared with the nominal SP controller (C3). All labeled configurations (e.g., C3) are also presented in Fig. 4*

Study 1	Baselines and nominal SP controller		
	Physiological (C1)	Constant speed (C2)	Nominal SP controller (C3)
Afterload variation	0	0.86	0.29
Preload variation	0	1.61	0.58
Contractility variation	0	0.31	0.54

Study 2A	Reference Speed N_{ref} (rpm)		
	3750 (C4)	4180 (C3)	4500 (C5)
Afterload variation	0.42	0	0.39
Preload variations	1.02	0	1.04
Contractility variation	0.64	0	0.82

Study 2B	Gain parameter k_{sp} (rpm/mm Hg)										
	0	10 (C6)	20	40 (C3)	60	80	100	120	140	200	220 (C7)
Afterload variation	0.65	0.36	0.24	0	0.17	0.33	0.46	0.74	0.88	-	-
Preload variation	1.24	1.05	0.55	0	0.28	0.61	0.47	0.86	0.81	0.88	1.08
Contractility variation	0.78	0.46	0.24	0	0.27	0.56	-	-	-	-	-

Study 3	Contractility parameter (%)										
	10 (C9)	15	20	25	30	35	40	45	50	55	60 (C8)
Afterload variation	0.39	0.33	0.21	0.21	0.12	0.06	0.14	0.22	0.28	0.35	0.40
Preload variation	1.11	0.88	0.64	0.36	0.23	0.18	0.31	0.64	0.93	1.19	1.46
Contractility variation	-	-	-	-	-	-	-	-	-	-	-

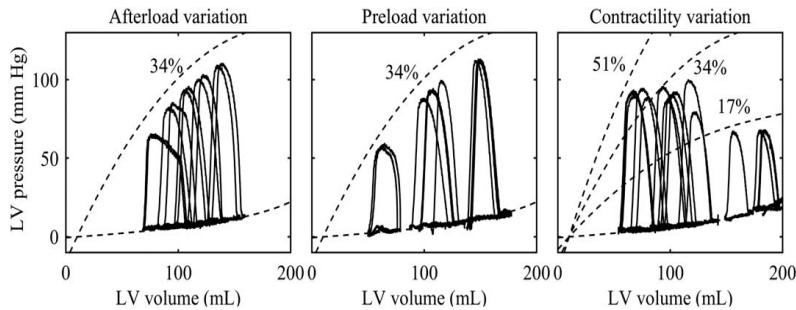| Study 4	Pressure sensor drift (mm Hg)										
	−25	−20	−15 (C10)	−10	−5	0 (C3)	5	10	15 (C11)	20	25
Afterload variation	0.61	0.39	0.35	0.23	0.14	0	0.12	0.20	0.24	0.30	0.33
Preload variation	1.38	1	0.64	0.38	0.16	0	0.34	0.47	0.67	0.78	0.93
Contractility variation	0.70	0.59	0.47	0.33	0.23	0	0.10	0.24	0.36	0.49	0.53

FIG. 5. Pressure–volume loops during after-, preload, and contractility variation experiments for the pathological circulation assisted with a tVAD controlled by the SP controller (C3). The dashed lines indicate the end-systolic and end-diastolic pressure–volume relationship curves for different contractility values, which are indicated in percent of the physiological contractility.
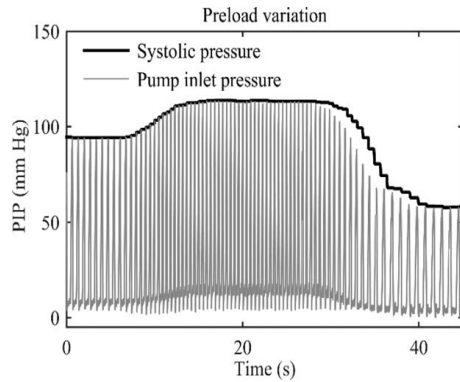
FIG. 6. The pump inlet pressure (PIP) and the extracted systolic pressure (SP) during the preload variation experiment.

and at $k_{sp} = 80$ rpm/mm Hg during the contractility variation. Suction only occurred at controller gain values below 10 rpm/mm Hg.

Sensitivity of the SP controller on the contractility

Figure 9 shows the influence of the contractility on the performance of the nominal SP controller during the preload variation. The contractility is increased from 34% (C3) to 60% (C8) (e.g.,
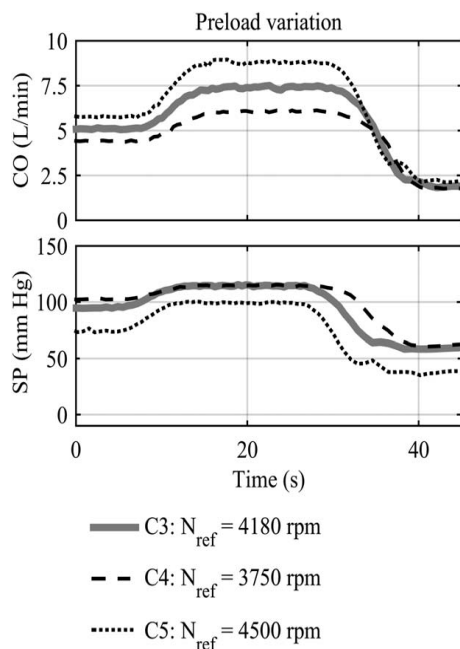

FIG. 7. Sensitivity analysis of the SP controller reference speed N_{ref} (C4, C5) in comparison with the nominal SP controller (C3).
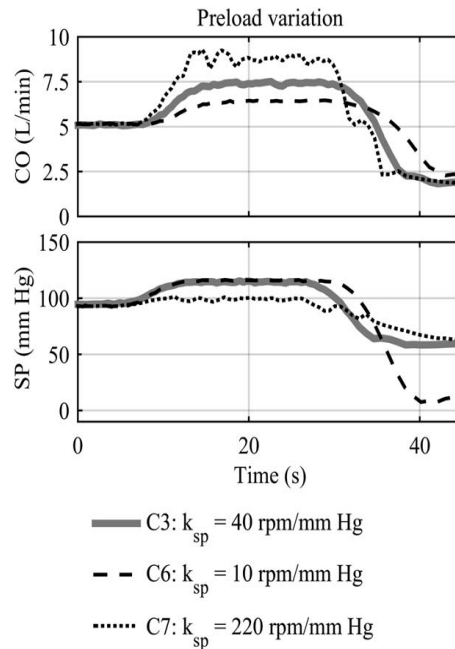
FIG. 8. Sensitivity analysis of the SP controller gain k_{sp} (C6, C7) in comparison with the nominal SP controller (C3).

myocardial recovery) and decreases from 34% (C3) to 10% (C9) (e.g., progressive heart failure). The contractility increase (C8) led to an increase of the CO up to nearly 10 L/min during the preload increase, which even exceeded the CO of the physiological circulation (Fig. 4, CO panel of preload variation). The contractility decrease (C9) led to a reduced CO during the preload increase. Furthermore, the pump was operating close to suction (minimum SP = 5 mm Hg at $t > 40$ s) during the preload decrease. The CO RMS values of all contractility values tested for both after- and preload variations are listed in Tables 2 and 3 (study 3). The contractility variations mainly influenced the performance of the nominal SP controller during the preload variations. Suction events (LV pressure < 0 mm Hg) did not occur for any tested contractility value during both experiments.

Sensitivity of the SP controller on pressure sensor drift

Figure 10 shows the effect of a sensor drift on the CO and the SP during the preload variation. The sensor drift is implemented by a constant offset in the LV pressure measurement. An offset of ±15 mm Hg, only has a small effect on the resulting CO. And even with ±25 mm Hg, no suction
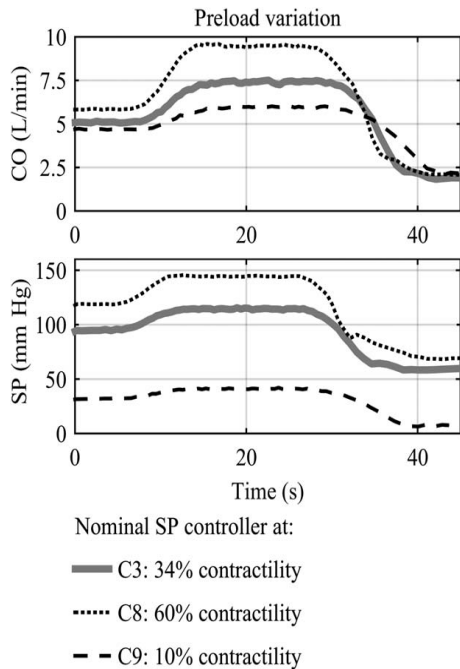
Nominal SP controller at:

— C3: 34% contractility

······ C8: 60% contractility

– – C9: 10% contractility

FIG. 9. Influence of contractility increase and decrease on the performance of the SP controller. The figure shows how CO and SP change when the contractility of a specific pathological LV increases (C8) or decreases (C9).

Nominal SP controller with:

— C3: 0 mm Hg sensor drift

······ C10: +15 mm Hg sensor drift

– – C11: -15 mm Hg sensor drift

FIG. 10. Influence of sensor drift on the performance of the SP controller. The figure shows how CO and SP change when the measurement of the pressure sensor is affected by a drift of ±15 mm Hg.

events occurred. Study 4 in Tables 2 and 3 lists the calculated CO RMS values for various values for the sensor drift with respect the values obtained with 0 mm Hg offset. A drift of −25 mm Hg led to a CO RMS value greater than 1 L/min.

DISCUSSION

A tVAD operated at constant speed is able to restore the hemodynamics of a patient suffering from severe heart failure to a physiological range. However, variations of the physiological requirements can lead to over- or underpumping. Figure 4 shows that the SP controller is able to avoid such events and yield a physiological adaptation of the CO. The performance of the SP controller is based on the strong dependence of the SP on after- and preload, when a tVAD assists a pathological circulation. During contractility variations, the SP controller (C3) behaved similarly to the physiological circulation (C1), with respect to CO changes, but more aggressively, that is, greater CO changes were observed when the contractility was changed.

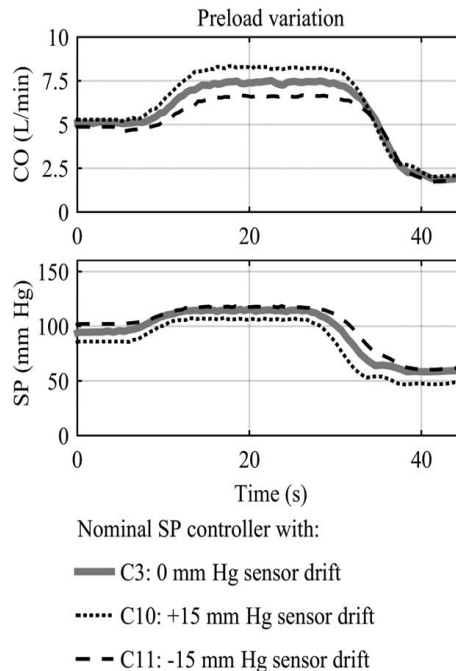We can categorize most published physiological controllers in three groups, according to their

concept. The first group consists of controllers that are directly based on preload (23,25,34), that is, they use a measure of preload as the input to the controller, for instance EDV, EDP, or left atrial pressure (LAP). These controllers are independent of the contractility. The second group consists of controllers which rely on an estimate of preload (18,20,35), for instance the pump flow or pressure pulsatility. These algorithms depend on preload as well as contractility but they also aim at imitating the response of the native heart, that is, the Frank–Starling mechanism. The third group consists of controllers, which aim at maintaining the perfusion in a physiological range (21,24,30–32,36–38) for instance through measurements of mean arterial pressure, EDP, pump flow, or pump pressure difference. The SP controller can be assigned to the second group, as the SP, just like most pulsatility indices, depends on preload as well as contractility.

In (39), the authors evaluated various physiological controllers from these three groups in vitro. Their results show that among the pressure controllers, those based on EDP present the best physiological performance (24,25). The performance of the pump-flow-pulsatility-based controller (18) is

slightly inferior, but still good (25,39). The SP controller is based on the estimation of the preload condition of the LV and therefore, it lacks preload sensitivity compared to direct preload-based controllers (23–25).

However, the novelty of the SP controller has a few advantages over most other controllers. First, only one pressure sensor at the inlet cannula of the pump is required in order to implement the controller, while the other pressure-based controllers require an additional sensor to measure either the pump flow (25) or the pressure at the outlet of the pump (aortic pressure) (20,21,24,30–32). Thus, the SP controller keeps the complexity of the system low. Second, sensor drift constitutes a major problem of implantable pressure sensors (33) and the SP controller is very robust toward this drift. Figure 5 shows that SP undergoes large variations (55–110 mm Hg) during after- and preload variations and therefore the influence of noise and sensor drift on the performance of the SP controller is small. Figure 10 and Table 2 (study 4) justify this statement by showing the influence of the sensor drift on the CO. In contrast, EDP undergoes small variations during after- and preload variations (Fig. 4), which makes it quite sensitive when sensor noise or drift are present. Third, the SP is the maximum value of the LV pressure signal, which is, compared to EDP, easier to extract.

The SP controller is simple in structure. It has only three parameters to be defined: the reference speed N_{ref}, the reference SP SP_{ref} and the gain k_{sp}. The reference speed can be adjusted in the same way as it is done in current clinical practice (40). For the SP controller, the physician will adjust an initial pump speed according to his or her clinical guidelines. For every tVAD, the N_{ref} will be different and based on the pressure–speed–flow characteristics. After choosing the reference speed, the SP_{ref} is automatically extracted, stored, and used in the control algorithm. Figure 7 shows that the performance of the SP controller when controlling the DP2 can be influenced by setting different reference speeds. For the DP2, a range of the N_{ref} between 3500 and 4500 rpm results in a good physiological performance without suction events.

In our study, we proposed a value of 40 rpm/mm Hg for the gain, which represents a physiological performance and large stability margins. Table 2 and study 2B show that within a gain range from 20 to 60 rpm/mm Hg the CO RMS value for all experiments is lower than 0.55 L/min and suction can be prevented. This gain and its margins would need to be redefined, when the SP controller is implemented on a clinically used tVAD. However, contractility variation study (study 3) showed that in case of a very low contractility (below 10%, i.e., ejection fraction <10%) the SP controller with a gain of 40 rpm/mm Hg will be unable to change the tVAD speed sufficiently and suction events may occur.

The occurrence of suction due to contractility variations could be avoided with a separate suction detection algorithm (22), which runs in parallel with the SP controller. Suction events are detected by such an algorithm and a separate algorithm to release suction is activated. A suction detection could also be implemented for a constant speed tVAD. However, the lack of physiological adaptation would still be present.

The parameter k_{sp} represents the gain from the SP to the pump speed. Due to the small stroke volume of tVAD supported patients, the contractility can be regarded as the gain from EDV to SP, defined by the slope of the ESPVR. The overall gain from EDV to pump speed is therefore the multiplication of k_{sp} and the contractility. For the overall gain from EDV to pump speed to be approximately constant, large variations of the contractility therefore require an adaptation of k_{sp}. Methods to assess the contractility or detect contractility variations based on pump flow or LV pressure have been proposed (41–43), which could also be implemented in the SP controller to detect contractility changes or even to automatically adapt k_{sp}. However, such an adaptation requires a thorough investigation, which is not in the scope of the current paper.

During an isolated acute contractility decrease, the SP controller decreased the pump speed causing a reduced pump support to the native heart, which in turn led to a strong increase in EDP (Fig. 4). The EDP increased due to the blood accumulation in the pulmonary circulation ultimately leading to a condition of decompensated heart failure. Such a response of the SP controller is regarded as undesirable and constitutes a limitation of the controller. However, changes in contractility are typically related to changes in after- and preload. The Frank–Starling mechanism and Anrep effect (28) (contractility increase following an afterload increase) are known manifestations of this interdependence and constitute parts of the compensatory mechanisms of the heart.

The systolic dysfunction seen in the dilated cardiomyopathies constitutes a result of reduced contractility. Genetic or acquired pathophysiological and biochemical disorders, such as ischemia, toxins,

inflammation, infection, and tachycardia can lead to an acute or chronic reduction of contractility and heart failure. All these causes of decreased contractility can theoretically cause either a net reduction in the preoperative myocardial contractility or a relative reduction of the increased post-LVAD contractility, compromising the unloading of the LV. In our study, we investigated the response of the SP controller against acute complications (Fig. 4 and Table 3), which could cause an abrupt decrease, like acute ischemia, inflammation (septic heart), or tachycardia. Such cases are life threatening and must be treated in the hospital anyway and, therefore, not through the response of the SP controller.

In a possible clinical implementation, the SP controller must perform properly during all clinical conditions. Arrhythmic events, such as premature ventricular contractions (44), are frequently observed in VAD patients. Furthermore, acute and strong variations in their LV pressure due to breathing or strain events may occur during their daily life. The performance of the SP controller has been investigated under such conditions and none of the aforementioned conditions caused a problem for the SP controller. Suction events were avoided and a physiological CO response was observed.

In this study, we do not address the lack of a pressure sensor at the inlet of the clinically used tVADs. A biocompatible, durable, and accurate blood pressure sensor has not yet been developed but is likely to be realized in the near future (33,45–47). Furthermore, the first implantable blood pressure sensor was approved by the Food and Drug Administration (FDA) after a premarket approval application (PMA) in 2014 (48). This pressure sensor developed by St. Jude Medical, named CardioMEMS HF System aims at monitoring the pressure of the pulmonary artery in heart failure patients and includes a method to recalibrate the pressure measurement in case of sensor drift. In addition, several groups have recently focused on the development of physiological controllers for tVADs based on pressure measurements (25,34,49).

The goal of the current study is to present the structure of a new physiological controller for tVADs. The controller was evaluated in vitro and it showed promising improvements over the constant speed operation of the tVAD. Acute in vivo experiments have recently been conducted using the exact structure of the nominal SP controller (C3) in order to further evaluate its performance and improve upon its limitations. However, the results of these experiments are not in the scope of the current paper.

CONCLUSION

The systolic pressure controller enables a physiological adaptation of the speed of a turbodynamic ventricular assist device to the perfusion requirements of a patient. The desired speed for the tVAD is generated based on a measurement of the pump inlet pressure. In vitro, a mimicked pathological circulation assisted with a tVAD controlled by the SP controller performed similarly to a physiological circulation with respect to the cardiac output. At the same time, over- and underpumping were eliminated. Physiological control is believed to improve the quality of life of tVAD patients and to reduce adverse event rates by providing appropriate perfusion of the organs. Therefore, the SP controller will in the future promote the tVAD treatment as a viable alternative to heart transplantation.

We confirm herewith that all named authors were fully involved in this study and in the preparation of the manuscript. Concept/design: AP, GO, RA, and MSD; data analysis/interpretation: AP, GO, RA, MSD, and PP; drafting article: AP, GO, RA, and MSD; critical revision of article: AP, GO, PP, MR, MM, and MSD; and approval of article: AP, GO, RA, PP, MR, MM, and MSD.

Conflict of Interest: The authors declare no conflict of interest

REFERENCES

1. Hall JE, Guyton AC. *Textbook of Medical Physiology*. London, UK: Saunders, 2011.
2. Mendez GF, Cowie MR. The epidemiological features of heart failure in developing countries: a review of the literature. *Int J Cardiol* 2001;80:213–9.
3. McMurray JJ, Adamopoulos S, Anker SD, et al. ESC guidelines for the diagnosis and treatment of acute and chronic heart failure 2012. *Eur J Heart Fail* 2012;14:803–69.
4. Garbade J, Barten MJ, Bittner HB, Mohr FW. Heart transplantation and left ventricular assist device therapy: two comparable options in end-stage heart failure? *Clin Cardiol* 2013;36:378–82.
5. Kirklin JK, Naftel DC, Pagani FD, et al. Seventh INTERMACS annual report: 15,000 patients and counting. *J Heart Lung Transplant* 2015;34:1495–504.
6. Timms D. A review of clinical ventricular assist devices. *Med Eng Phys* 2011;33:1041–7.

7. Mancini D, Colombo PC. Left ventricular assist devices: a rapidly evolving alternative to transplant. *J Am Coll Cardiol* 2015;65:2542–55.

8. Schumer EM, Ising MS, Slaughter MS. The current state of left ventricular assist devices: challenges facing further development. *Expert Rev Cardiovasc Ther* 2015;13:1–9.

9. Argiriou M, Kolokotron SM, Sakellaridis T, et al. Right heart failure post left ventricular assist device implantation. *J Thorac Dis* 2014;6:S52.

10. Moazami N, Dembitsky WP, Adamson R, et al. Does pulsatility matter in the era of continuous-flow blood pumps? *J Heart Lung Transplant* 2014;34:999–1004.

11. AlOmari AHH, Savkin AV, Stevens M, et al. Developments in control systems for rotary left ventricular assist devices for heart failure patients: a review. *Physiol Meas* 2013;34:R1–R27.

12. Chang Y, Gao B, Gu K. A model-free adaptive control to a blood pump based on heart rate. *ASAIO J* 2011;57:262–7.

13. Endo G, Kojima K, Nakamura K, Matsuzaki Y, Onitsuka T. The meaning of the turning point of the index of motor current amplitude curve in controlling a continuous flow pump or evaluation of left ventricular function. *Artif Organs* 2003;27:272–6.

14. Karantonis DM, Lim E, Mason DG, Salamonsen RF, Ayre PJ, Lovell NH. Noninvasive activity-based control of an implantable rotary blood pump: Comparative software simulation study. *Artif Organs* 2010;34:E34–45.

15. AlOmari AHH, Javed F, Savkin AV, et al. Non-invasive measurements based model predictive control of pulsatile flow in an implantable rotary blood pump for heart failure patients. Proceedings of the 19th Mediterranean Conference on Control and Automation, IEEE, Corfu, Greece, 2011, pp. 491–6.

16. Vollkron M, Schima H, Huber L, Benkowski R, Morello G, Wieselthaler G. Development of a reliable automatic speed control system for rotary blood pumps. *J Heart Lung Transplant* 2005;24:1878–85.

17. Lim E, Alomari AHH, Savkin AV, et al. A method for control of an implantable rotary blood pump for heart failure patients using noninvasive measurements. *Artif Organs* 2011;35:E174–80.

18. Gaddum NR, Stevens M, Lim E, et al. Starling-like flow control of a left ventricular assist device: In vitro validation. *Artif Organs* 2014;38:E46–56.

19. Kwan-Gett C, Crosby M, Schoenberg A, Jacobsen S, Kolff W. Control systems for artificial hearts. *ASAIO J* 1968;14:284–90.

20. Arndt A, Nüsser P, Graichen K, Müller J, Lampe B. Physiological control of a rotary blood pump with selectable therapeutic options: control of pulsatility gradient. *Artif Organs* 2008;32:761–71.

21. Wang Y, Koenig SC, Slaughter MS, Giridharan GA. Rotary blood pump control strategy for preventing left ventricular suction. *ASAIO J* 2015;61:21–30.

22. Saito I, Ishii K, Isoyama T, et al. Preliminary study of physiological control for the undulation pump ventricular assist device. Proceedings of 32nd Annual International IEEE Conference on Engineering in Medicine and Biology Society, IEEE, Buenos Aires, Argentina, 2010, pp. 5218–21.

23. Ochsner G, Amacher R, Wilhelm MJ, et al. A physiological controller for turbodynamic ventricular assist devices based on a measurement of the left ventricular volume. *Artif Organs* 2013;38:527–38. ISSN 0160-564X.

24. Bullister E, Reich S, Sluetz J. Physiologic control algorithms for rotary blood pumps using pressure sensor input. *Artif Organs* 2002;26:931–8.

25. Mansouri M, Salamonsen RF, Lim E, Akmeliawati R, Lovell NH. Preload-based Starling-like control for rotary blood pumps: numerical comparison with pulsatility control and constant speed operation. *PLoS ONE* 2015;10:e0121413.

26. Ochsner G, Amacher R, Amstutz A, et al. A novel interface for hybrid mock circulations to evaluate ventricular assist devices. *IEEE Trans Biomed Eng* 2013;60:507–16.

27. Colacino FM, Moscato F, Piedimonte F, Arabia M, Danieli GA. Left ventricle load impedance control by apical VAD can help heart recovery and patient perfusion: a numerical study. *ASAIO J* 2007;53:263–77.

28. Klabunde R. *Cardiovascular Physiology Concepts*. Philadelphia, PA: Lippincott Williams & Wilkins, 2011.

29. Moscato F, Vollkron M, Bergmeister H, Wieselthaler G, Leonard E, Schima H. Left ventricular pressure–volume loop analysis during continuous cardiac assist in acute animal trials. *Artif Organs* 2007;31:369–76.

30. Wu Y, Allaire P, Tao G, Wood H, Olsen D, Tribble C. An advanced physiological controller design for a left ventricular assist device to prevent left ventricular collapse. *Artif Organs* 2003;27:926–30.

31. Casas F, Orozco A, Smith WA, De Abreu-Garcia J, Durkin J. A fuzzy system cardio pulmonary bypass rotary blood pump controller. *Expert Syst Appl* 2004;26:357–61.

32. Giridharan GA, Pantalos GM, Gillars KJ, Koenig SC, Skliar M. Physiologic control of rotary blood pumps: an in vitro study. *ASAIO J* 2004;50:403–9.

33. Troughton RW, Ritzema J, Eigler NL, et al. Direct left atrial pressure monitoring in severe heart failure: long-term sensor performance. *J Cardiovasc Transl Res* 2011;4:3–13.

34. Stevens MC, Gaddum NR, Pearcy M, et al. Frank-Starling control of a left ventricular assist device. Proceedings of the IEEE Conference on Engineering in Medicine and Biology Society, IEEE, Boston, MA, 2011, pp. 1335–8.

35. Bakouri MA, Salamonsen RF, Savkin AV, AlOmari AHH, Lim E, Lovell NH. A sliding mode-based starling-like controller for implantable rotary blood pumps. *Artif Organs* 2014;38:587–93.

36. Verbeni A, Fontana R, Silvestri M, et al. An innovative adaptive control strategy for sensorized left ventricular assist devices. *IEEE Trans Biomed Circuits Syst* 2014;8:660–8.

37. Casas F, Ahmed N, Reeves A. Minimal sensor count approach to fuzzy logic rotary blood pump flow control. *ASAIO J* 2007;53:140–6.

38. Choi S, Boston JR, Antaki JF. Hemodynamic controller for left ventricular assist device based on pulsatility ratio. *Artif Organs* 2007;31:114–25.

39. Pauls JP, Stevens MC, Bartnikowski N, Fraser JF, Gregory SD, Tansley G. Evaluation of physiological control systems for rotary left ventricular assist devices: an in-vitro study. *Ann Biomed Eng* 2016;1–11.

40. Goldstein D, Oz M. *Cardiac Assist Devices*. New York: Wiley-Blackwell, 2000.

41. Naiyanetr P, Moscato F, Vollkron M, et al. Estimation of cardiac contractility during rotary blood pump support using an index derived from left ventricular pressure. IFMBE Proceeding EMBEC08 4th European Medical & Biological Engineering Conference, IFMBE European Conference on Biomedical Engineering. Springer, Antwerp, Belgium, pp. 1885–8.

42. Naiyanetr P, Moscato F, Vollkron M, Zimpfer D, Wieselthaler G, Schima H. Continuous assessment of cardiac function during rotary blood pump support: a contractility index derived from pump flow. *J Heart Lung Transplant* 2010;29:37–44.

43. Quiñones MA, Gaasch WH, Alexander J. Influence of acute changes in preload, afterload, contractile state and heart rate on ejection and isovolumic indices of myocardial contractility in man. *Circulation* 1976;53:293–302.

44. Amacher R, Ochsner G, Ferreira A, Vandenberghe S, Schmid Daners M. A robust reference signal generator for synchronized ventricular assist devices. *IEEE Trans Biomed Eng* 2013;60:2174–83.

45. Konieczny G, Opilski Z, Pustelny T, Gacek A, Gibinski P, Kustosz R. Results of experiments with fiber pressure

sensor applied in the Polish artificial heart prosthesis. *Acta Phys Pol A* 2010;118:1183–5.

46. Zhou MD, Yang C, Liu Z, Cysyk JP, Zheng SY. An implantable Fabry-Pérot pressure sensor fabricated on left ventricular assist device for heart failure. *Biomed Microdevices* 2012;14:235–45.

47. Potkay JA. Long term, implantable blood pressure monitoring systems. *Biomed Microdevices* 2008;10:379–92.

48. Abraham WT, Adamson PB, Hasan A, et al. Safety and accuracy of a wireless pulmonary artery pressure monitoring system in patients with heart failure. *Am Heart J* 2011; 161:558–66.

49. Stevens MC, Wilson S, Bradley A, Fraser J, Timms D. Physiological control of dual rotary pumps as a biventricular assist device using a master/slave approach. *Artif Organs* 2014;38:766–74.

Biomedical Physics & Engineering Express

PAPER

Acute changes in preload and the QRS amplitude in advanced heart failure patients

Seraina Anne Dual[1,5] , Panagiotis Pergantis[2,3,5] , Felix Schoenrath[2,3], Julian Keznickl-Pulst[2], Volkmar Falk[2,3,4], Mirko Meboldt[1] and Marianne Schmid Daners[1]

[1] Product Development Group Zurich, Department of Mechanical and Process Engineering, ETH Zurich, Zurich, Switzerland
[2] Department of Cardiothoracic and Vascular Surgery, German Heart Center Berlin, Berlin, Germany
[3] DZHK (German Centre for Cardiovascular Research), Partner Site Berlin, Germany
[4] Department of Cardiothoracic Surgery, Charité-Universitätsmedizin Berlin, Corporate Member of Freie Universität Berlin,
    Humboldt- Universität zu Berlin and Berlin Institute of Health Berlin, Germany
[5] These authors contributed equally.

E-mail: seraina.dual@alumni.ethz.ch

Abstract

To date, only invasive monitoring methods are available for continuous monitoring of the volume status of heart failure (HF) patients. The literature suggests that left ventricular (LV) volume status can in part be deduced from the electrocardiogram in healthy individuals in the experimental setting. The aim of this study was to evaluate if short-term changes in cardiac preload can be deduced from the QRS amplitude in advanced HF patients. We examined 19 non-decompensated advanced HF patients, listed for heart transplantation or in the process of evaluation for advanced HF treatment, during a leg raising maneuver. Electrocardiac (leads I, II, and V6) data was collected continuously in all patients along with preload indicators available in every specific patient: central venous pressure (n = 11), pulmonary arterial pressure (n = 9), pulmonary wedge pressure (n = 9), mitral inflow Doppler wave velocity (E- wave) (n = 17), and LV volume (n = 7). During leg raising, the increase of cardiac preload was significant with an increase in the E wave of $0.09 \, \text{m s}^{-1}$ (p = 0.029), but a change in LV volume or the QRS amplitude was not observed. In patients with a Swan-Ganz catheter, however, a statistically significant negative correlation between the mean pulmonary arterial pressure and the QRS amplitude in V6 and II was found with correlation coefficient (R) and 95% confidence intervals of R = −0.28 (−0.49, −0.04) and R = −0.29 (−0.50, −0.05), respectively. Although the identified correlation is not very strong, the findings of this study in advanced HF patients are in accordance with experimental data recorded in healthy individuals. The findings support the further investigation in settings where greater, acute LV volume changes are probable, such as in HF patients with mechanical circulatory support.

1. Introduction

Hemodynamic monitoring forms the basis of clinical decision-making in patients with cardiovascular disease. Cardiac preload is defined as the stretching of the cardiomyocytes directly before contraction and influences the cardiac output, according to the Frank-Starling law (Sequeira and van der Velden 2015). In the clinical setting, it is equivalent to either left ventricular (LV) end-diastolic volume or pressure. Therapeutic interventions, such as diuretic therapy, aim at optimizing cardiac preload, as a means of augmenting cardiac output and relieving symptoms. Goal directed therapy (Dellinger *et al* 2013, Stephens and Whitman 2015, Chong 2018) stresses the significance of hemodynamic monitoring; Interventions on fluid management should be based on objective, reliable and preferably continuous parameters in patients with critical conditions, such as sepsis, cardiogenic shock or after cardiac surgery (Osawa *et al* 2015, Levy *et al* 2018). Current clinical methods, used in the in-patient setting, typically evaluate preload at one specific point in time or with invasive measurements only (Fischer *et al* 2013, Bednarczyk *et al* 2017).

Invasive methods provide continuous hemodynamic data such as central venous pressure (CVP), pulmonary capillary wedge pressure (PCWP), pulmonary arterial pressure (PAP), or respiratory arterial pulse pressure variations. Unavoidably, the pressure catheter needs to be inserted invasively before the investigation via central veins or in arteries. Recent examples include the measurement of the PAP with the implantable pressure sensor CardioMEMS[TM] HF System (Abbott, Atlanta, GA, USA) (Magalski *et al* 2002). Patients whose treatment was based on data provided from CardioMEMS had lower re-hospitalization rates (Abraham *et al* 2011). Furthermore, continuous echocardiographic LV volume measurement has become available through a miniaturized transesophageal probe (Begot *et al* 2015).

Non-invasive methods are well established, but provide mostly non-continuous data, and thus, are limited in their usefulness for continuous monitoring. Among them are transthoracic or intermittent echocardiographic measurements of the end-diastolic LV volume or the diameter of the inferior vena cava (Yavasi *et al* 2014). Bio-impedance spectroscopy is non-invasively measured on the body surface, provides a continuous measurement, and hence is a promising candidate for the monitoring of volume status in heart failure (Weyer *et al* 2014, Saporito *et al* 2017). Its clinical utility remains limited, since the measurement method is not widely available in clinics and practices. On the contrary, the measurement of the thoracic impedance through pacemaker (PM) leads (OptiVol—Medtronic, Minneapolis, MN, USA) (Porterfield *et al* 2011) has been used as a remote monitoring parameter in heart failure (HF), but it requires the implantation of a device. Clinical studies have investigated automated data-driven monitoring techniques based on existing non-invasive hemodynamic parameters, which have yet to be widely applied (Vakily *et al* 2017). A clinically available method for non-invasive, continuous measurement of the volume status remains to become established.

The QRS amplitude has been previously investigated as a monitoring parameter for the long-term course of heart failure (HF) (Madias 2007) and transplantation (Eubel *et al* 2001), which is associated with but not limited to changes in volume status. A physics-based relationship between the QRS amplitude of the electrocardiogram (ECG) and the LV end-diastolic volume was first proposed in the 1950s by Brody *et al* (Brody 1956). Previous experimental studies in healthy animals and healthy humans have found contradicting results. Some studies suggest a correlation between the LV volume and the amplitude of the QRS complex or of the R-wave (Ishikawa *et al* 1979, Ishikawa *et al* 1983, Feldman *et al* 1985, Vitolo *et al* 1987, Vancheri and Barberi 1989); others could not confirm the correlation (Caiani *et al* 2013). Further, the directionality of the correlations was negative in some cases (Ishikawa *et al* 1979, Ishikawa *et al* 1983,

Vitolo *et al* 1987, Vancheri and Barberi 1989, Giraud *et al* 2013, Fresiello *et al* 2014) and positive in others (Feldman *et al* 1985). In all studies, the relationship has only been assessed in the short term and within subject; as the Brody effect appears to be based on a physical rather than physiological effect. The limited reproducibility of these results raises questions regarding the impact of confounders such as the position and movement of the heart in the thorax, the respiratory artefacts, the overall thoracic impedance, and the hematocrit.

The Brody effect has yet to be measured and evaluated in advanced HF patients. Advanced HF patients have altered hemodynamics compared to healthy individuals: LV and intravascular volume, myocardial contractility, and electrophysiological characteristics, e.g. paced rhythm. If the physics-based relationship described was confirmed in advanced HF patients in the acute setting, the relationship found could aid the continuous assessment of the volume status. The ECG is most widely available in the in-patient setting of every hospital as well as in most practices, while the recent integration in wearable accessories presents with future possibilities (Turakhia *et al* 2019). Data-driven algorithms, as described before (Meyer *et al* 2018), currently portray little understanding on which data is used for the prediction. The integration of the correlation between the volume status and the QRS amplitude has the potential to augment the efficacy of these automated surveillance systems.

This study investigated the relationship between acute changes in cardiac preload and the QRS amplitude measured with surface ECG in advanced HF patients, listed for heart transplantation or in the process of evaluation for advanced heart failure treatment. A passive leg raising (PLR) maneuver was performed in a group of advanced HF patients, during which electrocardiographic (ECG leads I, II and V6), hemodynamic and respiratory data were recorded. The maneuver was intended to provoke a volume shift from the lower half of the body into the thorax, therefore causing an increase in cardiac preload. Positive results would support the introduction of this parameter as a monitoring modality for the volume status of HF patients. This study is the first to show a significant correlation between cardiac preload as expressed through mean pulmonary arterial pressure (mPAP) and QRS amplitude from the surface ECG in nine HF patients.

2. Methods

2.1. Study design and population
The present study is a prospective, single-center clinical study involving 19 advanced HF patients. The study was approved by the ethics committee of the Charité Universtitätsmedizin Berlin, Germany (EA2/092/17) and informed consent was given by all participants. Patients were enrolled while presenting

Table 1. The three phases of the experiment.

	Phase		Leg angle	Duration
	0	Neutral, supine position	0°	4−6 min
	1	Passive leg raising	45°	3−6 min
	2	Neutral, supine position	0°	3−5 min

with non-decompensated advanced HF in the German Heart Center Berlin (DHZB). All patients were either in the evaluation process for heart transplantation and left ventricular assist device (LVAD) implantation, or already on the waiting list for a heart transplantation. Independent of the present study, in some patients a Swan-Ganz catheter (PAC) (Edwards Lifesciences Corporation, Irvine, CA, USA) was placed as part of the evaluation procedure such that its recordings were included in the study. A PAC is a soft catheter with an expandable balloon tip, placed in the pulmonary artery through the right heart and used for measuring pressures continuously in the right atrium and the pulmonary artery. The pulmonary capillary wedge pressure (PCWP), regularly used as an equivalent to the LV filling pressure is measured intermittently.

The experiment consisted of an adapted form of passive leg raising (PLR). The PLR is a positioning maneuver for autotransfusion, intended to provoke a volume shift from the lower half of the body into the thorax. As long as the right ventricle can adapt to the increased preload, the LV volume increases. Depending on the volume status of the patient's venous reservoir a shift of 150–450 ml of blood can be achieved (Monnet and Teboul 2015). As described by Pozzoli *et al* (Pozzoli *et al* 1997), a significant increase in LV volume in HF patients is possible by the PLR. The PLR was adapted slightly from its original form, with the intention of minimizing the relative movement of the heart in the thorax, bearing in mind the risk of being less effective in terms of volume displacement from the lower half of the body to the thorax. Traditionally the PLR is performed with a tilt of the patients' bed, so that the lower half of the body including the abdomen can be elevated in regard to the upper half. In our study, only the legs of the patients were raised and were placed on pillows. The main benefit of PLR is that it keeps the overall volume status and the blood composition constant, compared to previous studies of the QRS amplitude during hemodialysis (Ishikawa *et al* 1979, Vitolo *et al* 1987), hemorrage (Giraud *et al* 2013) or visits to the sauna (Ishikawa *et al* 1983).

The study design had three phases (table 1). In Phase 0, the patients laid on the patient bed on their back with a slight tilt to the left side in order to optimize echocardiographic conditions. The upper body was elevated from the horizontal position (~30°) during

the entire study. In Phase 1, only the lower extremities of the patients were raised by 45°, allowing the thorax and abdomen to stay in a stable position. In Phase 2, the lower extremities of the patients were returned to the initial position. Data recording was synchronized over the three phases between all devices. In every phase, three datasets were collected with a total of nine measurements for most parameters (continuously recorded parameters and LV volume data). The goal was to complete all three sets of measurements and achieve steady state by the last measurement of each phase. Therefore, the examiner aimed for a total duration of five minutes per phase. Considering the hemodynamic stability and well-being of the patient, slight differences in the exact duration of the phases occurred, with a duration range among the patients as reported in table 1.

2.2. Data acquisition

2.2.1. Echocardiography

The echocardiographic recordings of the LV end-diastolic volume (n = 7) were performed transthoracically in the 4-chamber and 2-chamber view. During collection of the echocardiographic data, the upper body of the patients remained stable. At the end of each phase, the following additional data was collected (n = 17): distance between the LV apex and the thoracic body surface (Feldman *et al* 1985) as an indicator of the stable position of the heart relative to the thorax; the ratio of peak velocity blood flow over the mitral valve in early diastole (E wave) to peak velocity flow in late diastole (E/A ratio); and the ratio of the E wave to the wall velocity at the lateral mitral valve annulus (E/E′) as an indicator of mitral flow and LV filling. An additional optimized 4-chamber view for the right ventricle was recorded at the end of each phase for the measurement of the right ventricular end-diastolic diameters ($RVEDD_1$, $RVEDD_2$). Further, we measured the diameter of the inferior vena cava (VCI) during normal breathing at the end of each phase. The echocardiographic recordings were taken with a Vivid S70 ultrasound device (GE Healthcare, Milwaukee, WI, USA). Maintaining a constant echocardiographic axis and thorax position in all phases of the study was favored over the echocardiographic data quality. The measurements were conducted by a

3

second examiner using IntelliSpace Cardiovascular 2.2 (Philips Medical Systems, Best, The Netherlands).

2.2.2. Electrocardiography

Continuous ECG of the leads V6, I and II was recorded during all phases at a frequency of 300 Hz at a resolution of 1 μV. A 10-lead ECG was placed at standard locations on the patient's thorax. The peripheral leads of the lower extremities were placed on the lower thorax in order to reduce movement artefacts, which could arise during PLR. All continuous data was acquired using a GE Patient monitor B850 (GE Healthcare, Milwaukee, WI, USA), which was connected to a laptop via USB. The signals were recorded with two simultaneously running versions of Collect (Datex-Ohmeda, S/5 Collect-System, GE Healthcare, Milwaukee, WI, USA). The number of recordable ECG leads was restrained to three by the data transmission rate of the hardware connection between monitor and laptop. The normal QRS axis in healthy individuals is between $-30°$ and $+90°$ generating large positive QRS amplitudes in Leads I (0°) and II (60°) (Surawicz and Knilans 2008); these two leads have also been successfully used in previous studies regarding changes in the QRS amplitude (Vancheri and Barberi 1989, Madias 2007, Kataoka and Madias 2011). We chose these two leads, as it was impossible to anticipate the incidence of axis deviations and bundle branch blocks in our cohort of mostly paced HF patients. Lead V6 was chosen as the third lead, because the QRS amplitude in the precordial leads is more influenced by the relative movement of the LV wall to the thorax (Feldman *et al* 1985), and because of the proximity of V6 to the cardiac apex.

Relative thoracic impedance (ΔZ) was derived by the GE monitor using both electrodes of Lead II and the signal was sampled at 25 Hz. The heart rate (HR) was computed by the GE module every 10 s. Additionally to the surface ECG, print-outs of the ECG recorded by the PM leads were obtained in each phase for all patients with such a device. The printouts typically featured 9–10 QRS complexes, which were manually measured to obtain the intra-thoracic QRS amplitude collected from the leads of the implanted PM devices (Medtronic, Minneapolis, MN, USA; BIOTRONIK GmbH & Co. KG, Erlangen, Germany).

2.2.3. Hemodynamic and respiratory data

Hemodynamic and respiratory data was acquired continuously from a PAC, if applicable (n = 9), and from a respiratory module (E-sCOVX-Modul, GE Healthcare, Milwaukee, WI, USA) for all patients (n = 17). Patients were asked to breathe through the mouthpiece of the respiratory module during the entire experiment. Tidal volume (TV_{insp}) was acquired at 0.1 Hz, while the concentration of carbon dioxide (CO_2) was recorded at 100 Hz. The availability of a PAC was independent of the study and the PAC was inserted prior to the study in patients who required it

as part of the (re-)evaluation process for heart transplantation. The reference pressure was measured at constant chest height, which was not altered between the phases. The PAC obtained systolic (sPAP), diastolic (dPAP) and mean pulmonary arterial pressure (mPAP), and central venous pressure (CVP) by measuring continuously at 0.1 Hz. PCWP was obtained once, at the end of each phase. Manual blood pressure (BP_{med}) values were obtained in every phase with a cuff attached to the left upper arm.

2.3. Data processing

Time-series data of the continuous recordings were post-processed semi-automatically with MATLAB (R2018a, The Mathworks Inc., Natick, MA, USA). The beat-wise QRS amplitude was derived from the peak maxima and peak minima of the QRS complex. If either maxima or minima was undefined, its value was replaced by the value of the isoelectric line. The detection of the QRS amplitude for each patient was verified by a clinical practitioner in one heart-beat and subsequently repeated automatically for the remaining heartbeats. Figure 1 shows two examples for QRS amplitude detection in a patient with and a patient without PM. Beat-wise QRS amplitudes were subsequently averaged over 10 s. The thoracic impedance signal was filtered with a Gauss filter of the 6th order and a cut-off frequency of 0.05 Hz. All other continuous data such as CO_2, HR and hemodynamic parameters were averaged over 10 s, provided their sampling frequency exceeded 0.1 Hz.
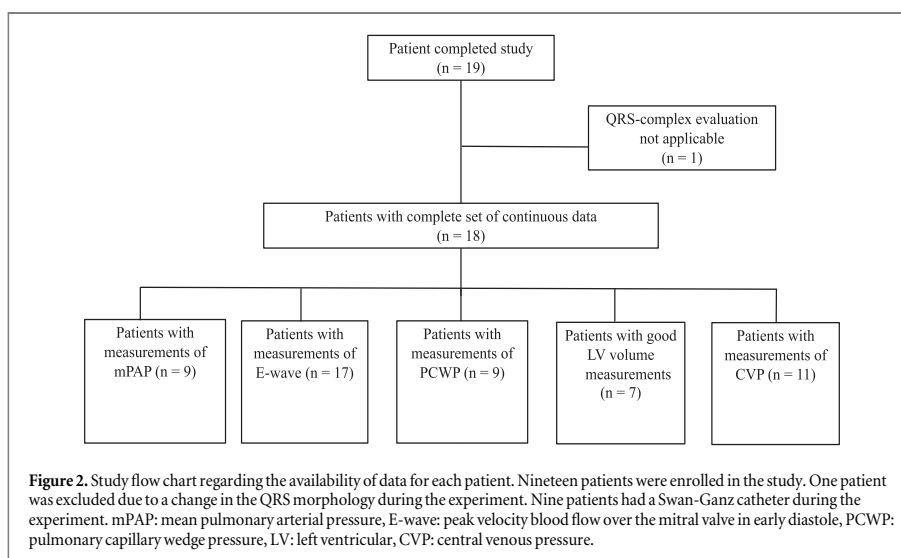
2.4. Statistical analysis

All statistical analyses were conducted with R, Version 3.3.1 (R Core Team 2016. R: A language and environment for statistical computing. R Foundation for Statistical Computing, Vienna, Austria). Categorical variables are presented as numbers and percentages, and continuous variables as median and interquartile range (IQR) unless otherwise stated. Differences between two independent groups were examined by the χ2-test and Fisher's exact test for categorical variable, and by the Mann-Whitney U test for continuous variables. The Friedman test was used for differences among the three phases (Phase 0, 1 and 2). The correlation between mPAP and QRS amplitude was analyzed by means of repeated measures correlation (Bakdash and Marusich 2017) per individual for each phase and tested against the null-hypothesis of the slope being zero. All tests are two-sided and explorative in nature. Therefore, p-values were not adjusted for multiple testing and were considered significant at p-value < 0.05.

3. Results

3.1. Patient characteristics

Nineteen advanced HF patients in the process or already being listed for heart transplantation were

Figure 1. Extraction of the beat-wise QRS amplitude in (a) native heart rhythm and (b) paced heart rhythm. In (a) the QRS amplitude was derived from the peak maxima (circle) and peak minima (cross) of the QRS complex and in (b) between the peak minima (cross) and the isoelectric line (double circle). (c) Example of continuously collected data (unbroken) over a time period of 20 s. The average value for relative impedance (ΔZ) is shown (dashed). ECG: electrocardiogram leads I, II and V6, $C0_2$: carbon dioxide.

Figure 2. Study flow chart regarding the availability of data for each patient. Nineteen patients were enrolled in the study. One patient was excluded due to a change in the QRS morphology during the experiment. Nine patients had a Swan-Ganz catheter during the experiment. mPAP: mean pulmonary arterial pressure, E-wave: peak velocity blood flow over the mitral valve in early diastole, PCWP: pulmonary capillary wedge pressure, LV: left ventricular, CVP: central venous pressure.

included in this study. One patient had to be excluded from the analysis because of a sudden change in the heart rhythm during the experiment. A PAC was available in nine of the remaining 18 patients. LV volume data from seven patients was incorporated into the analysis (figure 2), considering the limited quality of the echocardiographic data in the other cases.

Table 2 lists the most relevant demographics. Fifteen patients were male and four female. Their median and interquartile range age was 53 [43, 60] years. All

patients had dilated cardiomyopathy, in 26% of ischemic etiology. The majority of the patients had a normal to mildly reduced right heart ejection fraction (49%). In 68% of the patients, the rhythm was triggered by a pacemaker.

3.2. Preload
An increase in all pressure measurements, as well as the mitral inflow (E wave) was observed during PLR (see table 3), while the geometric echocardiographic

Table 2. Patient characteristics: demographics, heart failure and electrocardiogram (ECG). Assessments in percentage (%) with respect to all 19 patients. We depict median and interquartile range.

Patient characteristics		
Demographics		
Sex (number)	Female	4
	Male	15
Age (y)		53 [43, 60]
BMI (kg m^{-2})		28.1 [25, 31.2]
Heart failure		
Etiology		
Dilated cardiomyopathy (%)		
	Idiopathic	36.8
	Inflammatory	31.6
	Toxic	5.3
Ischemic cardiomyopathy (%)		26.3
RVEF (%)		
	Normal	47
	Mildly reduced	42
	Moderately reduced	11
Pro- BNP (ng ml^{-1})		2060 [855, 3659]
Creatinine (mg dl^{-1})		1.2 [0.9, 1.45]
Hematocrit (%)		42.9 [40.9, 46.8]
Beta-blocker (%)		78.9
Amiodarone (%)		52.6
ECG		
Pacemaker triggered rhythm (number)		12
	Biventricular pacing	11
	Atrial sensing and univentricular pacing	1

BMI: Body mass index, NYHA: New York Heart Failure Association, RVEF: right ventricular ejection fraction, CRT: cardiac resynchronization therapy.

Table 3. Effect of the passive leg raising (PLR) on all collected preload indices. Statistically significant changes in mPAP, CVP, PCWP, E Wave, E/A and E/E'. We depict median and interquartile ranges.

	N	Phase 0	Phase 1	Phase 2	p_{all}	p_{01}	p_{12}	p_{02}
Swan-Ganz catheter								
mPAP (mmHg)	10	30.3 [16.4, 35.8]	32.8 [20.9, 38.6]	31.7 [19.2, 40]	0.014	0.011	ns	ns
CVP (mmHg)	11	6 [0, 10]	9 [2, 12]	5 [1, 8]	0.009	ns	0.011	ns
PCWP (mmHg)	9	11 [8, 21]	17 [12, 28.5]	11 [9.5, 22]	0.001	0.003	0.003	ns
Transthoracic echocardiography								
LVV (mL)	8	251 [216, 283]	233 [213, 262]	247 [227, 283]	ns	ns	ns	ns
E Wave (m s^{-1})	17	0.72 [0.61, 0.94]	0.81 [0.66, 1.13]	0.75 [0.54, 1.02]	0.015	0.029	0.012	ns
E/A ($\sim$)	16	1.55 [0.75, 2.02]	1.71 [0.8, 2.4]	1.36 [0.74, 2]	0.002	ns	0.003	0.020
E/E' ($\sim$)	17	12.9 [8.4, 16.8]	11.8 [9.3, 18]	13.5 [9.3, 19.3]	0.047	ns	ns	0.029
VCI (mm)	13	13 [10.5, 17]	14 [10.5, 16]	14 [11.5, 16.5]	ns	ns	ns	ns
RVEDD$_1$ (mm)	12	38.5 [33, 48.8]	40 [35.8, 53.3]	36 [30, 46.5]	ns	ns	ns	ns
RVEDD$_2$ (mm)	10	28 [22.8, 32.5]	27 [23.8, 33]	25.5 [18.8, 27.3]	ns	ns	ns	ns

p_{all}: p-value over all three phases, p_{01}: p-value between Phase 0 to Phase 1, p_{12}: p-value between Phase 1 to Phase 2, p_{02}: p-value between Phase 0 and Phase 2. mPAP: mean pulmonary arterial pressure, CVP: central venous pressure, PCWP: pulmonary capillary wedge pressure, VCI: vena cava inferior, RVEDD$_1$: right ventricular end-diastolic diameter one, RVEDD$_2$: right ventricular end-diastolic diameter two, N: number of patients, ns: not significant.

measurements, for example LV volume, remained unchanged (see table 4). In the entire patient cohort, the statistically significant increase of the mitral inflow of 0.09 m s^{-1} suggests an increase in LV volume ($p_{01} = 0.029$) (see figure 3(a)). In the subgroup of patients with a PAC, a statistically significant increase in mPAP of 1.5 mmHg ($p_{01} = 0.011$) (see figure 3(b))

and in PCWP of 6 mmHg ($p_{01} = 0.003$) (see figure 3(c)) from Phase 0 to Phase 1 was noted, and a significant change was also noted for CVP over all phases ($p_{all} = 0.009$). All changes were reversible since there was no significant difference in these values between Phase 0 and Phase 2. On the contrary, no increase was noted in the LV volume among the
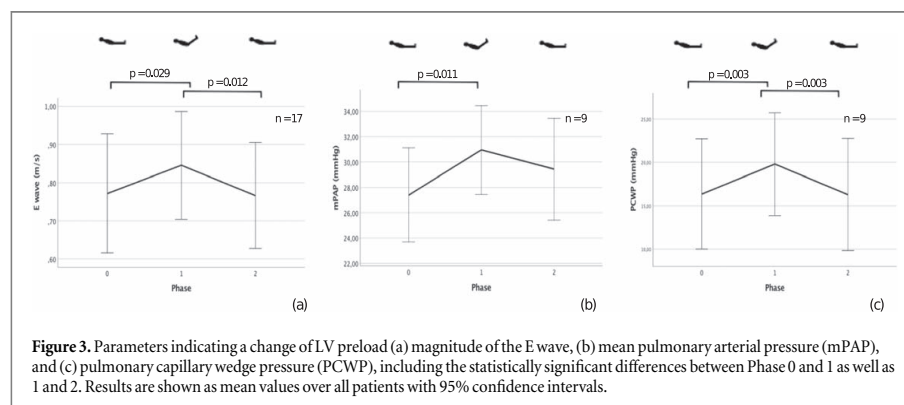
Figure 3. Parameters indicating a change of LV preload (a) magnitude of the E wave, (b) mean pulmonary arterial pressure (mPAP), and (c) pulmonary capillary wedge pressure (PCWP), including the statistically significant differences between Phase 0 and 1 as well as 1 and 2. Results are shown as mean values over all patients with 95% confidence intervals.

Table 4. The possible confounders of the relationship between the QRS amplitude and cardiac preload. No changes were seen in any parameter during passive leg raising (PLR). We depict median and interquartile ranges.

	N	Phase 0	Phase 1	Phase 2
Monitoring data				
HR (bpm)	19	73 [66.2, 82]	73.2 [66.3, 81.8]	70.3 [66, 81.5]
Impedance (mΩ)	18	-20 [-92, 49.3]	-51.1 [-328.3, 17.7]	121.1 [-136, 312.7]
TV_{insp} (mL)	14	438.6 [275.7, 664]	371.2 [286.8, 499]	292.8 [267.8, 493.1]
BP_{med} (mmHg)	16	75 [66.8, 82.8]	74 [65, 84]	75 [63.3, 84.3]
Transthoracic echocardiography				
Thorax-apex distance (mm)	18	30.5 [26, 35.5]	31 [27.8, 34.5]	29.5 [26.8, 36.3]

HR: heart rate, TV_{insp}: inspiratory tidal volume, BP_{med}: mean blood pressure, N: number of patients.

patients included in the analysis. Further echocardiographic parameters of volume status, such as $RVEDD_1$, $RVEDD_2$ and VCI remained unchanged, indicating that the additional volume coming from the legs during PLR does not accumulate in the right ventricle or vena cava.

3.3. Physiological monitoring

The evaluated confounding factors remained unchanged during the experiment. HR, impedance, TV_{insp}, BP_{med} and echocardiographic thorax-apex distance did not differ with statistical significance after PLR (table 4). One patient with a sudden increase in HR was excluded from the analysis, due to a rapid change in heart rhythm.

3.4. QRS amplitude

The data processing for the QRS amplitude was straightforward and the signals were stable over the time period of the experiment in all but one patient. Over all patients, no significant changes were noticeable between the Phases 0, 1 and 2 of the PLR in the QRS amplitude in any of the leads I, II or V6 (see table 5). In several patients, reversible changes of the QRS amplitude occurred in Phase 1, but the changes mostly remained within the natural variation (noise) of the QRS amplitude. Finally, yet importantly, no significant difference, but a slightly lower median

value in the QRS amplitude of the intra-thoracic PM ECG (QRS_{pm}, table 5) was noted in Phase 1.

The repeated measures correlation per individual between mPAP and QRS amplitude showed a negative correlation for the two leads V6 and II in the subgroup of patients with PAC (see figure 4). The correlation coefficient (R) with 95% confidence intervals for the leads V6 and II was R = -0.28 (-0.49, -0.04) and R = -0.29 (-0.50, -0.05), respectively, with statistical significance of p = 0.024 (V6) and p = 0.016 (II). The negative changes in QRS amplitude were as high as one milli Volt, which is equivalent to a 20% change for low QRS amplitudes. Six of the nine patients with a PAC also had a triggered rhythm, which could have supported a uniform distribution of values of the QRS amplitude. In lead I, no significant correlation was found. Although changes in the PCWP and E wave were more pronounced than those in the mPAP no statistical significance was seen in the repeated measures correlation analysis. Since there is no apparent physiological explanation for this discrepancy, the reason is probably the single PCWP value and E wave value, compared to three mPAP values, mitigating the level of statistical significance.

3.5. Beat-to-beat analysis

A beat-to-beat analysis was performed to show (1) the natural variability of the QRS amplitude compared to
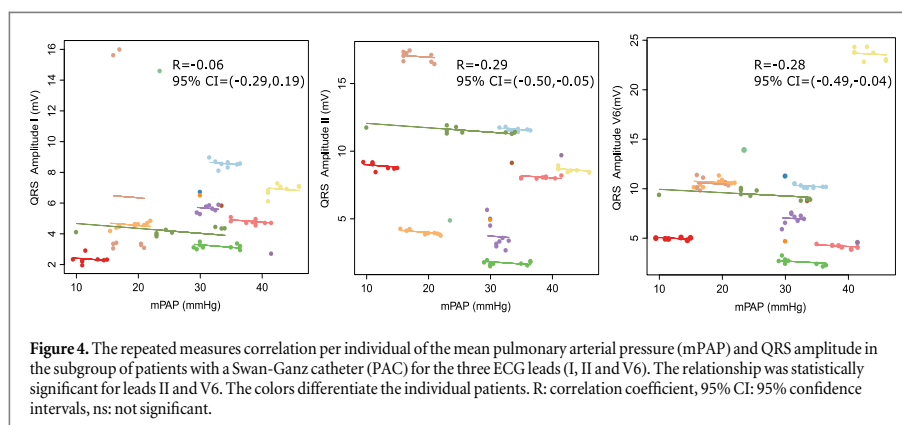
Figure 4. The repeated measures correlation per individual of the mean pulmonary arterial pressure (mPAP) and QRS amplitude in the subgroup of patients with a Swan-Ganz catheter (PAC) for the three ECG leads (I, II and V6). The relationship was statistically significant for leads II and V6. The colors differentiate the individual patients. R: correlation coefficient, 95% CI: 95% confidence intervals, ns: not significant.

Table 5. The QRS response to the PLR. No significant changes were seen in any of the leads V6, I and II.

	N	Phase 0	Phase 1	Phase 2
QRS amplitude V6 (mV)	18	9.33 [4.99, 11.23]	8.93 [5.25, 10.69]	9.65 [5.12, 10.69]
QRS amplitude I (mV)	18	6.55 [4.30, 7.65]	6.44 [4.12, 7.97]	6.31 [3.85, 7.24]
QRS amplitude II (mV)	17	7.82 [4.74, 10.20]	7.73 [4.79, 9.97]	7.53 [4.37, 9.29]
QRS amplitude I + II (mV)	17	13.09 [11.21, 16.79]	13.65 [10.75, 16.50]	13.05 [10.66, 15.50]
QRS_{pm} (mV)	6	6.59 [3.19, 11.52]	6.36 [3.5, 11.3]	6.7 [3.56, 11.06]

QRS_{pm}: QRS amplitude from pacemaker electrocardiogramm.

the observed changes in QRS amplitude during the PLR and (2) the effect of averaging five consecutive heartbeats to account for respiratory changes. The natural variability of the QRS amplitude is similar for a paced and an unpaced rhythm (see figure 5). The variability of the measured QRS amplitude is greater than the changes in QRS amplitude over time in this patient. Averaging the QRS amplitude over five consecutive beats (dark circles) improved the prediction intervals by a factor of two with respect to the raw QRS amplitude (bright circles), as it eliminated artefacts due to the respiration.
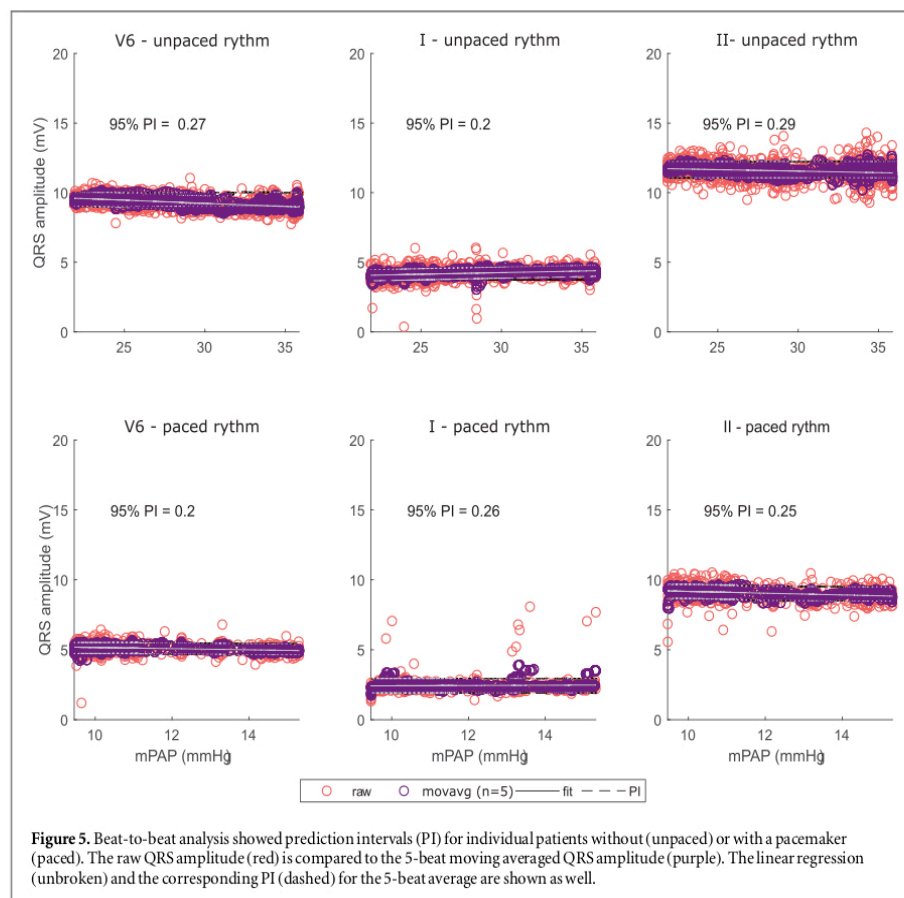
3.6. Subgroup analysis

Insertion of the PAC was completely independent of this study. Since the correlation between mPAP and QRS amplitude could only be evaluated in the patients with a PAC, we performed a descriptive subgroup analysis to investigate possible differences between the two groups (see table A1 in the appendix). To summarize the results, the PAC group was ten years older (p = 0.043) and had a five more breaths per minute respiratory rate (p = 0.019) than the group without a PAC. Both are not considered relevant regarding the hypothesis investigated. No difference was found between the two groups regarding their anti-arrhythmic medication (Amiodarone, Beta blocker).

4. Discussion

The study evaluated the effect of acute preload changes on the QRS amplitude of the surface ECG in advanced HF patients. An increase in cardiac preload was achieved with the PLR, as filling pressures and mitral inflow increased. No change in the QRS amplitude was observed, which might be due to the small relative changes in LV volume induced. However, in the subgroup of patients with a PAC, a negative correlation was detected between mPAP and QRS amplitude in leads V6 and II. Based on these findings, further investigations are foreseen that assess the correlation in HF patients with the potential for bigger LV volume changes than the patient cohort in this study.

The PLR maneuver induced a change in cardiac preload that significantly increased cardiopulmonary pressures as well as mitral inflow. The increase in mitral inflow suggests an augmentation of absolute LV volume (Pozzoli *et al* 1997). However, the echocardiographic measurements of LV volume did not detect a significant increase. Compensatory tachycardia could leave the LV volume unchanged despite higher mitral inflow. No change in the HR was noted, which was expected because of the failing compensatory mechanisms in the advanced stages of HF (Eckberg and Sleight 1992). Considering the advanced dilatation of the ventricles (LV end-diastolic volume = 251 ml), the added volume was probably not sufficient to cause

8

Figure 5. Beat-to-beat analysis showed prediction intervals (PI) for individual patients without (unpaced) or with a pacemaker (paced). The raw QRS amplitude (red) is compared to the 5-beat moving averaged QRS amplitude (purple). The linear regression (unbroken) and the corresponding PI (dashed) for the 5-beat average are shown as well.

a detectable relative augmentation of the LV volume. Furthermore, advanced HF patients mostly have congested cardiovascular systems that operate at the steep part of the Frank-Starling curve. Hence, large increases in cardiopulmonary pressures result in small increases in LV volume only (Sequeira and van der Velden 2015). Indeed patients with a PAC showed reversible changes in mPAP, CVP and PCWP, which confirm the increase in cardiac preload, despite no measurable LV volume increase.

No change in QRS amplitude was seen over all patients during PLR. Since the Brody effect describes the reaction of the QRS amplitude to changes in LV volume, a small or absent relative volume change could explain why there were no observable changes in QRS amplitude. In congested patients, the induced preload changes correlate more with pressure changes than with LV volume changes, such that it must become difficult to use the QRS amplitude as an indicator for preload. Thus, the variability of the QRS amplitude shadowed the small changes in the QRS amplitude induced by the PLR in these patients. In summary, pressure measurement, such as Cardio-Mems, should be preferred over LV volume dependent measurements, such as the QRS amplitude, as a

monitoring modality for acute preload changes in advanced HF patients.

Still, in the nine patients with PAC, the QRS amplitude and the mPAP in leads V6 and II correlated negatively. These results compared well with previous experimental findings in healthy individuals. The detection of a correlation in lead V6 and lead II only, is unexpected as lead I and lead V6 measure in similar direction. Because V6 is measured in close vicinity to the heart, this measurement might therefore be influenced heavily by the positioning of the heart with respect to the thorax. Indeed, Vancheri *et al* (Vancheri and Barberi 1989) have previously omitted the precordial leads, claiming them to be strongly influenced by the position of the heart with respect to the thorax in an attempt to eliminate the positioning effect. Feldmann *et al* (Feldman *et al* 1985) measured full 9-lead ECG and found a correlation of V5 and V6 only, which they explain by the positioning effect, in particular, by a change in the distance of the LV to the thoracic wall. In contrast to Feldman *et al* our study is the first to find a significant correlation in lead II. In summary, the findings in these nine patients provide further evidence of a correlation between preload indicators and QRS amplitude in advanced HF patients and of the effect being observable in precordial and limb

leads. The applicability of this correlation in the clinical setting still remains uncertain, since in this specific patient population the acute LV volume variations are too small to easily be detected by changes in the QRS amplitude.

Since the 1950s many efforts have been made to separate the physical Brody effect (Brody 1956) from possible confounding factors. Our study adressed a series of confounding factors previously described in the literature, such as respiration, impedance, hematocrit, potassium and the positioning of the heart. Impendance did not change before and after PLR: only a transient effect was observed during the movement of the legs. HCT and potassium were very unlikely to change because PLR does not influence blood composition. The positioning of the heart is most difficult to assess, yet the QRS amplitude is highly sensitive to it. An increase in LV volume could lead to changes in the surface ECG through the approximation of the heart walls to the thoracic chest wall. Madias *et al* (Madias 2007, 2014) argue that changes seen in the QRS amplitude of the surface ECG in HF patients are related to the changes of total blood fluid or myocardial edema. Our findings offer an alternative explanation, since the acute preload change should not affect the total body fluid, or the consistency of the myocardial tissue. In summary, the correlations we found can be explained by either the physical Brody effect, the location of f the heart in the thorax or a combination of the two. For the clinical application, however, the most important factor is the observability and reliability of the effect, which could not be confirmed in this heavily congested cohort of advanced HF patients.

This study had the following limitations. The patient selection, although random, happened from a HF patient pool, which is not representative for the entire advanced HF population. The patients, presenting routinely for (re-) evaluation for heart tranplantation or LVAD implantation, fulfill selection criteria outside the scope of our investigation. Overall, we did not see a significant change in QRS amplitude during PLR, since the relative volume changes were small and the non-invasive study design was limited to a preload reference from transthoracic echocardiography, omitting a pressure-volume catheter. As the experiment required the position of the thorax to remain stable, the quality of the echocardiographic data was not optimal. Finally, the ECG derived from print-outs of the PM provided very limited resolution of the QRS amplitude, which might have shadowed any effects in the intra-cardiac ECG.

The correlation between LV volume and QRS amplitude should further be investigated in HF patients where substantial LV volume changes occur and maximum benefit is expected. Such patients are HF patients with less congested cardiovascular systems and patients with mechanical circulatory support, e.g. left ventricular assist devices (LVADs). In HF patients with less congested cardiovascular systems, under diuretic therapy and HF medication and probably in earlier stages of the disease, larger LV volume changes are expected. Volume overload can usually be seen under acute deterioration of the heart function or hypovolemia occurs because of HF therapy. The detection of such changes using the widely available surface ECG could enhance the monitoring of both the course of the disease and the course of treatment, allowing further, targeted adjustments of the therapeutic intervention. However, the experimental investigation in this patient group can be very complicated, because of the many confounders that would have to be controlled for and regarding patient safety.

Currently, LVADs operate at a constant speed and lack continuous preload monitoring as well as physiologic feedback control. According to clinical and echocardiogaphic data the pump speed is set by the physicians, opting at the best hemodynamic status regarding the goal of the therapy. Variations in LV volume and cardiac contractility can lead to underpumping or overpumping, since the pump speed is constant and consequently, may cause serious adverse events, like suction or pulmonary edema. Early detection of such changes could alert the treating physicians or activate an automated response from the control system leading to a manual or automatic targeted adjustment of the pump speed. For physiological feedback control of LVADs, integrated pressure or volume sensors are necessary (Ochsner *et al* 2016, Petrou *et al* 2018), but they are not commercially available as yet (Tchantchaleishvili *et al* 2017, Dual *et al* 2018). Simply by integrating electrodes in the cannula of an LVAD, an ECG-based preload estimate could provide the input variable needed for physiological control in the future. Given the manifold determinants of the QRS amplitude, a robust measure of preload will likely require a combination with additional signals.

An experimental setting, where controlled and easily reversible, acute and substantial changes in LV volume can be induced, like in patients with an LVAD, would enable to bring the correlation under investigation forward. The loading status of the LV of LVAD patients mainly depends on the pump speed of the device, thus the LV volume is largely affected and easily manipulated through pump speed changes (Addetia *et al* 2018). Protocols for the assessment of the patients' hemodynamics are regularly used in the clinic to further adjust their therapy. Therefore, an experimental protocol including LV volume manipulations through pump speed changes could be applied quite safely as a next step in the investigation process and even combined with protocolls already in use in the clinical setting. Pump speed changes in an experimental setting lead to significant changes in LV volume, and hence most probably induce bigger changes of the QRS amplitude. In summary, not only would LVAD patients greatly profit from the application of this correlation, but they also provide the most optimal conditions for the further investigations.

In conclusion, this study supports existing literature on the correlation between cardiac preload and QRS amplitude of the surface ECG (Brody 1956) and extends its application to the complex ECG waveform of advanced HF patients. Patients with mildy congested cardiovascular systems and especially HF patients with mechanical circulatory support could profit from this correlation. This could be an aid for adequately setting the pump speed, an input method for a preload estimator for physiological control algorithms or a monitoring technique to prevent possible complications resulting from LV volume changes. Yet, further investigations in HF patients with mechanical circulatory support are required.

Acknowledgments

Appendix

Table A1. All variables that were investigated to characterize the difference between the PAC group and the no-PAC group. Only age and the respiratory rate were statistically significant. The Exact Fischer test was used for nominal, not normally distributed variables and the Mann-Whitney-U test for continuous, not normally distributed variables.

Variables
Previous cardiothoracic operations
Sex
Ischemic etiology
Pacemaker device implanted
CRT- D device implanted
Ventricular tachycardia in the past
Ventricular ablation (EP)
Advanced CKD (KDOQI III, IV, V)
Beta blocker
Amiodarone
NYHA II versus NYHA III
Weight gain during the previous 4 weeks
Admission to a hospital over 3 times in the previous 6 months (equal to/over)
Clinical edema
Sinus rhythm
PM-triggered ECG
RV function moderately or severely reduced
Mitral valve insufficiency moderate or severe
Tricuspid valve insufficiency moderate or severe
Age (p = 0.043)
Weight
Height
BMI
Weight gain in percentage during the previous 4 weeks
Weight loss in percentage during the previous 4 weeks
Respiratory rate (p = 0.019)
Systolic blood pressure
Diastolic blood pressure
Mean blood pressure
Hematocrit
Potassium
Pro-BNP
Creatinine
Heart rate
QRS duration
QRS amplitude in external basis ECG
QTc time
PQ time
LVEDD
RVOT

ORCID iDs

Seraina Anne Dual ⓘ https://orcid.org/0000-0001-6867-8270

Panagiotis Pergantis ⓘ https://orcid.org/0000-0001-9635-2999

Marianne Schmid Daners ⓘ https://orcid.org/0000-0002-6411-8871

References

Abraham W T *et al* 2011 Wireless pulmonary artery haemodynamic monitoring in chronic heart failure: a randomised controlled trial *The Lancet* **377** 658–66

Addetia K *et al* 2018 3D morphological changes in LV and RV during LVAD ramp studies *JACC: Cardiovascular Imaging* **11** 159–69

Bakdash J Z and Marusich L R 2017 Repeated measures correlation *Frontiers in Psychology* Frontiers **8** 456

Bednarczyk J M *et al* 2017 Incorporating dynamic assessment of fluid responsiveness into goal-directed therapy: a systematic review and meta-analysis *Critical Care Medicine* **45** 1538–45

Begot E *et al* 2015 Hemodynamic assessment of ventilated ICU patients with cardiorespiratory failure using a miniaturized multiplane transesophageal echocardiography probe *Intensive Care Medicine* **41** 1886–94

Brody D A 1956 A theoretical analysis of intracavitary blood mass influence on the heart-lead relationship *Circ. Res.* **4** 731–7

Caiani E G *et al* 2013 Evaluation of the relation between changes in R-wave amplitude and LV mass and dimensions in a model of 'reversed hypertrophy' *Computing in Cardiology* **40** 867–70

Chong M A 2018 Does goal-directed haemodynamic and fluid therapy improve peri-operative outcomes?: a systematic review and meta-analysis *European Journal of Anaestehsiology* **35** 469–83

Dellinger R P *et al* 2013 Surviving sepsis campaign *Critical Care Medicine* **41** 580–637

Dual S A *et al* 2018 Ultrasonic sensor concept to fit a ventricular assist device cannula evaluated using geometrically accurate heart phantoms *Artif. Organs* **42** E29–E42

Eckberg D and Sleight P 1992 Human baroreflexes in health and disease *Monographs of the Physiological Society* (Cambridge: Cambridge University Press) (https://doi.org/10.1017/CBO9781107415324.004)

Eubel A *et al* 2001 *Nicht-invasive Überwachung von Abstoßungsreaktionen nach Herztransplantation* **126** 1223–8

Feldman T E D *et al* 1985 Relation of electrocardiographic R-wave amplitude to changes in left ventricular chamber size and position in normal subjects *American Journal of Cardiology* **55** 1168–74

Fischer M O *et al* 2013 Prediction of responsiveness to an intravenous fluid challenge in patients after cardiac surgery with cardiopulmonary bypass: a comparison between arterial pulse pressure variation and digital plethysmographic variability index *Journal of Cardiothoracic and Vascular Anesthesia* **27** 1087–93

Fresiello L *et al* 2014 The relationship between R-wave magnitude and ventricular volume during continuous left ventricular assist device assistance: experimental study *Artif. Organs* **39** 446–450

Giraud R *et al* 2013 Respiratory change in ECG-wave amplitude is a reliable parameter to estimate intravascular volume status *J. Clin. Monit. Comput.* **27** 107–11

Ishikawa K, Nagasawa T and Shimada H 1979 Influence of hemodialysis on electrocardiographic wave forms *Am. Heart J.* **97** 5–11

Ishikawa K, Shirato C and Yanagisawa A 1983 Electrocardiographic changes due to sauna bathing. Influence of acute reduction in circulating blood volume on body surface potentials with special reference to the Brody effect. *British Heart Journal* **50** 469–75

Kataoka H and Madias J E 2011 Changes in the amplitude of electrocardiogram QRS complexes during follow-up of heart failure patients *Journal of Electrocardiology* Elsevier Inc. **44** e1–394

Levy M M, Evans L E and Rhodes A 2018 The surviving sepsis campaign bundle: 2018 update *Intensive Care Medicine* **44** 925–928

Madias J E 2007 The resting electrocardiogram in the management of patients with congestive heart failure: Established applications and new insights *PACE—Pacing and Clinical Electrophysiology* **30** 123–8

Madias J E 2014 *Transient Attenuation of the Amplitude of the QRS Complexes in the Diagnosis of Takotsubo Syndrome'* (https://doi.org/10.1177/2048872613504311)

Magalski A *et al* 2002 Continuous ambulatory right heart pressure measurements with an implantable hemodynamic monitor: a multicenter, 12-month follow-up study of patients with chronic heart failure *J. Cardiac Failure* **8** 63–70

Meyer A *et al* 2018 Machine learning for real-time prediction of complications in critical care: a retrospective study *The Lancet Respiratory Medicine* 905–914

Monnet X and Teboul J-L 2015 Passive leg raising: five rules, not a drop of fluid! *Critical Care* **19** 18

Ochsner G *et al* 2016 *In vivo* evaluation of phsiological control algorithms for LVADs based on left ventricular volume or pressure *ASAIO Journal.* **63** 568–577

Osawa E A *et al* 2015 Effect of perioperative goal-directed hemodynamic resuscitation therapy on outcomes following cardiac surgery *Critical Care Medicine* **44** 1

Petrou A *et al* 2018 Standardized comparison of selected physiological controllers for rotary blood pumps: *in vitro* study *Artif. Organs* **42** E29–E42

Porterfield J E *et al* 2011 Left ventricular epicardial admittance measurement for detection of acute LV dilation. *Journal of applied physiology (Bethesda, Md.: 1985)* **110** 799–806

Pozzoli M *et al* 1997 Loading manipulations improve the prognostic value of Doppler evaluation of mitral flow in patients with chronic heart failure *Circulation.* **27** 174

Saporito S *et al* 2017 Comparison of cardiac magnetic resonance imaging and bio-impedance spectroscopy for the assessment of fluid displacement induced by external leg compression *Physiol. Meas.* IOP Publishing **38** 15–32

Sequeira V and van der Velden J 2015 Historical perspective on heart function: the Frank–Starling law *Biophys. Rev.* **7** 421–47

Stephens R S and Whitman G J R 2015 Postoperative critical care of the adult cardiac surgical patient. Part I: routine postoperative care *Critical Care Medicine* **43** 1477–97

Surawicz B and Knilans T K 2008 Left bundle branch block *Chou's Electrocardiography in Clinical Practice* 6th edition (Philadelphia: Elsevier) 75–94

Tchantchaleishvili V *et al* 2017 Clinical implications of physiologic flow adjustment in continuous-flow left ventricular assist devices *ASAIO Journal* **63** 241–250

Turakhia M P *et al* 2019 Rationale and design of a large-scale, app-based study to identify cardiac arrhythmias using a smartwatch : the apple heart study *Am. Heart J.* **207** 66–75

Vakily A *et al* 2017 A System for continuous estimating and monitoring cardiac output via arterial waveform analysis *Journal of Biomedical Physics & Engineering* **7** 181–90

Vancheri F and Barberi O 1989 Relationship of QRS amplitude to left ventricular dimensions after acute blood volume reduction in normal subjects *Eur. Heart J.* **10** 341–5

Vitolo B Y E *et al* 1987 Relationship between changes in R wave voltage and cardiac volumes. A vectorcardiographic study during hemodialysis *J. Electrocardiology* **20** 138–46

Weyer S *et al* 2014 Bioelectrical impedance spectroscopy as a fluid management system in heart failure *Physiol. Meas.* **35** 917–930

Yavasi Ö *et al* 2014 American journal of emergency medicine monitoring the response to treatment of acute heart failure patients by ultrasonographic inferior vena cava collapsibility index *American Journal of Emergency Medicine* **32** 403–710

CURRICULUM VITAE

Mein Lebenslauf wird aus datenschutzrechtlichen Gründen in der elektronischen Version meiner Arbeit nicht veröffentlicht

Publikationsliste

Artikel:

Dual, S. A., Pergantis, P., Schoenrath, F., Keznickl-Pulst, J., Falk, V., Meboldt, M., & Daners, M. S. (2019). Acute changes in preload and the QRS amplitude in advanced heart failure patients. *Biomedical Physics & Engineering Express*, *5*(4), 045015. Noch kein Impact Factor zugeteilt.

Petrou, A., Kanakis, M., Boës, S., Pergantis, P., Meboldt, M., & Daners, M. S. (2018). Viscosity prediction in a physiologically controlled ventricular assist device. *IEEE Transactions on Biomedical Engineering*, *65*(10), 2355-2364. Impact Factor 2018: 4,4891

Sargut, T. A., Pergantis, P., Knosalla, C., Knierim, J., Hummel, M., Falk, V., & Schoenrath, F. (2018, December). Adjusting preoperative risk models of post heart transplant survival to a European cohort in the age of a new cardiac allocation score in Europe. In *The heart surgery forum* (Vol. 21, No. 6, pp. E527-E533). Impact Factor 2018: 0,564

Petrou, A., Ochsner, G., Amacher, R., Pergantis, P., Rebholz, M., Meboldt, M., & Schmid Daners, M. (2016). A physiological controller for turbodynamic ventricular assist devices based on left ventricular systolic pressure. *Artificial organs*, *40*(9), 842-855. Impact Factor 2016: 2,403

Petrou, A., Pergantis, P., Ochsner, G., Amacher, R., Krabatsch, T., Falk, V., Mebold M. & Daners, M. S. (2017). Response of a physiological controller for ventricular assist devices during acute patho-physiological events: an in vitro study. *Biomedical Engineering/Biomedizinische Technik*, *62*(6), 623-633. Impact Factor 2017: 1,096

Pieri, M., Scandroglio, A. M., Müller, M., Pergantis, P., Kretzschmar, A., Kaufmann, F., Falk, V., Krabatsch, T., Arlt, G., Potapov, E. & Kukucka, M. (2016). Surgical management of driveline infections in patients with left ventricular assist devices. *Journal of cardiac surgery*, *31*(12), 765-771. Impact Factor 2016: 0,518

Pieri, M., Müller, M., Scandroglio, A. M., Pergantis, P., Kretzschmar, A., Kaufmann, F., Falk, V., Krabatsch, T., Arlt, G., Potapov, E. & Kukucka, M. (2016). Surgical treatment of mediastinitis with omentoplasty in ventricular assist device patients: report of referral center experience. *Asaio Journal*, *62*(6), 666-670. Impact Factor: 2.190

Scandroglio, A. M., Kaufmann, F., Pieri, M., Kretzschmar, A., Müller, M., Pergantis, P., Dreysse, S., Falk V., Krabatsch, T. & Potapov, E. V. (2016). Diagnosis and treatment algorithm for blood flow obstructions in patients with left ventricular assist device. *Journal of the American College of Cardiology*, *67*(23), 2758-2768. Impact Factor 2016: 19,896

Pergantis, P., Krabatsch, T., Potapov, E., & Schoenrath, F. (2016). Therapy forms for advanced heart failure. Ventricular assist devices. *KARDIOLOGE*, *10*(2), 119-128.

Pedde, D., Soltani, S., Kaufmann, F., Müller, M., Pergantis, P., Falk, V., Krabatsch, T. & Potapov, E. (2016). Impact of Atrial Fibrillation on Pump Thrombosis and Thromboembolic Events in Long-Term Left Ventricular Assist Device Therapy. *The Journal of Heart and Lung Transplantation*, *35*(4), S251. Impact Factor 2016: 7,114

Abstracts

Schoenrath, F. F., Roehrich, L., Mulzer, J., Mueller, M., Starck, C., Potapov, E., Falk, V., Knierim, J. & Pergantis, P. (2019). Implementation of the 2016 ESC guidelines for treatment of heart failure in patients after continuous flow LVAD implantation. In *EUROPEAN JOURNAL OF HEART FAILURE* (Vol. 21, pp. 87-87). 111 RIVER ST, HOBOKEN 07030-5774, NJ USA: WILEY.

Roehrich, L., Knierim, J., Hajduczenia, M., Mulzer, J., Mueller, M., Pergantis, P., Hummel, M., Falk, V., Potapov, E., Suendermann S. & Schoenrath, F. (2019). Early-and Late-Onset Arrhythmias after Bioelectrical Impedance Analysis in End-Stage Heart Failure Patients under Inotropic Support. *The Journal of Heart and Lung Transplantation*, *38*(4), S377.

Pergantis, P., Dual, S. A., Daners, M. S., Keznickl-Pulst, J., Schoenrath, F., & Falk, V. (2019). The Effect of Preload Change on QRS Amplitude in Advanced Heart Failure Patients. *The Journal of Heart and Lung Transplantation*, *38*(4), S378-S379.

Scandroglio, A., Kaufmann, F., Pieri, M., Kretzschmar, A., Muller, M., Pergantis, P., Dreysse, S., Falk, V., Krabatsch, T. & Potapov, E. (2016). Diagnosis and Treatments of Three Different Types of Blood Flow Abnormalities in Patients Supported with HeartWare HVAD: Analysis of More Than 600 Cases. *The Journal of Heart and Lung Transplantation*, *35*(4), S96.

Krabatsch, T., Kaufmann, F., Hörmandinger, C., Müller, M., Kretzschmar, A., Pergantis, P., Falk, V. & Potapov, E. V. (2015). Management of Pump Thrombosis in Heartware Hvad Patients. *Circulation*, *132*(suppl_3), A19675-A19675.

Eidesstattliche Versicherung

„Ich, Panagiotis Pergantis, versichere an Eides statt durch meine eigenhändige Unterschrift, dass ich die vorgelegte Dissertation mit dem Thema: ‚Physiologische Regelung für linksventrikuläre Herzunterstützungssysteme/ Physiological control for left ventricular assist devices' selbstständig und ohne nicht offengelegte Hilfe Dritter verfasst und keine anderen als die angegebenen Quellen und Hilfsmittel genutzt habe.

Alle Stellen, die wörtlich oder dem Sinne nach auf Publikationen oder Vorträgen anderer Autoren/innen beruhen, sind als solche in korrekter Zitierung kenntlich gemacht. Die Abschnitte zu Methodik (insbesondere praktische Arbeiten, Laborbestimmungen, statistische Aufarbeitung) und Resultaten (insbesondere Abbildungen, Graphiken und Tabellen) werden von mir verantwortet.

Meine Anteile an etwaigen Publikationen zu dieser Dissertation entsprechen denen, die in der untenstehenden gemeinsamen Erklärung mit dem Erstbetreuer/in, angegeben sind. Für sämtliche im Rahmen der Dissertation entstandenen Publikationen wurden die Richtlinien des ICMJE (International Committee of Medical Journal Editors; www.icmje.og) zur Autorenschaft eingehalten. Ich erkläre ferner, dass ich mich zur Einhaltung der Satzung der Charité – Universitätsmedizin Berlin zur Sicherung Guter Wissenschaftlicher Praxis verpflichte.

Weiterhin versichere ich, dass ich diese Dissertation weder in gleicher noch in ähnlicher Form bereits an einer anderen Fakultät eingereicht habe.

Die Bedeutung dieser eidesstattlichen Versicherung und die strafrechtlichen Folgen einer unwahren eidesstattlichen Versicherung (§§156, 161 des Strafgesetzbuches) sind mir bekannt und bewusst."

Datum   **Unterschrift**

Danksagung

Ich möchte mich bei Prof. Dr. med. Volkmar Falk, Prof. h.c. Dr. med. habil. Thomas Krabatsch, PD Dr. med. Evgenij Potapov und Dr. med. Felix Schönrath für die Überlassung des Themas sowie die Ermöglichung und Begleitung meiner wissenschaftlichen Tätigkeit im Deutschen Herzzentrum Berlin bedanken.

Ein herzlicher Dank geht an meine Freunde und Kollegen Dr.-Ing. Seraina Dual und Dr.-Ing. Anastasios Petrou für die traumhafte Zusammenarbeit, die Unterstützung und die Inspiration. Besonders möchte ich mich bei Dr.-Ing. Marianne Schmid Daners für das Mentoring und das Vertrauen bedanken. Es war mir eine Ehre und eine echte Freude an ihrer Arbeitsgruppe an der ETH Zürich teilnehmen zu dürfen.

Ich möchte mich bei meinen Freunden Dr. med. Antonia Schulz und Dr. med. Darach O h-ici für die langen Gespräche, ihre Geduld und die Motivation bedanken. Besonders dankbar bin ich Katerina Tsantila für die Begleitung und Unterstützung in den schwierigen Phasen dieser Doktorarbeit.

Für vieles in meinem Leben, inklusiv der Unterstützung während meiner Promotion, bedanke ich mich ganz herzlich bei meinen engsten Freunden Georgia Tsampouka, Triantafylli Nikolopoulou, Artemis Vekrakou und Diana Vardaxi.

Bei meinen Eltern Vassiliki und Dimitris bedanke ich mich ganz herzlich, weil sie mir alles zur Verfügung gestellt haben, damit ich meine Träume verwirklichen kann. Meinem lieben Bruder Aggelos danke ich für die Inspiration in meinem Leben und meiner Doktorarbeit.

Ein spezieller Dank geht an meinen Partner Stijn Harry Kox für die Begleitung dieses Prozesses, das Vertrauen und den Ausgleich.

Diese Arbeit widme ich meiner Großmutter Aggeliki Pantazou. Alles was ich von ihr über das Leben und mich selbst lernen durfte, hat meinen Weg zu diesem Punkt begleitet.